International Journal of
Fine Chemicals, Applied Chemistry and Biotechnology

chimica oggi
CHEMISTRY TODAY

PEER REVIEWED

ISSN 0392-839X CHOGDS

Poste Italiane Spa - Sped. in Abb. Postale - D.L. 353/2003 (conv. In L. 27/02/2004 n. 46) - art.1 comma 1 - DCB Milano • Chimica Oggi / Chemistry Today - vol 33(6) - November/December 2015 • Published by Tekno Scienze Srl

ALDRICH Chemistry

Rediscover Aldrich catalysis with the *repriced* Buchwald portfolio

Add Aldrich™

Now the most competitively priced Buchwald offering!

Experiment with our Buchwald portfolio of products, which we are now offering at up to 69% off of our former list prices without compromising the high quality that you have come to expect from Aldrich. Examples of the new competitive price reductions are shown below.

Easily activated Palladium Precatalysts for facile C–N and C–C bond formations.

Buchwald palladium precatalysts are highly reactive, air-stable, and crystalline white solids that generate the active monoligated Pd(0) species in situ, providing a more efficient and easily accessible catalytic system.

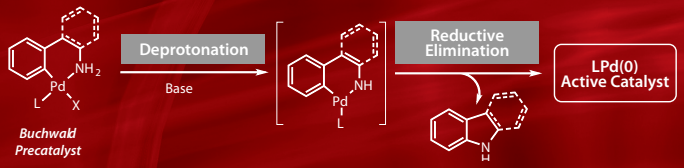

G1 = 1st Generation Precatalysts

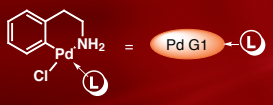

G2 = 2nd Generation Precatalysts

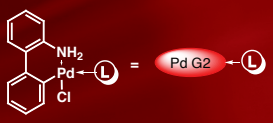

G3 = 3rd Generation Precatalysts

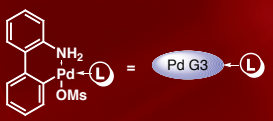

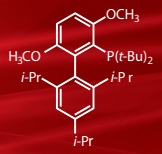

730998-500MG
tBuBrettPhos
New Price—reduced 69%

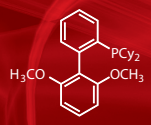

638072-5G
SPhos
New Price—reduced 38%

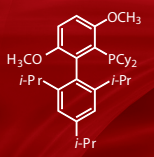

718742-100MG
BrettPhos
New Price—reduced 37%

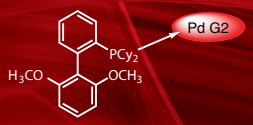

753009-5G
SPhos Pd G2
New Price—reduced 34%

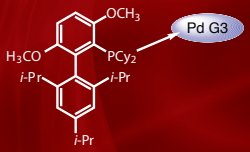

761605-5G
BrettPhos Pd G3
New Price—reduced 35%

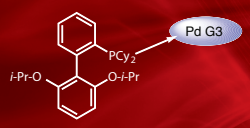

763403-250MG
RuPhos Pd G3
New Price—reduced 21%

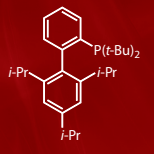

638080-5G
tBuXPhos
New Price—reduced 41%

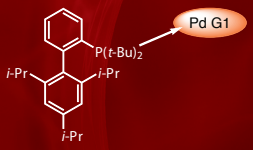

708739-1G
tBuXPhos Pd G1
New Price—reduced 35%

To see the complete list of available Buchwald Precatalysts and Ligands, visit **Aldrich.com/Buchwald**

84073

SIGMA-ALDRICH®

BE INSPIRED !

OmegaChem

Inspiring Your Imagination

OC-0717	OC-0755	OC-0701	OC-0677	OC-0750	OC-0745
OC-0632	OC-0721	OC-0704	OC-0709	OC-0731	OC-0708
OC-0706	OC-0697	OC-0707	OC-0700	OC-0556	OC-0747
OC-0734	OC-0742	OC-0740	OC-0725	OC-0735	OC-0746
OC-0557	OC-0576	OC-0564	OC-0738	OC-0579	OC-0736

CONTENTS

TEKNO SCIENZE SRL
Viale Brianza, 22 - 20127 Milano (Italy)
Tel +39-02-26809375/28381260 - Fax +39-02-2847226
e-mail: info@teknoscienze.com - web: www.teknoscienze.com

Editor in Chief
Carla Scesa - info@teknoscienze.com
Editorial Director
Silvana Maini - silvana@teknoscienze.com
Associate Editors
Gayle De Maria - gayle@teknoscienze.com
Florian Weighardt- florian@teknoscienze.com
Luigi Lo Forti - luigi@teknoscienze.com
Marketing & Sales
Giulio Fezzardini - giulio@teknoscienze.com
Silvia Baldina - silvia@teknoscienze.com
Simona Rivarollo - simona@teknoscienze.com
Marketing & Events
Paola Passadore - paola@teknoscienze.com
Production Manager
Elisa Novaresi - elisa@teknoscienze.com
Production Assistants & IT Department
Luis Alburqueque Diaz - luis@teknoscienze.com
Matteo Cattane - matteo@teknoscienze.com
Administrative & Account
Alba Aprea - alba@teknoscienze.com

PRINTING AND LAY-OUT OFFICE:
Arti Grafiche Colombo (Muggiò - MB, Italia)
Authorization from *Tribunale di Milano* n. 514 of July 27th 2006
(Autorizzazione del *Tribunale di Milano* n. 514 del 27 Luglio 2006).

Chimica Oggi - Chemistry Today is a peer-reviewed journal devoted to fine chemistry, pharmaceuticals and biotechnology addressed to a readership belonging to the industry. An **impact factor of 0,390** is listed in the 2014 Journal Citation Reports (ISI Web of Knowledge).

Chimica Oggi - Chemistry Today
vol. 33(6) November/December 2015


Mario Pagliaro

MARIO PAGLIARO
Sicily's Solar Pole and Istituto per lo Studio dei Materiali Nanostrutturati, CNR, via U. La Malfa 153, 90146 Palermo, Italy

Member of *Chimica Oggi - Chemistry Today* Scientific Advisory Board

Green chemistry in APIs manufacturing:
A forthcoming revolution now mature

Faced by increasing manufacturing cost and by numerous quality problems, the fine chemicals and pharmaceutical industries are slowly, but inevitably, shifting to green chemistry synthetic methods: Biocatalysis and homogeneous catalysis first; and then to heterogeneous catalysis, well beyond typical hydrogenation reactions over Pt/C or Pd/C conventional catalysts. We have explained in detail elsewhere how, dwarfed by the typical E-factor = 0.1 value of the petrochemicals industry, the E-factor (kilogram of waste per kilogram of API manufactured) approaching 200 typical of homogeneously catalyzed API synthetic processes has marked for the last decade the industry's *process* obsolescence (1).

Yet this situation is now changing thanks to the concomitant introduction of new heterogeneous catalysts coupled to manufacturing under flow conditions. Second-generation commercial heterogeneous catalysts suitable for carbon-carbon coupling, debenzylation, hydrosilylation and many other industrially relevant reactions, including conversion of natural terpenes into fragrances, perfumes, flavours, pharmaceuticals and synthetic intermediates, are now commercially available.

Using 3-D encapsulated, rather than 2-D surface-derivatized materials, heterogeneously catalyzed processes make use of entrapped enzyme, organo- or metal catalyst to selectively mediate the desired reaction, avoiding waste generation while attaining higher conversion and yield than reaction under batch.

As we write, furthermore, we witness to the first small molecule fine chemicals and pharmaceuticals being produced continuously in flow, in what Trout has called the "ultra-lean way of manufacturing" (2). Regulatory problems have indeed been overcome, with the first harmonized regulatory guidelines accepted across various regulatory authorities.

Contrary to mainstream thinking, China and India not only give every year eminent contributes to advance the science and technology of heterogeneous catalysis for fine chemical and API manufacturing, but companies based in these huge countries where the production of APIs and fine chemicals has been largely outsourced from Europe and the US, already lead the field along with companies based in Switzerland, Germany, Sweden, the US and Austria.

This global effort, we argue in conclusion, will help to regain control on product quality, ending what Grayson, has called in this Journal (2) the «madness» of fine chemistry during two decades of economic globalization. Eventually, within the next decade, the pharmaceutical and fine chemicals industries will rely on chemical manufacturing with little or no waste generation, minimal energy and resource utilization, based on continuous manufacturing in flow reactors equipped with solid catalysts, located in industrial plants 20 or 30 times smaller than today's batch plants of similar output.

It is the task of us chemistry scholars, to make flow and nanochemistry-based catalysis a part of the course curriculum for chemists, filling the "talent shortage" lately identified by us (3) and by Jamison (4), a professor and pioneer in flow chemistry, as today's main barrier to the industry's adoption of nanochemistry and catalysis under flow as the most promising green chemistry technologies.

REFERENCES

1. R. Ciriminna, M. Pagliaro, Org. Process Res. Devel. 17, 1479-1484 (2013)
2. B. Trout, "Continuous manufacturing: the ultra lean way of manufacturing," Biochemical Engineering XVI, Burlington (VT), July 2009.
3. M. Pagliaro, Chem. Eur. J. 21, 11.931-11.936 (2015).
4. Interview to D. Stanton, In-PharmaTechnologist.com, 13 maggio, 2015.

Orange lichens are source for potential anticancer drug

An orange pigment, found in lichens and rhubarb, called parietin may have potential as an anti-cancer drug, scientists at Winship Cancer Institute of Emory University have discovered.
The results were published in *Nature Cell Biology* on October 19.
Parietin, also known as physcion, could slow the growth of and kill human leukemia cells obtained directly from patients, without obvious toxicity to human blood cells, the authors report. The pigment could also inhibit the growth of human cancer cell lines, derived from lung and head and neck tumors, when grafted into mice.
A team of researchers led by Jing Chen, PhD, discovered the properties of parietin because they were looking for inhibitors for the metabolic enzyme 6PGD (6-phosphogluconate dehydrogenase). 6PGD is part of the pentose phosphate pathway, which supplies cellular building blocks for rapid growth. Researchers have already found 6PGD enzyme activity increased in several types of cancer cells.
"This is part of the Warburg effect, the distortion of cancer cells' metabolism," says Chen, professor of hematology and medical oncology at Emory University School of Medicine and Winship Cancer Institute. "We found that 6PGD is an important metabolic branch point in several types of cancer cells."
This work represents a collaboration among three laboratories at Winship led by Chen, Sumin Kang, PhD, assistant professor of hematology and medical oncology, and Jun Fan, PhD, assistant professor of radiation oncology. Co-first authors are postdoctoral fellows Ruiting Lin, PhD, and Changliang Shan, PhD, and former graduate student Shannon Elf, PhD, now at Harvard.
The Winship team obtained cancer cells from a patient with acute lymphoblastic leukemia, and found doses of physcion/parietin that could kill half the leukemia cells in culture within 48 hours, while the same doses left healthy blood cells unscathed. A more potent derivative of the pigment called S3 could cut the growth of a lung cancer cell line by a factor of three over 11 days, when the cells were implanted into mice.
Although 6PGD inhibitors appear to be nontoxic to healthy cells, more toxicology studies are needed, both to assess potential side effects and to see whether people with inherited conditions would be more sensitive to the drugs. Parietin is present in some natural food pigments, but has not been tested as a drug in humans.
The research at Emory was supported by the Winship Cancer Institute, the National Cancer Institute, the Department of Defense, the Charles Harris Run for Leukemia and the Georgia Research Alliance. Some co-authors of the paper are employees of Cell Signaling Technology Inc.
Emory Health Sciences

3-D printed parts from some commercial devices toxic to zebrafish embryos

The recent boom in 3-D printing has driven innovations in fields as disparate as haute couture and medical implants. But little is known about the safety of the materials used. In a new study in ACS' journal Environmental Science & Technology Letters, scientists showed that some 3-D printed parts are highly toxic to zebrafish embryos. Their findings could have implications not only for aquatic life but also for hobbyists, manufacturers and patients.

In 2012, the market for 3-D printing was worth $288 million, according to an analysis by Canalys, Inc. By 2018, its value is projected to soar to $16.2 billion. The driver for this market has largely been use in medical applications, but with prices dropping for 3-D printers, more hobbyists and small businesses are expected to adopt the technology. Some research has already raised concerns that the printed materials might cause inflammatory or allergic reactions in patients. But little work has been done to explore their potential effects on an organism's overall health and development. William H. Grover and colleagues wanted to fill that void.

The researchers exposed zebrafish embryos to discs printed by two kinds of commercial 3-D printers: fused deposition modeling (FDM) printers and stereolithography (STL) printers. Among other problems, the embryos exposed to either type of disc showed lower survival, reduced lengths and decreased hatching rates compared to the controls. In addition, all embryos exposed to STL-printed parts had malformations and died within seven days. The researchers found that treating 3-D printed pieces with ultraviolet (UV) light for 30 minutes on each side seemed to reduce some side effects. They conclude that safe disposal strategies for 3-D printed products and waste materials are needed to protect aquatic life.
American Chemical Society

RAPID EVAPORATION SOLUTIONS FOR NATURAL PRODUCT EXTRACTION

Genevac reports on how their Rocket Synergy automated evaporator systems are replacing rotary evaporators as the tool of choice for rapid and sample-safe evaporation of natural product extracts. Working with natural products to derive potential pharmaceutical drug candidates or to identify new flavours and fragrances has a reputation of being very difficult. Sample collection, preparation, extraction, and drying are extremely labour intensive and not easily reproducible from a process standpoint. The traditional bottleneck in the natural product pipeline has been the drying of solvent extracted samples. Historically natural product researchers have used rotary evaporators to remove solvent from the extract, a tedious process that sometimes can take days per sample. Recently researchers have found the unique design of the Rocket Synergy used in conjunction with Genevac SampleGenie™ technology has allowed them to dry down samples in just 1-2 hours under low vacuum and low temperature conditions which do affect the integrity of the sample. The Rocket Synergy is able to dry or concentrate up to six flasks, each containing a maximum of 450ml of solvent, or 18 ASE® vials, with no user intervention or attention. To extend operational versatility the Rocket Synergy flask rotor may be quickly removed and replaced with a stainless steel vessel allowing unattended automated batch processing of up to 5 litres per run. It has been found that a single Rocket Synergy evaporator is capable of replacing several rotary evaporators, saving valuable bench space and improving your productivity.
www.genevac.com/naturalproducts

UNDERTAKING HEATED EXPERIMENTS IN NMR TUBES

Asynt has developed DrySyn NMR Heating Blocks to enable safe, effective and uniform heating of up to 10 NMR tubes on a conventional hotplate stirrer. This new DrySyn unit allows you to use standard NMR tubes as a reaction vessel for applications including catalyst screening experiments and reaction monitoring as well as studying broad peaks, temperature dependent solubility issues and conformational changes. Unlike heating in problematic oil baths, using a DrySyn NMR Heating Blocks allows you to analyse the contents of your NMR tube almost immediately without removal of residual oil on the outside of the glassware. To compliment the DrySyn NMR heating blocks, Asynt also offer an affordable range of NMR tubes and a Liquid Nitrogen Generator for NMR spectrometers to keep liquid helium cool and prevent boil off. The DrySyn heating block range is a safe and productive alternative to oil baths and heating mantles. The system offers clean, safe synthesis for single or multiple reactions. Compatible with any magnetic hotplate stirrer, DrySyn heating blocks provide rapid temperature ramping to over 300 °C. All DrySyn heating blocks are manufactured in the UK with a chemical and solvent resistant clear anodised finish to ensure long trouble-free operation.
For further information please contact Asynt on +44-1638-781709 / **sales@asynt.com**

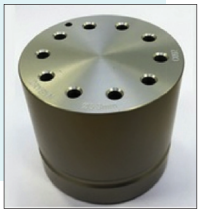

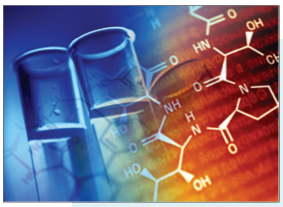

POST PURIFICATION SAMPLE HANDLING

Genevac, specialists in solvent removal, have developed a suite of proprietary technological solutions to facilitate post purification sample handling, including reformatting. For labs undertaking purification using Normal Phase HPLC, SFC or Flash chromatography – removal of organic solvents can be simply, productively and safely carried out in a Genevac centrifugal evaporator (EZ-2, ROCKET, Rocket Synergy or HT Series III). Where the nature of the sample being concentrated can lead to solvent bumping (e.g. natural products) - Genevac's DriPure® technology is proven to completely eliminate this troublesome and time-consuming problem. The evaporation of aqueous acetonitrile (or methanol / ethanol) fractions resulting from Reverse Phase HPLC is a widely carried out application on many Genevac evaporator systems. A multiple stage method has been developed for the EZ-2 evaporator to remove the organic solvent without freezing the water, remove the water, and then dry any remaining stubborn solvent. Alternatively, the unique LyoSpeed™ fast lyophilisation method can be used in Genevac HT series evaporators to produce dry (solvent-free) powders from samples that previously could only be produced as gums and oils. Recent advances in condenser technology, in particular the high power -75°C cold trap, available on HT Series III and Rocket Synergy evaporators, has led to significant advances in lyophilisation success rates. During post purification handling - samples typically need to be reformatted from fraction tubes or flasks, into a small vial for compound storage. For this specific time consuming task, Genevac developed SampleGenie™ technology. SampleGenie™ enables a large volume to be dried (or lyophilised) directly into a small storage vial in a fraction of the time taken by traditional evaporation methods that require you to reformat samples from a flask or multiple tubes into a vial.

www.genevac.com/purification

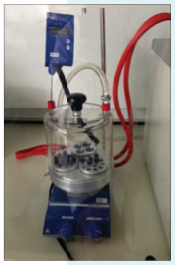

IMPROVING SUB-AMBIENT REACTION REPRODUCIBILITY

The DrySyn Snowstorm MULTI from **Asynt** provides a simple and highly effective way to perform multiple reactions in parallel across a large temperature range including sub-ambient chemistries such as organometallic syntheses and controlled rate crystallisation studies down to -60°C. Sub-ambient reactions have traditionally been difficult to undertake reproducibly on a small to medium scale. The DrySyn Snowstorm MULTI is able to accommodate up to 12 vials or three 100ml round bottom flasks offering sub ambient reactions in parallel without the need for jacketed reaction vessels, or ice baths. Operating with a suitable chiller / circulator, a DrySyn SnowStorm MULTI provides accurate, stable temperature control down to -60°C and up to +150°C. Being able to maintain a sub-ambient temperature, sometimes for significant periods, is important for reaction reproducibility. The DrySyn SnowStorm MULTI connects to an external chiller unit and holds temperatures at a set-point for as long as is required. Setting temperature ramping profiles is also possible on the DrySyn Snowstorm MULTI which is important in crystallisation studies.

www.asynt.com/product/drysynsnowstormreactor/

ABBVIE'S COMMITMENT TO ONCOLOGY DEMONSTRATED AT THE 57TH AMERICAN SOCIETY OF HEMATOLOGY ANNUAL MEETING

AbbVie presented data from clinical trials evaluating the company's oncology portfolio during the 57th American Society of Hematology Annual Meeting (ASH), December 5-8, in Orlando, Fla. Notably, data scheduled for presentation include results from studies of venetoclax, an investigational oral B-cell lymphoma-2 (BCL-2) inhibitor, in chronic lymphocytic leukemia (CLL) and other hematological malignancies. Additionally, researchers presented data from studies of ibrutinib (IMBRUVICA®), an inhibitor of Bruton's tyrosine kinase (BTK), as a single-agent and in combination with other therapies in several hematologic malignancies, including CLL, mantle cell lymphoma (MCL), follicular lymphoma (FL), multiple myeloma (MM) and diffuse large B-cell Lymphoma (DLBCL). "The breadth and depth of the data we are presenting at ASH underscore our commitment to developing treatment options for people affected by blood cancers" said Michael Severino, M.D., executive vice president of research and development and chief scientific officer, AbbVie. "We have made significant progress in advancing our deep and robust pipeline and are excited to share the results of some of our key clinical trials".
Meeting abstracts are available at http://www.hematology.org/Annual-Meeting/Abstracts/.

www.abbvie.com

DR. REDDY'S ANNOUNCES THE COMPLETION OF FONDAPARINUX INTELLECTUAL PROPERTY PURCHASE

Dr. **Reddy's Laboratories** has announced that it has completed the purchase of worldwide exclusive intellectual property rights for Fondaparinux sodium, its generic anti-coagulant drug from its Australian partner, Alchemia Limited. Earlier, the company had signed a term sheet for this transaction in September, 2015. Alchemia's shareholders approved the sale of Fondaparinux at the Company's annual general meeting held on 10 November 2015, post which Dr. Reddy's and Alchemia have executed a purchase and sale agreement, together with various patent assignment deeds. Alchemia has received USD 17.5 million from Dr. Reddy's as consideration for the sale. The agreement is effective July, 2015.

www.drreddys.com

Virginia Tech Carilion Research Institute scientists gain insight in cause of Alzheimer's symptoms

Virginia Tech Carilion Research Institute scientists have uncovered a mechanism in the brain that could account for some of the neural degeneration and memory loss in people with Alzheimer's disease.

The researchers, together with scientists at the University of Alabama at Birmingham School of Medicine, discovered that a common symptom of Alzheimer's disease – the accumulation of amyloid plaques along blood vessels – could be disrupting blood flow in the brain. The results have been published in the journal Brain.

"We've always been interested in how glial cells interact with blood vessels," said Harald Sontheimer, director of the Center for Glial Biology in Health, Disease, and Cancer at the Virginia Tech Carilion Research Institute and senior author of the paper. "Astrocytes are the most populous cell type in the brain and even outnumber neurons."

Sontheimer also noted the importance of astrocyte function in the brain.

"Astrocytes serve many support functions, such as shuttling nutrients from blood vessels to nerve cells or removing their waste products," said Sontheimer, who is also the I. D. Wilson Chair in Virginia Tech's College of Science. "They also control the diameter of blood vessels to assure proper nutrient and oxygen delivery to the brain and maintenance of the blood-brain barrier. In response to injury and disease, however, astrocytes become reactive and change many of their supportive properties."

Sontheimer's team discovered that the astrocytes' blood flow regulation is disrupted by plaques formed of misfolded proteins around blood vessels. In a healthy brain, amyloid protein fragments are routinely broken down and eliminated.

The presence of amyloid proteins around blood vessels in the brain is a hallmark of Alzheimer's disease, yet it wasn't understood if the proteins did any harm. Now, Sontheimer's team has found that they do.

"We found that amyloid deposits separated astrocytes from the blood vessel wall," said Stefanie Robel, a research assistant professor at the Virginia Tech Carilion Research Institute and a coauthor of the paper. "We also found that these amyloid deposits form an exoskeleton around the blood vessels, a kind of cast that reduces the pliability of the vessels."

The exoskeleton is known as a vascular amyloid. Its inelasticity might result in lower blood flow, which could account for Alzheimer's symptoms, such as memory lapses, impaired decision-making, and personality changes.

"Vascular amyloid may be the culprit in Alzheimer's disease symptoms, especially considering that the amyloid exoskeleton might limit the supply of oxygen and glucose to the brain regions that need them most," Sontheimer said. "This could also explain the cognitive decline in people with Alzheimer's disease, as the disease is associated with reduced cerebral blood flow."

While the scientists don't fully understand the role of vascular amyloid in Alzheimer's disease, they now have a possible therapeutic target to study.
"It may be helpful to remove the deposits to allow for appropriate blood flow," Robel said. "The problem is we don't know. It might be harmful to remove vascular amyloid at late stages of the disease; maybe they're actually holding the vessels together."
The researchers' next step will be to examine blood vessels once the amyloid deposits are removed.
"Vascular amyloid is strangling the blood vessels," Sontheimer said. "By removing them, maybe we'll be able to restore blood flow regulation. Perhaps it'll turn out vascular amyloid is preventing further degeneration. Whatever the case, we'll certainly learn something new."
The Virginia Tech Carilion Research Institute joins the life science, physical science, computational science, informatics, engineering, and social science strengths of Virginia Tech with the medical education expertise of the Virginia Tech Carilion School of Medicine and the medical practice experience of Carilion Clinic.
Virginia Tech

EUR 60 MILLION INVESTMENT FOR SALTIGO
Specialty chemicals company **LANXESS** is investing around EUR 60 million in the expansion of the Leverkusen production facilities of Saltigo GmbH – a leading supplier in the field of exclusive synthesis. The biggest single investment in Saltigo since it was founded as a fine chemicals company in 2006 should sustainably strengthen the LANXESS subsidiary's market position. "Once again this year, we have many projects in the pipeline and see further growth potential" says Saltigo Managing Director Wolfgang Schmitz. This is why the LANXESS subsidiary is significantly expanding its multi-purpose production facilities in the Central Organics Pilot Plant (ZeTO). "This expansion will further expand our flexibility and also ensure in the future that Saltigo remains optimally positioned in the dynamic custom manufacturing market" adds Schmitz. "In the crop protection segment alone we anticipate annual market growth of 3 percent on average through 2025 despite weaker demand at the moment. To grow with our customers, we are expanding synthesis capacities for custom manufacturing in the ZeTO by around a third" says Schmitz. A part of these future capacities is already contractually secured. Saltigo will use a large share of this investment to add further reactors to its existing multi-purpose facilities and to construct two new solids isolation and drying lines. In addition, it will ensure an even more efficient raw material and solvent supply of the production facilities through the installation of a new container warehouse next to the plant. Planning also leaves scope for further expansion of this storage capacity. The complete facility will be equipped with a modern new process control system to combine the highest possible qualitative requirements with maximum productivity. The construction launch is scheduled for the middle of next year, while production should start at the end of 2017. The expansion should create 10 new jobs.
www.saltigo.com

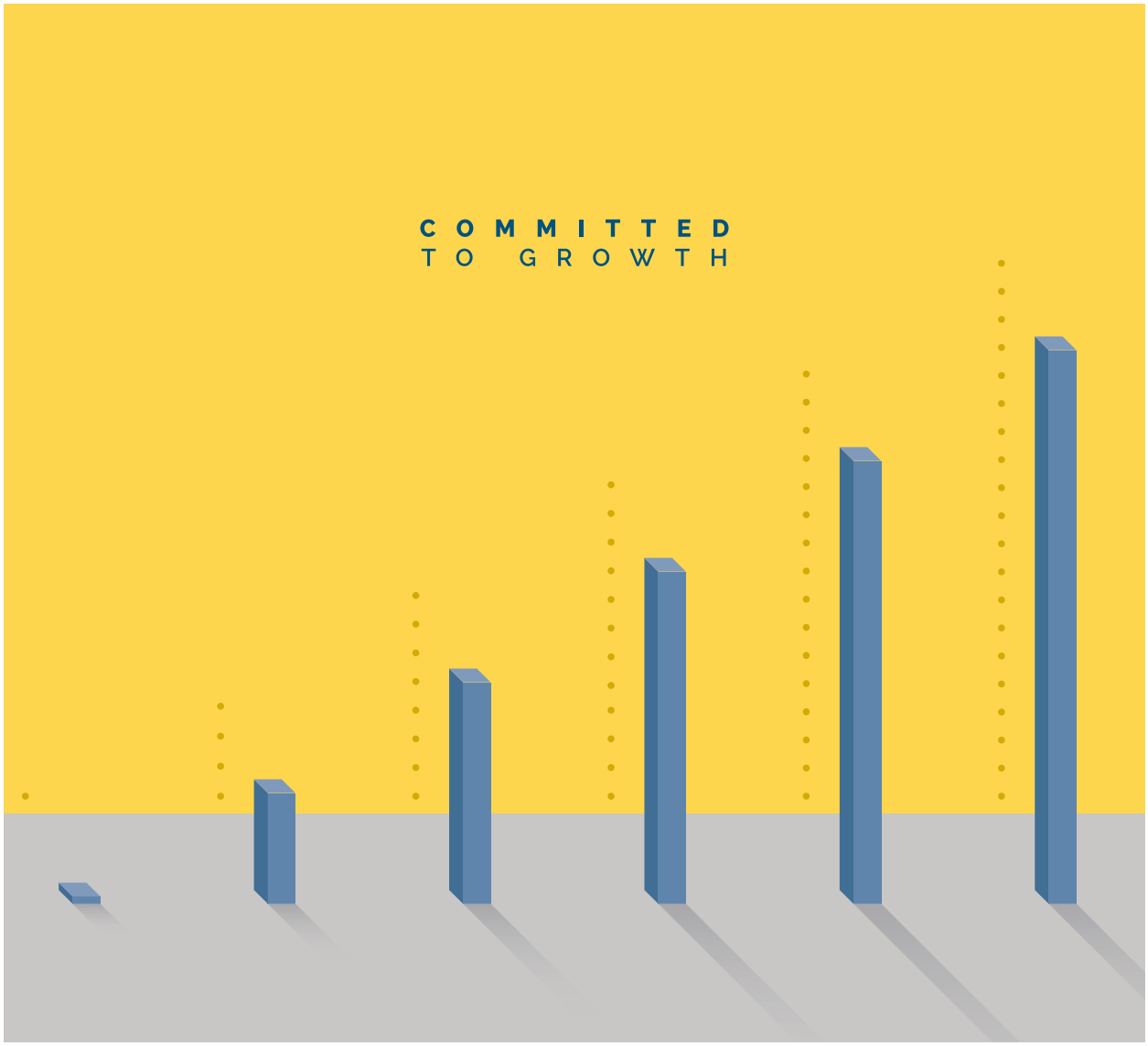

Growing is important. To us growing means to define new standards and to attain more and more advanced service performances. We are grateful to the companies that have cooperated with us through this journey and to those who will join us in the future. Challenges and new needs are to us, day after day, our starting points.

Ask for more.

JETPHARMA
Micronization Expertise

www.jetpharma.com

THOMAS HAHN, FABIAN HAITZ, SUSANNE ZIBEK*
*Corresponding author
Fraunhofer Institute for Interfacial Engineering and Biotechnology,
Nobelstraße 12, 70569 Stuttgart, Germany

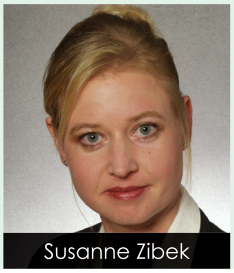
Susanne Zibek

PEER REVIEWED

Enzymatic hydrolysis of solid substrates
Critical notes and experimental guidelines for improvements

KEYWORDS: Design of experiments, experimental guidelines, enzyme optimization, solid substrate hydrolysis, lignocellulose, cellulase.

Abstract Optimization strategies of enzymatic reactions on solid substrates often suffer from unsystematic strategies and selection of unsuitable parameters. We present an efficient three-step guideline for optimization of enzymatic digestion processes taking the hydrolysis of cellulose by cellulases as an example. In the first step, intrinsic properties of the cellulases are addressed by the identification of optimal pH and temperature via design of experiments and subsequent evaluation. Process engineering parameters for the use of solid substrates greatly affecting the enzymatic reaction are further identified. These parameters are optimized in separate investigations and can be used for scale-up. The conclusive step contains the determination of product concentration with ongoing time, which can be performed in heterogeneous Michaelis-Menten approaches to achieve scientifically relevant data.

RELEVANT PARAMETERS FOR CELLULOSE HYDROLYSIS

Enzymatic solid substrate hydrolysis is, due to increased utilization of renewable resources, a major economic factor in biotechnology. Pretreatment, purification and succeeding enzymatic hydrolysis of the solid substrates are of great scientific and economic interest. But there are still many challenges to face including the minimization of enzyme amount which represents a large cost factor, for example in cellulose hydrolysis (1). Optimization of hydrolysis was often carried out software-assisted by using many parameters with unsuitable boundary conditions resulting in non-expressive values. The present manuscript addresses the optimization of a solid substrate hydrolysis in a three-step procedure. Simultaneously we focus on common mistakes performed and provide facts that attention should be paid on. This is elucidated using the example of cellulose hydrolysis.
On the one hand, enzyme performance can be improved by outside or extrinsic ascendancies which in general increase the accessible surface of the solid substrate.
To improve these extrinsic conditions ultrasound and microwave irradiation (2-4), non-conventional reaction media such as super-critical fluids, ionic liquids (5) or combinations (6) thereof are sequently or simultaneously applied. Further factors that are known to affect the accessibility of e. g. the cellulosic solid substrate to enzymatic hydrolysis like pore size, pore size distribution, lignin content (7) or the degree of polymerization and crystallinity (8) are likewise seen as extrinsic factors by the authors because these parameters are essentially determined by the pretreatment of the lignocellulosic material and cannot be affected strongly by the enzymatic hydrolysis process itself. Therefore these parameters can be supposed to be constant during optimization of cellulose hydrolysis for a specific substrate. Variation of the "intrinsic" reaction conditions like pH and temperature and "extrinsic" variables not resulting from pretreatment such as liquid ratio, enzyme-to-substrate ratio, initial particle size or stirrer velocity result in an optimization of the overall performance of the enzymatic hydrolysis.
One-factor-at-a-time methods for optimization of these variables are time- and resource intensive and are often not suitable to find the global optimum. Thus, new approaches were pursued to identify the overall optimum while decreasing number of trials. To decrease the extent of experimental approaches, design of experiments (DOE) was used. This statistical tool was also reported to be applied for cellulose hydrolysis by cellulases (9, 10). The parameters as well as the factor values applied are defined in DOE. Obtaining the results, analysis of variance (ANOVA) was performed in order to confirm the significance of the factors affecting the target size glucose yield. Response Surface Methodology (RSM) was applied to statistically analyze and model the linkage between the response or target size and variables. The aim was to quantify the correlation in the form of a polynominal equation to adjust variables for optimization. In applied science, knowledge about the empirical correlation between enzyme usage and product yield is more

important than kinetic parameters or Michalis-Menten kinetics. Above all, for the digestion of a solid substrate, as is the case for cellulose degradation by cellulases, determination of these parameters is hindered as process engineering conditions strongly affect kinetics. Within this article we want to provide useful modifications and information to achieve expressive results for the enzymatic degradation of a solid substrate using the example of cellulose digestion by cellulases. The authors focused on parameters that are in general significant for most of the solid substrate hydrolyses although from case to case special factors have to be added.

SOLID SUBSTRATE HYDROLYSIS PARAMETERS

Factors affecting cellulase activity in aqueous phase are temperature (T; °C), pH (pH; -), cellulase-to-cellulose (Enzyme-to-substrate, ETS; U/g_S) relation and incubation time (t; min). The target size, which is the magnitude that needs to be measured and optimized equates for example glucose yield per cellulose applied (P; gP/gS). Glucose yield varies in function of the variables and parameter conditions. With the help of these values a response-surface model can be determined. Equation 1 is an empirically determined first-order linear model without interaction that relates the value of the target size to the values of the variables mentioned. C_0 and C_i provide constants that accommodate the contribution of the term to the target size. Equation 2 displays a generalized form of the product yield as function of the variables (X) concerning significant interactions that contribute to the empirical determined relation.

Variable (T, pH, ETS, t) → Target size (P)

$$P = C_0+C_1\cdot T+C_2\cdot pH+C_3\cdot ETS+C_4\cdot t \quad (1)$$

General linear model

$$P = C_0+\sum_{i=1}^{k} C_iX_i+\sum_{i=1}^{k-1}\sum_{j=i+1}^{k} C_{ij}X_iX_i \quad (2)$$

We will focus on the provision of significant factors contributing to the efficacy of a solid substrate, respectively, cellulose hydrolysis provided in linear form (see equation 1). This was carried out to simplify and illustrate the derivation of the experimental guideline. In the specific case of cellulosic material digestion, two additional factors could be considered but were often lacking because they were underrated: The liquor ratio (S/L; g_S/mL) and the initial particle size. The liquor ratio describes the relation of the cellulose amount in the approach to the liquid applied. The particle size (c_S; mm or µm) directly affects the cellulose amount that is available at the freely accessible cellulose particle surface. Although these parameters are often disregarded, they greatly affect especially kinetic of the hydrolysis. The same applies to the stirring velocity (SV; rpm). The first-order model should be extended in this case to equation 3.

$$P = C_0+C_1\cdot T+C_2\cdot pH+C_3\cdot ETS+C_4\cdot t+C_5\cdot S/L+C_6\cdot SV+C_7\cdot c_S \quad (3)$$

Velocity of diffusional migration of the cellulose hydrolysis products into the bulk solution depends on the concentration gradient of the product from the pore or surface of cellulose particles to bulk liquid. Thus, after certain time of incubation at high solid-to-liquid ratios product concentration reaches high yields lowering the diffusion velocity. Furthermore, high solid-to-liquid-ratios generally increase viscosity and thus decrease cellulase activity due to diffusional restrictions. Investigations by Kirstensen *et al.* showed an inhibition of enzyme adsorption on the solid substrate by hydrolysis products during high-solids enzymatic hydrolysis that resulted in decreased yields (11). Commonly, ß-glucosidases would be applied to cleave the emerging cellobiose to glucose avoiding inhibitory concentrations. Activity of β-glucosidases would greatly depend on the number of coincidences between the enzyme and cellobiose, which is also decreased by high viscosity. Due to this knowledge, low solid-to-liquid ratios will therefore be advantageous. Additionally low solid-to-liquid ratios offer good separation properties and the solubility limit of the product generated is commonly not reached. Furthermore, migration of cellobiose and glucose from the boundary layer to the bulk liquid is accelerated by the means of a high concentration gradient. In contrary to this, high solid-to-liquid ratios up to 30 wt % or even higher are proposed in terms of efficiency or economy (11, 12). These thoughts should result in a compromise which has to be considered in the examination of RSM conclusions.

Increasing stirring velocity or shaking frequency is normally beneficial on an enzymatic reaction up to the point where shearing forces start to denature the enzyme. Otherwise, to define a range of investigation, the experimenter has to pay attention that appropriate mixing takes place and the enzymatic hydrolysis does not undergo diffusional limitations. Thus, a turbulent flow at low stirrer speed in a batch reactor would be suitable without the occurrence of water spouts. Laminar flow forces both cellulolytic enzymes and the substrates to move in an orbit perpendicular to the stirrer axis. As in cultivation of microorganisms, mixing time and hydrodynamics can be selected due to the appropriate choice of shaking frequency of different vessels (13, 14). The stirring velocity or shaking frequency is also a determining factor that affects the thickness of the laminar layer surrounding the cellulose particles. It is obvious that a smaller particle size increases homogeneity and provides a larger cellulose surface and thus a higher availability of the substrate for the cellulases. Additionally, minimization of the laminar layer results in a more rapid diffusion into the bulk solution. In terms of kinetics, the smaller the initial particle size the better it is. For later purification, the drawback consists of membrane blocking and low centrifugation efficiencies due to smaller particle size.

A STEP-TO-STEP PROCEDURE FOR IMPROVEMENT

A DOE concerning all relevant parameters for cellulase degradation leading to overall equation 3 results in numerous trials. Since the mentioned factors can be categorized, a sequential determination of different optima or parameters can be taken into account. The suggested step-to-step procedure is depictured in Figure 1 and would result in equation 4 and 5 that may be extended by interaction terms and heterogeneous Michaelis-Menten type kinetics (Equation 6).

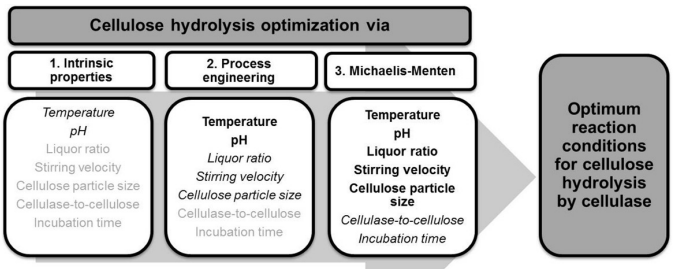

Figure 1. Optimization of enzyme reaction via succeeding process steps. Grey: Fixed factors; italic: Factors varied at the given process step; in bold: Fixed and already optimized or determined parameters.

$$P_1 = C_0+C_1 \cdot T+C_2 \cdot pH \quad (4)$$

$$P_2 = C_3+C_4 \cdot S/L+C_5 \cdot SV+C_6 \cdot c_S \quad (5)$$

$$P_3 = f(ETS, t) \quad (6)$$

Temperature and pH optima of the cellulase are intrinsic properties and therefore constant while varying other parameters. It has to be stated that the optimal activity at different pH and temperature conditions can vary from the optimal stability conditions of the enzymes. The decision which temperature or pH will be selected should consider high activity with sufficient stability. These main parameters largely affect the enzyme performance and therefore present the first step of the optimization. DOE and succeeding response-surface methodologies are suitable tools to find a global optimum in function of these parameters. One-factor-at-a-time methods often result in local optima and do not access interaction effects (15). In a more practical way of thinking, optimization of process engineering parameters via three factor DOE should succeed. It is suggested to perform the investigation of the intrinsic parameters previous to the process engineering parameters. Intrinsic parameters hold the property to be approximately invariant from other conditions. Extrinsic conditions can be adapted by the experimenter and can be adjusted in respect to the intrinsic parameters.
The fixation of the process engineering parameters also greatly affects prospective works especially scale-up procedures. Stirring velocity affects mixing time, power input, turbulence as well as Reynolds number and therefore presents a highly significant parameter for scale-up as provided by Schmidt for the scale-up of fermentation processes (16). To the best of the author's knowledge, process engineering parameters for the calculation of dimensionless numbers were only applied one time for the scale-up of cellulose hydrolysis with cellulases (12). It is obvious to mention, that all investigations already presented have to be carried out in cellulose excess. This corresponds to the expression that the cellulase always works under saturated conditions. Comparable and expressive results can only be obtained at time points succeeding initial hydrolysis period when concentration difference is at highest between two approaches (see Figure 2). Initially, the concentration difference is low and slightly varying ambient conditions or standard deviation within response analysis may impede the determination of significant differences between sets of different process conditions. If hydrolysis converges total conversion at given conditions, product formation rate is apparently lowered. This causes sensitivity problems of commonly applied assays for glucose determination and standard deviations exceed different glucose concentrations based on different parameter sizes. This results in miscalculation of the parameter significance. The authors thus advice to perform preliminary experiments to determine *raw* kinetics and suggest low incubation time for the experiments performed for block 1 and block 2 investigations. Since the end of the linear range often greatly differs concerning the time point of the experiments measuring product concentration at earlier time points would be suitable rather than at late incubation times.

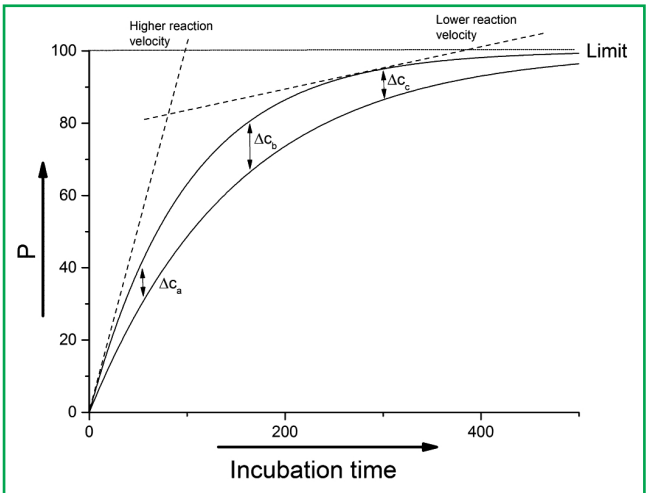

Figure 2. Glucose concentration in function of incubation time (min). Absolute yield (%) difference between two cellulose hydrolysis approaches applying different conditions is low at the beginning and at time points when conversion is finished.

For determination of optimum incubation time, progress of glucose or cellobiose concentration was measured. Kinetic measurements only apply for the given conditions and should thus present the last step of optimization. It is suggested, that the recording of glucose concentration with ongoing incubation time at varying cellulase-to-cellulose relations can be used for the preparation of overall Michaelis-Menten kinetics (17). This has the advantage, that the kinetic is investigated for the already optimized system that will also be applied in prospective works. Furthermore, kinetic values as K_M and v_{max} are investigated with that experiment enabling to gain scientifically relevant data and conclusions can be drawn with respect to an economic application of the cellulolytic enzymes.

As the results indicate, more preliminary studies need to be performed in order to find the right conditions resulting in significant factors. In common, it is suggested to find optimal pH and temperature for enzyme activity in one solely DOE approach, since optima pH depends from temperature and vice versa. They can be defined as determinant or intrinsic factors. Especially in enzymatic hydrolysis of solid substrates, as cellulose, evaluation of process engineering parameters is advisable in a successive step. These factors do not influence the work or activity of the cellulase itself, but do alter availability of substrate, diffusion and so on. It is stated that these parameters should be paid more attention in prospective works since these are reactions with large economic impact and of high scale-up relevance. It is advised to carry out heterogeneous Michaelis-Menten kinetics succeeding to the process engineering parameters. In the case of combined cellulase and glucosidase application, an overall kinetic can be identified, whereas the relative amount of enzymes used has to be previously optimized.

ACKNOWLEDGMENTS

The authors would gratefully like to thank PD Dr. Steffen Rupp and Prof. Dr. Thomas Hirth for constructive discussions, helpful advices and the opportunity to perform the studies resulting in this publication.

REFERENCES AND NOTES

1. Singhvi, M.S., Chaudhari, S., Gokhale, D.V. "Lignocellulose processing: a current challenge", *Rsc Advances*, 4 (16), 8271-8277 (2014)
2. Rufino, A.R., Biaggio, F.C., Santos, J.C., et al. "Screening of lipases for the synthesis of xylitol monoesters by chemoenzymatic esterification and the potential of microwave and ultrasound irradiations to enhance the reaction rate", *International Journal of Biological Macromolecules*, 47 (1), 5-9 (2010)
3. Zhongdong, L., Yongmei, Y., Hui, et al. "Study on technology of ultrasound-microwave assisted improves preparation of porous starch", *Advanced Materials Research*, 476-478 744-750 (2012)
4. Uluko, H., Zhang, S.W., Liu, L., et al. "Effects of microwave and ultrasound pretreatments on enzymolysis of milk protein concentrate with different enzymes", *International Journal of Food Science and Technology*, 48 (11), 2250-2257 (2013)
5. Sheldon, R.A., Van Rantwijk, F., Lau, R.M., *Biotransformations in ionic liquids: An overview*, in *Ionic Liquids as Green Solvents: Progress and Prospects*, R.D. Rodgers and K.R. Seddon, Editors. 2003, Amer Chemical Soc: Washington. p. 192-205.
6. Wang, Y., Pan, Y., Zhang, Z.Q., et al. "Combination use of ultrasound irradiation and ionic liquid in enzymatic isomerization of glucose to fructose", *Process Biochemistry*, 47 (6), 976-982 (2012)
7. Mooney, C.A., Mansfield, S.D., Touhy, M.G., et al. "The effect of initial pore volume and lignin content on the enzymatic hydrolysis of softwoods", *Bioresource Technology*, 64 (2), 113-119 (1998)
8. Mansfield, S.D., Mooney, C., Saddler, J.N. "Substrate and enzyme characteristics that limit cellulose hydrolysis", *Biotechnology progress*, 15 (5), 804-816 (1999)
9. Ezhumalai, S., Thangavelu, V. "Kinetic and optimization studies on the bioconversion of lignocellulosic material into ethanol", *Bioresources*, 5 (3), 1879-1894 (2010)
10. Ruangmee, A., Sangwichien, C. "Response surface optimization of enzymatic hydrolysis of narrow-leaf cattail for bioethanol production", *Energy Conversion and Management*, 73 381-388 (2013)
11. Kristensen, J., Felby, C., Jorgensen, H. "Yield-determining factors in high-solids enzymatic hydrolysis of lignocellulose", *Biotechnology for Biofuels*, 2 (1), 11 (2009)
12. Ludwig, D., Michael, B., Hirth, T., et al. "High Solids Enzymatic Hydrolysis of Pretreated Lignocellulosic Materials with a Powerful Stirrer Concept", *Applied Biochemistry and Biotechnology*, 172 (3), 1699-1713 (2014)
13. Kato, Y., Hiraoka, S., Tada, Y., et al. "Mixing time and power consumption for a liquid in a vertical cylindrical vessel, shaken in a horizontal circle", *Chemical Engineering Research & Design*, 74 (A4), 451-455 (1996)
14. Peter, C.P., Suzuki, Y., Rachinskiy, K., et al. "Volumetric power consumption in baffled shake flasks", *Chemical Engineering Science*, 61 (11), 3771-3779 (2006)
15. Farinas, C.S., Loyo, M.M., Baraldo Junior, et al. "Finding stable cellulase and xylanase evaluation of the synergistic effect of pH and temperature", *New Biotechnology*, 27 (6), 810-815 (2010)
16. Schmidt, F.R. "Optimization and scale up of industrial fermentation processes", *Applied Microbiology and Biotechnology*, 68 (4), 425-435 (2005)
17. Michaelis, L., Menten, M.L. "The kinetics of invertin action", *Febs Letters*, 587 (17), 2712-2720 (2013)

Realigning the Fine Chemicals Division
for increased customer access to unmatched complex chemistry capabilities

Johnson Matthey Fine Chemicals supplies efficient and sustainable products and services for companies developing pharmaceuticals, agrochemicals and other fine and specialty chemicals.

The division has developed a diverse range of innovative chemistry capabilities and pharmaceutical manufacturing technologies across its 11 global sites since the first facility was founded in Scotland 200 years ago. These include catalysis and chiral technologies, world-leading opiates and narcotics, global API development, life cycle management and manufacturing facilities.

The company recently rebranded the Fine Chemicals Division to realign these capabilities into four core offerings: Custom Pharma Solutions, Controlled Substances, Catalysts and APIs & Life Cycle Management, forming a more cohesive Fine Chemicals brand. The realignment aims to increase access for customers to the company's complex chemistry capabilities and differentiating technologies. It will also enhance collaboration and knowledge sharing between the core offerings, helping to advance product development and bring even more value to customer projects.

The Custom Pharma Solutions offering provides a full range of bespoke drug development, scale-up and manufacturing services, through pre-clinical and toxicological studies, to development and commercial manufacturing. The company's expert teams can solve the most challenging chemistry and scale-up problems, bringing a unique blend of deep R&D knowledge and large-scale global capabilities.

Johnson Matthey Fine Chemicals' Controlled Substances are extensively used in therapeutic classes including analgesia, CNS disorders and anti-addiction treatments. With state-of-the-art poppy production facilities for key opiate raw materials as well as GMP-compliant bulk production plants, Johnson Matthey Fine Chemicals provides customers with assured security of supply for all their controlled substance requirements.

Through the APIs & Life Cycle Management offering, Johnson Matthey Fine Chemicals provides customers with broad technologies, an extensive API portfolio and a network of compliant facilities for collaborative working and API development. The company has products expertise covering a wide range of therapeutics classes such as anti-cancer, anti-rheumatic, addiction, psychiatric disorders and ophthalmic indications.

The unmatched Catalysts offering includes a high technology portfolio of heterogeneous and homogeneous catalysts, chiral and biocatalysts that can be applied for developing smarter ways to enable chemistry and optimise customers' processes. Global technical teams have market leading expertise offering the best solution with efficient and sustainable chemistry.

Johnson Matthey Fine Chemicals draws on its significant industry experience, large portfolio of specialist technologies and deep knowledge to provide customers with expert solutions, optimising their chemical processing requirements. Ultimately, accelerating customers' innovation and ensuring reliable commercial supply of their API, intermediates and catalyst requirements.

Johnson Matthey Fine Chemicals
28 Cambridge Science Park,
Milton Rd, Cambridge, CB4 0FP, UK
Email: Finechemicals@matthey.com
http://jmfinechemicals.com

Johnson Matthey

Fine Chemicals

Fine Chemicals

REALISE YOUR
TRUE POTENTIAL AT
INFORMEX BOOTH 533

Custom Pharma Solutions

Controlled Substances

APIs & Life Cycle Management

Catalysts

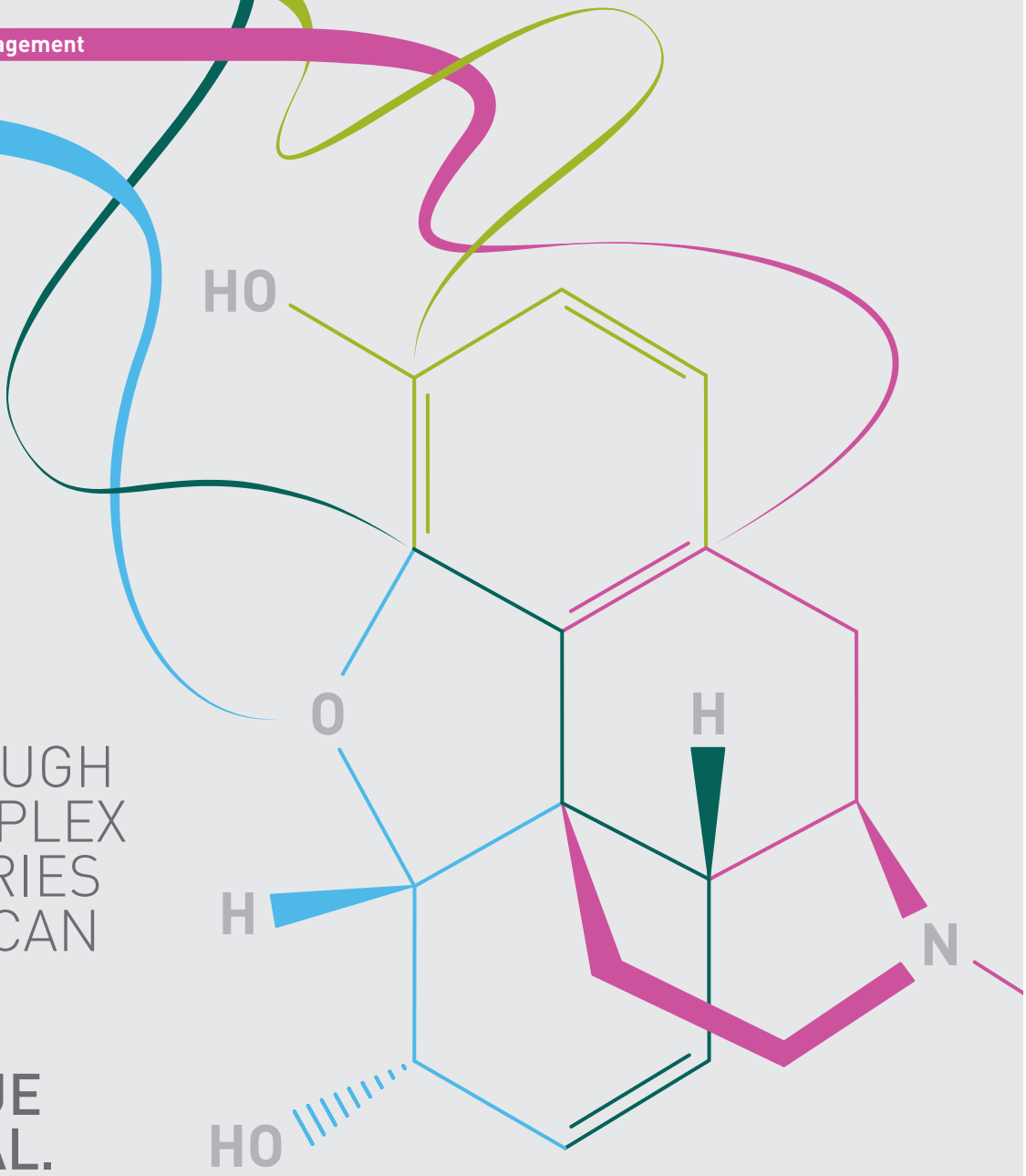

IT'S THROUGH OUR COMPLEX CHEMISTRIES THAT WE CAN HELP YOU REALISE **YOUR TRUE POTENTIAL.**

Johnson Matthey Fine Chemicals combines our proven specialist expertise and 200-year heritage, to deliver a collaborative service offering focused on strengthening your products to ensure they get to market more efficiently. Built around core offerings of Custom Pharma Solutions, Controlled Substances, Catalysts, APIs & Life Cycle Management and using our complex chemistries, we're ensuring that your goals aren't just met, but surpassed.

To discover your true potential, visit JMFineChemicals.com or email us at FineChemicals@matthey.com

JM
Johnson Matthey

OLGA O. BABICH*, ALEXANDER YU. PROSEKOV,
LYUBOV S. DYSHLYUK, SVETLANA A. IVANOVA
*Corresponding author
Kemerovo Institute of Food Science and Technology,
Department of Bionanotechnology
47 Stroiteley Boulevard, 650056, Kemerovo, Russian Federation

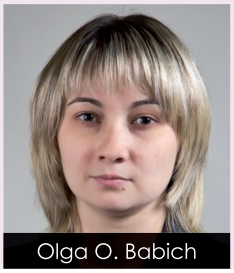
Olga O. Babich

Investigation of kinetic aspects of L-phenylanine ammonia-lyase production in pigmental yeast

Kinetic aspects of L-phenylanine production

KEYWORDS: enzyme, L-phenylalanine ammonia lyase, pigmentary yeast Aureobasidium pullulans, kinetics, biosynthesis, product yield, Luedeking-Piret kinetic equation.

Abstract A model of a continuous L-phenylalanine ammonia-lyase (PAL) fermentation process by Aureobasidium pullulans (Y863) pigment yeast strain was developed. As a basis of the kinetic model, differential equations of Luedeking-Piret model combined with Monod were used. It was found that the kinetic growth of Aureobasidium pullulans (Y863) and synthesis of PAL were carried out not only in case of decrease of phenylalanine content in the substrate, but also in the course of biosynthesis of the desired product. As an effective criterion of the biokinetics' selected performance, the PAL target product was selected, determined by the quantity of the substrate stream and the concentration of the target product in the culture medium. The obtained dependencies of the phenylalanine concentration in the nutrient solution for every fixed value of the feed stream have a unified dynamics of change. The obtained kinetic dependences can be used for both qualitative and quantitative characteristics of the process in the development of PAL production technology.

INTRODUCTION

The issue of use of enzymes in different areas of the economy has attraced a lot of interest from around the world, making the search for novel commercial primary sources particularly important.
L-phenylalanine ammonia-lyase (PAL, EC 4.3.1.5) is one of the enzymes that can be used in various medical applications, i.e. for direct phenylketonuria therapy, in high-grade phenylalanine-free food manifacture, and for malignant cells growth inhibition (1,2). In addition, this enzyme can be used for L-phenylalanine production in biotechnology using trans-cinnamic acid (3).
L-phenylalanine ammonia-lyase belongs to the family of lyases catalyzing the reaction of the nonoxidative deamination of L-phenylalanine with the formation of trans-cinnamic acid and free ammonium ion.
In most cases, PAL molecule has a molecular weight ranging from 300 to 340 kDa (4). According to various researchers, there are exceptions to this rule: molecules with molecular weight of 152 kDa, 226 kDa, 250 kDa, 560 kDa.
Conformations of PAL, isolated from different sources, are more or less spherical (5). Usually, L-phenylalanine ammonia-lyase is a homotetrametric protein consisting of four identical subunits.

PAL activity is found in algae (6), actinomycetes and 12 wood-destroying species of Basidiomycetes (7). Among the microorganisms having PAL-activity, there are several strains of red yeast Rhodotorula, Rhodosporidium and Sporobolomyces (8), and two representatives of actinomycetes which are producers of mitomycin (9). PAL was not found in bacteria.
PAL is common in natural sources (beans, parsley, sweet potatoes, etc.) (10-14). In plants, the highest level of PAL was detected in Pteridium aguilinum fern. In most plants, PAL is coded by the region of 3-5 genes. The exception is the sequence of PAL in potatoes, which consists of 40-50 genes. In most cases, the size of the genes is in the range from 2.1 to 2.4 kDa.
Typically, PAL does not require metal ions, although there is evidence of a weak influence of Mg^{2+} and Ba^{2+} ions on PAL activity. A wide range of compounds, such as carbonyl, thiol or sulfhydryl reagents, phenolic acids or heavy metal ions, can cause the suppression of activity of PAL. In most cases, PAL is sensitive to synthetic inhibitors, such as (S)-2-aminooxy-3-phenylpropanoic acid, (R)-(1-amino-2-phenylethyl)phosphonic acid and 2-aminoindan-2-phosphonic acid; such inhibitors are often used to block the biosynthesis of phenolpropanoid components in plant cells and tissues (5, 15).
Studies aiming to identify novel biotechnological approaches

to L-phenylalanine ammonia-lyase production attracts researchers' interest (16). Data on L-phenylalanine ammonia-lyase activity among microorganisms (32 strains) is also available (17).
A number of papers are dedicated to the study of the conditions of PAL formation in yeast cells. PAL activity was not detected in the intact yeast cells (18).
PAL activity was detected in yeasts cultured on natural and synthetic media. Maximum formation of PAL in different yeast genera and species was found in the presence of L-phenylalanine, L-tyrosine, L- and DL-isoleucine (19-25).
Currently, one of the limiting factors for using biotechnological systems in PAL production is the lack of theoretical approaches for analysis and interpretation of experimental data. Mathematical simulation the biotechnology processes used a set of kinetic equations, describing the processes of fermentation. A simplified model of Luedeking-Piret (26):

$$\frac{dX}{dt} = \mu X \qquad (1),$$

$$\frac{dP}{dt} = \alpha \frac{dX}{dt} + \beta X \qquad (2),$$

in conjunction with the equation

$$\frac{dS}{dt} = -\gamma \cdot \frac{dX}{dt} \qquad (3),$$

with the initial conditions $X(0)=X_0$, $P(0)=0$, $S(0)=S_0$, where $X=X(t)$ is biomass concentration at time point t (g/l), $P=P(t)$ is the concentration of the target product at time point t (g/l), $S=S(t)$ is the substrate concentration at time point t (g / l), μ, α, β, γ are process parameters. Based on the mathematical meaning of equations (1) - (3), the parameters μ, β are defined as the intensity with the dimension of the inverse time, and α, γ are constants.
Parameter is generally interpreted as a specific rate of growth of biomass and determined by Monod model, as a function of substrate concentration limit (27):

$$\mu = \frac{\mu_{\max} S}{K_s + S} \qquad (4),$$

where μ_{max} is the maximum specific growth rate of biomass (h^{-1}), K_S is the saturation constant or Monod constant (g/l).
Linear differential equations of the types (1) - (3), in a first approximation, describe a rather wide class of real processes, therefore the qualitative level of the model is always valid, but its quantitative results should be confirmed each time.
It should be noted that stochastic modeling methods (the so-called processes of birth and death), according to their methods and approaches, lead to the same equations with their own interpretations of the parameters and dimensions of conservation (28-31).
Kinetic equations are used for description of the biosynthesis process of microorganisms of various strains, including pigmented yeasts. The papers in which modeling was employed were studied: ethanol production by *Saccharomyces cerevisiae* mutant strain (32,33), *Candida Pseudotropicalis* strain (34), *Aureobasidium pullulans* strain (35); lipase synthesis by *Candida rugosa* yeasts (36) and Aureobasidium pullulans polysaccharides strain (37-41).
The purpose of the study was the development of a technology for producing L-phenylalanine ammonia-lyase by pigmented yeast based on the kinetic model, the parameters of which take into account the impact of various factors of biotechnological process, both individually and in conjunction.

MATERIALS AND METHODS

Microorganisms

The present study was conducted with the pigmented yeast strain *Aureobasidium pullulans (Y 863)* from the Russian National Collection of Industrial Microorganisms of FSUE GosNIIGenetika (Federal State Unitary Enterprise State Scientific and Research Institute for Genetics).

Chemicals

All the chemicals used in this study were obtained from the Institute of Biotechnology of Kemerovo Institute of Food Science and Technology (University), Kemerovo, Russia: Bacto-agar, yeast extract (Difco, USA); D-glucose; peptone (Merck, Germany); L-phenylalanine ammonia-lyase (Sigma, USA); L-phenylalanine (Acros Organics, Belgium).

Media and culture conditions

The pure culture was cultured for 24 hours at 26°C in agarized layer containing medium. The prepared samples were stored at 4°C.
Culture medium (according to the passport of GosNIIGenetika) included yeast extract (5.0 $g \cdot l^{-1}$), glucose (20.0 $g \cdot l^{-1}$), peptone (10.0 $g \cdot l^{-1}$); pH of the nutrient medium after the addition of all the components was 7.0 and thus was unregulated. Culture medium was prepared by the preliminary sterilization in autoclave at 121°C, pressure of 1 atm and 0.5 atm, during 1 and 0.5 h respectively for a solution of peptone and salts, and yeast extract solution.
The inoculum in volume of 5.0 ml was transferred to the flask with 100 ml of medium of the same composition. The flasks were incubated at 26°C in a shaker incubator LSI-3016A / LSI-3016R (Daihan Labtech, India) with a speed of 250 rpm in unregulated pH mode (initial pH is 7.0). After 20 h of incubation period, the culture was centrifuged at 6000 rpm (cooling centrifuge SIGMA 3-16PK (Sigma, USA)) for 40 minutes at 4°C. The final concentration was adjusted to 10^7 - 10^8 cells per ml.
Deep culturing of a pure culture was performed using Biostat A plus MO fermenter, (Sartorius, Germany) containing 5 l of fermentation broth at 26°C. Sterile syringes and needles were used for sampling during fermentation without breaking the tightness of the fermenter. Measurements were made of the following indicators samples: concentrations of biomass, phenylalanine and PAL.
The biomass concentration was measured with UV-1800 spectrophotometer (Shimadzu, Japan) by the absorption of light at 540 nm, followed by recalculation on the weight of dry biomass. The biomass of the cells dry matte was measured gravimetrically. The cells were pelleted at Buprog filters (pre-boiled) with a pore size of 0.24 microns, washed, dried at 80°C, and weighed.
Protein concentration was determined spectrophotometrically by absorbance at 260 nm and 280 nm by Warburg and Christian method. For calculations, the following formula was used:
Protein concentration (mg/ml) = $1.55 \times OD_{280} - 0.76 \times OD_{260}$, where OD is optical density.
In purified preparations (after chromatography), the absorbance at 280 nm was used to calculate PAL solution at

the concentration of 1 mg·ml^{-1} which had the optical density of 0.49. This factor was calculated by PAL BioEdit software based on its primary amino acid sequence.

Mathematical modeling

The process of continuous culturing of pigment yeast was described by kinetic model which was obtained based on Luedeking-Piret model for batch culture. The process was arranged in such a way that the same initial conditions were provided at any time; it was considered that the conditions of stationary process were formed, where (42)

$$\frac{dX}{dt}=0 \quad \frac{dP}{dt}=0 \quad \frac{dS}{dt}=0 \qquad (5).$$

Considering that the fermentation process was accompanied by presence of a constant incoming flow of substrate and biomass withdrawn, and the final product, from the equations (1) - (3), was as follows:

$$\frac{dX}{dt}=\mu X-DX \quad \frac{dP}{dt}=(\alpha\cdot\mu+\beta)X-DP \quad \frac{dS}{dt}=-\gamma\cdot\mu\cdot X+D(S_0-S) \qquad (6)$$

where D is the flow rate, h^{-1}; $\gamma=1/Y_{x/s}$, $Y_{x/s}$ is biomass yield based on phenylalanine utilized (g·g^{-1}).
Considering the presence of biosynthesis inhibition of the target product by the substrate concentration, one component of the nutrient medium (limiting component) isolated, that influenced the growth rate of the microorganisms biomass. Other components of the culture medium were regarded as being in excess with respect to consumption. The system of equations was obtained from the equations (6) and conditions (4), (5) , which took into account the inhibition of substrate concentration:

$$\mu_{max}\frac{S}{Ks+S}X-DX=0 \qquad (7),$$

$$\left(\alpha\cdot\mu_{max}\frac{S}{Ks+S}+\beta\right)X-DP=0 \qquad (8),$$

$$-\gamma\cdot\mu_{max}\cdot\frac{S}{Ks+s}X+D(S_0-S)=0 \qquad (9),$$

with the independent variable D or S_0.

Computations and data analyses

Each experiment was performed in triplicate. The considered characteristics were determined as average values of the obtained samples; PAL performance during the fermentation period was calculated using them. The model parameters were determined from the experimental data at periodic cultivation for 24 hours (Table 1). The parameter values were determined and refined in Excel 2007 (Microsoft). The parameter μ_{max} was interpreted as the maximum specific growth rate of biomass, which is typical for a limited time span of an exponential growth phase. The equations of lines, passing through any two points of the experimental curve, were written out for this purpose. Considering the physical meaning of the derivative from the obtained angular coefficients of the lines (Table 2), the one with the greatest value was chosen. This value was set to the maximum specific rate. The maximum deviation from the relationship between the experimental and theoretical values and the experimental value was multiplied by 100% of the estimated modeling error. The accuracy of the mathematical model, obtained according to the experimental results, was analyzed employing variance analysis (ANOVA).

The system of equations (7) - (9) was solved using Mathematica software (for Students Versions 5.2.0, Wolfram Research Inc).

RESULTS AND DISCUSSION

The data was obtained from culturing pigment yeasts *Aureobasidium pullulans (Y 863)* with different initial concentrations of phenylalanine (Figures 1-2). The model parameters (7) - (9) are shown in Table 1. The greatest specific growth rate was chosen from the values given in Table 2. The stability trend in the reduction of the growth rate of the biomass was observed in the following ranges. The average share value of the resulting protein per unit of the formed biomass of pigmented yeasts strain while culturing was γ=1.69g/g, not only for the studied one, but also for other types of pigmented yeast. The existence terms of the system solution (7) - (9) are formulated in the study (43). In our case, they satisfy only one of the three solutions found by numerical methods.

μ_{max}	α	β	K_s	@=1/$Y_{x/s}$
1.856	2.10	0.80	320.0	1.69

Table 1. Parameter values for the kinetic model of *Aureobasidium pullulans (Y 863)*.

$t_i - t_{i+1}$	0.0-0.5	0.5-1.0	1.0-1.5	1.5-2.0	2.0-2.5	2.5-3.0	3.0-3.5	3.5-4.0	4.0-4.5	4.5-5.0
k	0	-0.313	-0.228	0.124	0.426	1.856	1.655	1.098	1.096	0.583

Table 2. Slope values of the tangent to the experimental curve over time intervals of batch cultivation of *Aureobasidium pullulans (Y 863)*.

From Figure 1 and Figure 2 follows that in terms of the magnitude of flow 0.50 and 0.25 h^{-1}, product concentration PAL (curve 2) changes ambiguously. In the first case, the interval of values were observed in the phenylalanine concentration of the substrate in which the concentration of PAL increases (reaches maximum 200 g·l^{-1}) and decreases (up to 40 g·l^{-1}). In the second, after the growth, the concentration stabilized at the value of 135 g·l^{-1}, and further increase of the phenylalanine concentration (more than 80 g·l^{-1}) in the substrate was not required. Regardless of the magnitude of the flux values, it is evident that for the biokinetics process of the considered arrangement method, the phenylalanine concentration in the substrate should not exceed 80 g·l^{-1}. The value analysis of the biomass concentration suggests that the concentration of phenylalanine in the culture fluid, practically, has no restraining effect, especially at concentrations not exceeding 80 g·l^{-1}. Termination of biomass growth *Aureobasidium pullulans (Y 863)* with the flux value of 0.25 h^{-1} and 0.5 h^{-1} occurred at the concentration of phenylalanine in the substrate of 40-60 g·l^{-1}, indicating that it limits the impact. A similar trend was observed for the biosynthesis of the desired product only at the substrate concentration of 80 – 100 g·l^{-1}. Comparing the values of theoretical and experimental values, it is possible to note a good enough match for the substrate concentration (the error rate of not more than 4%) and worse for the biomass concentration and the concentration of the desired product (up to 25%), especially with the increase of the concentration of phenylalanine in the substrate to more than 100 g·l^{-1}. This indicates that the used model parameters do not completely describe the process in question. At the same time, the selected Luedeking-Piret model in combination with Monod equation describes the biosynthesis processes trends,

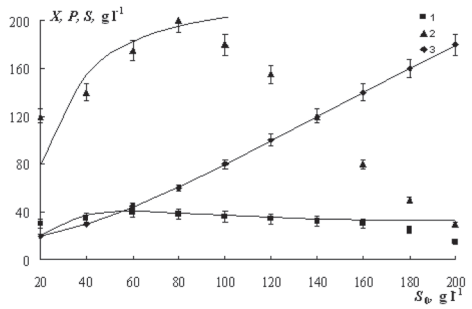

Figure 1. Dependencies between Biomass (1), Product Concentration (2) and Substrate Concentration (3), and Substrate Flux Concentration (S_0) for Flux Magnitude D = 0.50 h^{-1}.

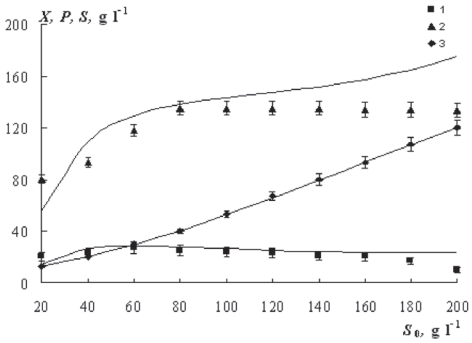

Figure 2. Dependencies between Biomass (1), Product Concentration (2) and Substrate Concentration (3), and Substrate Flux Concentration (S_0) for Flux Magnitude D = 0.25 h^{-1}.

but for quantitative description, the refinement by means of the introduction of additional parameters is required, as the factors limiting the formation of the desired product and biomass were not taken into account. There are known works (35,37–40) which studied the biokinetics of pigmented yeast by modeling the process of periodic and/or continuous culturing employing the modified Luedeking-Piret model. Relevant findings indicate either a good match of the experimental and model data or a qualitative description of the process of establishing the laws of the process, while others used models giving a better quantitative description without demonstration of the mechanisms. No works from the mentioned above doscussed the aspects of PAL pigmented yeast production, which are the subject of this work. Comparison of the parameter values found and obtained in other papers is quite problematic, since they are consistent with models of different processes. As a result, the additional studies and further development of the model and obtaining a better understanding of PAL pigmented yeasts mechanisms in the fermentation process are required.

Further study of continuous fermentation process of PAL pigmented yeast *Aureobasidium pullulans (Y 863)* corresponds to the study of its productivity Q_p with different methods of arrangement, i.e., depending on the incoming stream with phenylalanine of 20 and 40 g·l^{-1}:

$$Q_p = D \cdot P \qquad (10)$$

The results are shown in Figure 3. The curves corresponding to the concentration of the incoming flow of 80 and 120 g·l^{-1}, demonstrated uniform behavior: they reached single maximum (14.8 и 14.4 g·(l·h)$^{-1}$) in the range of the incoming flow of 0.4 – 0.5 and 0.4 – 0.6 h^{-1} respectively. A further increase in the quantity of flow at a fixed concentration of phenylalanine leads to a decrease in the performance primarily by reducing the rate of formation of the desired biosynthesis product (PAL). A similar picture is preserved at other concentrations of phenylalanine in the stream. The highest productivity in each case has the minimal value corresponding to one of the quantity values of flow from the range 0.1 – 0.6 h^{-1}.

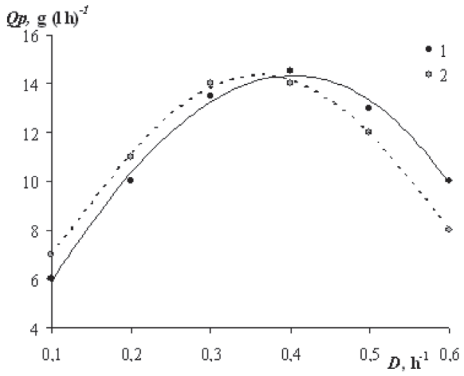

Figure 3. Dependences of Productivity on Flux Mmagnitude at Various Substrate Concentrations in the Flux: 1 – S_0 =80 g·l^{-1}, 2 – S_0 =120 g·l^{-1}.

CONCLUSIONS

The obtained model provides a specific understanding of the various factors that influence the kinetics of growth, phenylalanine consumption and PAL production by

Aureobasidium pullulans (Y 863) during continuous fermentation. From the parameters analysis and the model itself, it follows that the biomass growth and formation of the desired fermentation product (PAL) depends not only on the quantitative characteristics of the substrate, but is apparently limited by the content of the desired product in the culture medium. For the concentration of the substrate (phenylalanine) in the incoming flow, such dependence cannot be traced. It was established that when changing the quantity of flow from 0.5 to 0.25 h^{-1}, the target pattern of accumulation of product changes, and its greatest value decreases. The highest concentration was achieved when the flow rate was 0.5 h^{-1}. The increase of the concentration of phenylalanine in the incoming stream of more than 100 $g \cdot l^{-1}$ did not increase the quantity of the target biosynthesis product and performance of the process.

The kinetic model described in this study can be used for forecasting the efficiency of the process of L-phenylalanine-ammonium-lyase biosynthesis by cultivation of pigment yeast using continuous method of arrangement thereof, depending on both initial concentration of phenylalanine in the culture solution and the intensity of the substrate inflow (feed of phenylalanine into the fermenter).

Also, the proposed kinetic model can be used for regulating the output of the end product (L-phenylalanine-ammonium-lyase) by way of changing the parameters of the process of continuous cultivation of pigment yeast.

Furthermore, the proposed kinetic model can be used for computation of the main parameters of a continuous biotechnology process of L-phenylalanine-ammonium-lyase production with the use of pigment yeast: biomass, substrate concentration, product concentration, concentration of substrate in the flow, flow rate, production performance.

REFERENCES AND NOTES

1. Sarkissian CN, Shao Z, Blain F, et al. "A different approach to treatment of phenylketonuria: phenylalanine degradation with recombinant phenylalanine ammonia lyase", Proc Natl Acad Sci U S A, 96 (5), 2339–44 (1999).
2. Sarkissian CN, Gámez A. "Phenylalanine ammonia lyase, enzyme substitution therapy for phenylketonuria, where are we now?" Mol Genet Metab, 86(1), 6-22 (2005).
3. Evans CT, Hanna K, Payne C, et al. "Biotransformation of trans-cinnamic acid to l-phenylalanine: Optimization of reaction conditions using whole yeast cells", Enzyme Microb Technol, 9(7), 417–21 (1987).
4. Jiang Y, Joyce DC. "ABA effects on ethylene production, PAL activity, anthocyanin and phenolic contents of strawberry fruit", Plant Growth Regul, 39(2), 171–4 (2003).
5. Appert C, Logemann E, Hahlbrock K, et al. "Structural and catalytic properties of the four phenylalanine ammonia-lyase isoenzymes from parsley (Petrosselinum crispum Nym.)", Eur J Biochem, 225(1), 491–8, (1994).
6. Heo JW, Kang DH, Bang HS, et al. "Early growth, pigmentation, protein content, and phenylalanine ammonia-lyase activity of red curled lettuces grown under different lighting conditions", Korean J Hortic Sci Technol, 30(1), 6–12, (2012).
7. Kim SH, Kronstad JW, Ellis BE. "Induction of phenylalanine ammonia-lyase activity by tryptophan in Ustilago maydis", Phytochemistry, 58(6), 849–57, (2001).
8. MacDonald MJ, D'Cunha GB. "A modern view of phenylalanine ammonia lyase", Biochem Cell Biol, 85(3), 273–82, (2007).
9. Calabrese JC, Jordan DB, Boodhoo A, et al. "Crystal structure of phenylalanine ammonia lyase: Multiple helix dipoles implicated in catalysis", Biochemistry, 43(36), 11403–16. (2004)
10. Dixon R, Paiva N. "Stress-Induced Phenylpropanoid Metabolism", Plant Cell, 7(7), 1085–97, (1995).
11. Alunni S, Cipiciani A, Fioroni G, et al. "Mechanisms of inhibition of phenylalanine ammonia-lyase by phenol inhibitors and phenol/glycine synergistic inhibitors", Arch Biochem Biophys, 412(2), 170–5, (2003).
12. Allwood EG, Davies DR, Gerrish C, et al. "Phosphorylation of phenylalanine ammonia-lyase: Evidence for a novel protein kinase and identification of the phosphorylated residue", FEBS Lett, 457(1), 47–52 (1999).
13. Kuliyeva SV, Gyul'akhmedov SGO, Kuliyev AAO. "Study the activity of phenylalanine ammonia-lyase, the amount of anthocyanins and flavonoids in the growth and maturation of apple fruit on the mother tree (in Russia)", Vestn Mosk Gos Obl Univ Seriya Yestestvennyye Nauk, 5, 24–31 (2014).
14. Nadernejad N, Ahmadimoghadam A, Hossyinifard J, et al. "Evaluation of PAL activity, Phenolic and Flavonoid Contents in Three Pistachio (Pistacia vera L.) Cultivars Grafted onto Three Different Rootstocks", J Stress Physiol Biochem, 9(3), 84-97 (2013).
15. Appert C, Zoń J, Amrhein N. "Kinetic analysis of the inhibition of phenylalanine ammonia-lyase by 2-aminoindan-2-phosphonic acid and other phenylalanine analogues", Phytochemistry, 62(3), 415–22. (2003).
16. Kane JF, Fiske MJ. "Regulation of phenylalanine ammonia lyase in Rhodotorula glutinis", J Bacteriol, 161(3), 963–6 (1985)
17. Mushi NI, Kupletskaia MB, Bab'eva IP, et al. "Phenylalanine ammonia-lyase of pigmented yeasts", Mikrobiologiia, 49(2), 269–73, (1980).
18. Jeandet P, Delaunois B, Aziz A, et al. "Metabolic engineering of yeast and plants for the production of the biologically active hydroxystilbene, resveratrol", J Biomed Biotechnol, doi: 10.1155/2012/579089 (2012).
19. Shiman R, Gray DW. "Substrate activation of phenylalanine hydroxylase. A kinetic characterization", J Biol Chem, 255(10), 4793–800 (1980).
20. Sikora LA, Marzluf GA. "Regulation of l-phenylalanine ammonia-lyase by L-phenylalanine and nitrogen in Neurospora crassa", J Bacteriol, 150(3), 1287–91 (1982).
21. Marusich WC, Jensen RA, Zamir LO. "Induction of L-phenylalanine ammonia-lyase during utilization of phenylalanine as a carbon or nitrogen source in Rhodotorula glutinis", J Bacteriol, 146(3), 1013–9 (1981).
22. Yamada S, Nabe K, Izuo N. "Production of L-phenylalanine from trans-cinnamic acid with Rhodotorula glutinis containing L-phenylalanine ammonia-lyase activity", Appl Environ Microbiol,42(5), 773–8 (1981).
23. Zhang B-Z, Cui J-D, Zhao G-X, et al. "Modeling and optimization of phenylalanine ammonia lyase stabilization in recombinant Escherichia coli for the continuous synthesis of l-phenylalanine on the statistical-based experimental designs", J Agric Food Chem, 58(5), 2795–800 (2010).
24. Zhang Y, Shen Y, Zhu Y, et al. "Assessment of the correlations between reducing power, scavenging DPPH activity and anti-lipid-oxidation capability of phenolic antioxidants", LWT - Food Sci Technol, 63(1), 569–74, (2015).
25. Zhu L, Cui W, Fang Y, et al. "Cloning, expression and characterization of phenylalanine ammonia-lyase from Rhodotorula glutinis", Biotechnol Lett, 35(5), 751–6 (2013).
26. Luedeking R, Piret EL. "A kinetic study of the lactic acid fermentation. Batch process at controlled pH". J Biochem Microbiol Technol Eng, 1(4), 393–412, (1959)
27. Monod J. "The growth of bacterial cultures", Annu Rev Microbiol, 3, 371–94 (1949).
28. Kendall DG. "Stochastic processes and population growth", J R Stat Soc Ser B, 11(2), 230–82 (1949).
29. Haefner JW. "Modeling Biological Systems: Principles and Applications", Springer Science & Business Media, (2005).
30. Ivanova SA, Pavsky VA, Poplavskaya MA, et al. "Studying the biokinetics of pigmented yeast by stochastic methods", Foods Raw Mater, 2(1),17–21 (2014).

GAYLE DE MARIA
Chimica Oggi - Chemistry Today (TKS Publisher)

NEWS OLIGOS NEWS PEPTIDES NEWS OLIGOS NEWS PEPTIDES

Identified genetic interaction offers possible new target for glaucoma therapy

Scientists at the University of California, San Diego School of Medicine have elucidated a genetic interaction that may prove key to the development and progression of glaucoma, a blinding neurodegenerative disease that affects tens of millions of people worldwide and is a leading cause of irreversible blindness.

The findings, published in the September 10 online issue of Molecular Cell, suggest a new therapeutic target for treating the eye disease.

Primary open-angle glaucoma (POAG) is the most common form of glaucoma, affecting more than 3 million Americans, primarily after the age of 50. Pressure inside the eye (known as intraocular pressure) and age are the leading risk factors for POAG, resulting in progressive degeneration of retinal ganglion cells, optic nerve damage and eventual vision loss.

Genetics also plays a role. Recent genome-wide association studies have identified two genes – SIX1-SIX6 and p16INK4a – as strongly associated with POAG. SIX6 is required for proper eye development. P16INK4a irreversibly arrests cell growth, a phenomenon called senescence.

In their new paper, principal investigator Kang Zhang, MD, PhD, professor of ophthalmology and chief of Ophthalmic Genetics at Shiley Eye Institute at UC San Diego Health, and colleagues report that some variants of SIX6 boost expression of p16INK4a, which in turn accelerates senescence and death of retinal ganglion cells.

"We also show that high intraocular pressure in glaucoma increases expression of p16INK4a, making it a key integrator of inherent genetic and environmental risk factors that can result in glaucoma," said Zhang.

The findings suggest that inhibiting p16INK4a could offer a new therapeutic approach for glaucoma, which is currently treated by drugs that lower intraocular pressure. "Although lowering intraocular pressure can slow worsening of the disease, it does not stop it and prevent further cell death or possible blindness," said co-author Robert N. Weinreb, MD, Distinguished Professor of Ophthalmology and director of the Shiley Eye Institute.

The authors note that earlier studies in mouse models have shown that selective elimination of p16INK4a-positive senescent cells can prevent or delay age-related tissue deterioration.

According to the UC San Diego team, the next step is to conduct preclinical studies to assess the efficacy and safety

of antisense oligonucleotides – strands of synthesized DNA or RNA that can prevent transfer of genetic information – which might inhibit p16INK4a expression and prevent worsening of glaucoma. "If they are effective, we may contemplate a human clinical trial in the future," Zhang said.

Funding for this research came, in part, from the 973 Program, the State Key Laboratory of Ophthalmology, the National Institutes of Health and Research to Prevent Blindness.

University of California, San Diego School of Medicine

Boulder Peptide Society announced the 2015 Roche Meienhofer award recipient: Richard DiMarchi

Richard DiMarchi, Ph.D. the Standiford H. Cox Distinguished Professor of Chemistry and the Linda & Jack Gill Chair in Biomolecular Sciences at Indiana University has been named as the 2015 recipient of the Meienhofer Award for Excellence in Peptide Sciences. The award was presented to Dr. DiMarchi on September 30, 2015 at the Boulder Peptide Symposium, which took place from September 28 to October 1, 2015 in Boulder, Colorado, where Dr. DiMarchi gave a presentation of highlights from his prodigious record of research achievements.

Dr. DiMarchi's contributions in peptide & protein sciences consist of three decades of work in academia, the pharmaceutical industry and biotechnology companies. He is a co-founder of Ambrx, Inc., Marcadia Biotech, Assembly, Calibrium and MB2 Biotech. He has served as a scientific advisor to multiple pharmaceutical companies (Kai, Ferring, Lilly, Merck, and Roche), three venture funds; 5AM, TMP, Twilight and a former board member of BIO, Isis and Millenium-Bio. He is currently Chairman of the Peptide Therapeutics Foundation and external board member at Assembly Biosciences and On-Target Therapeutics.

Dr. DiMarchi earned his Ph.D. from Indiana University in 1979. He completed post-doctoral training at Rockefeller University under the mentorship of Noble Laureate Prof. Bruce Merrifield after which he began a twenty-two year career as a scientist and executive at Eli Lilly and Company. For more than two decades at Lilly Research Laboratories he provided leadership in biotechnology, endocrine research and product development, retiring as Group Vice President in 2003. The focus of much of Dr. DiMarchi's research has been the chemical biology of endocrine hormones, and more specifically those pertaining to diabetes and obesity. He is readily recognized for discovery and development of rDNA derived Humalog® (LisPro-human insulin) and the advancement of mixed incretin agonists for treatment of the metabolic syndrome. As scientist and executive, Dr. DiMarchi also significantly contributed to the commercial development of Humulin®, Humatrope®, rGlucagon®, Evista®, and Forteo®.

His current research is focused on developing macromolecules with enhanced therapeutic properties through biochemical and chemical optimization, an approach he has termed chemical-biotechnology. He is the author of nearly two hundred scientific publications and holds more than a hundred patents.

Dr. DiMarchi is the recipient of numerous awards including the 2005 AAPS Career Research Achievement Award in Biotechnology, the 2006 ACS Barnes Award for Leadership in Chemical Research Management, the 2006 ACS Esselen Award for Chemistry in the Service of Public Interest, the 2007 Carothers Award for Excellence in Polymer Sciences, the 2009 Watanabe Award for Life Sciences Research, the 2011 Merrifield Award for Career Contributions in Peptide Sciences, the 2012 Phillip Nelson Innovation Award, the 2014 Erwin Schrödinger-Preis, a 2014 inductee to the National Inventors Hall of Fame, a 2015 winner of the Patient Advocacy award of the philanthropic society Cures within Reach, a 2015 inductee to the National Association of Inventors.

www.boulderpeptide.org

Jammed up cellular highways may initiate Dementia and ALS

Molecular therapy partially relieves havoc wreaked by gene mutation in human and fly cells

Johns Hopkins researchers say they have discovered some of the first steps in how a very common gene mutation causes the brain damage associated with both amyotrophic lateral sclerosis (ALS) and frontotemporal dementia (FTD).

They report that the altered C9orf72 gene, located on human chromosome 9, causes RNA molecules to block critical pathways for protein transport, causing a molecular traffic jam outside brain cell nuclei and affecting their operations and survival. In a proof-of-concept experiment, the researchers also say that a molecular therapy eased the jam and restored molecular flow into the cell's core.

A report on the work was published online on Aug. 26 in the journal Nature.

"The discovery several years ago of this mutation — the most common one linked to ALS and FTD — was really a game changer for the field because it wasn't a typical genetic mutation," says Jeffrey Rothstein, M.D., Ph.D., a professor of neurology and director of the Brain Science Institute and the Robert Packard Center for ALS Research at the Johns Hopkins University School of Medicine. "Now we have some information about what it is doing early on to damage brain and spinal cord cells."

The mutation, the most common of the known genetic risk factors for the diseases, is associated with 40 percent of inherited ALS cases, 25 percent of inherited FTD and around 10 percent of noninherited cases of each disease. Both diseases are characterized by degeneration of nerve cells over time. In the case of FTD, the damage causes problems with speech, understanding language and processing emotions. In ALS, the degeneration affects cells in the spinal cord as well as the brain, and patients gradually lose the ability to control their muscles.

According to Rothstein, researchers knew that the C9orf72 mutation, rather than changing one building block of DNA to another, caused a stretch of six DNA nucleotides to repeat hundreds of times. Based on the mutated DNA, affected cells create long strands of repetitive RNA, genetic material normally responsible for transferring DNA's genetic code outside the nuclei, to the machinery that translates it into proteins.

In 2013, Rothstein's lab identified more than 400 proteins in the cell with which the repetitive RNA strands might directly interact. Now, that research group, along with that of Thomas Lloyd, M.D., Ph.D., an associate professor of neurology at Johns Hopkins, have homed

in on one of those proteins, RanGAP, as key to mediating the mutated RNA's effect on cells.

"The key breakthrough came from using a fruit fly model of human ALS and FTD that allowed us to screen these 400 candidates for ones that block brain cell death in a living organism," says Lloyd. "This work identified RanGAP as a critical target of the C9orf72 repeats that could prevent brain cell death when its function was restored."

In healthy cells, RanGAP helps transport molecules through nuclear pores that connect a cell's cytoplasm — the liquid that fills most of a cell — and the nucleus — the central compartment containing genetic material.

But in their experiments with both fly and human brain cells made from patients with the ALS-associated C9orf72 mutation, Rothstein and Lloyd discovered RanGAP is clumped up outside the nucleus. Moreover, proteins that rely on RanGAP for transportation into the nucleus don't flow through the nuclear pores.

"The group had the data in human stem cells and a fly model, but we really wanted to know whether we could see this in the brains of patients," says Rothstein. "So we went to our autopsy bank of human brain tissue and started looking."

Examinations of slices of brain tissue from patients with ALS and FTD showed similar clumps of RanGAP and other proteins — including some vital to neuron function — stuck outside the nuclei of brain cells. "Now, flies, human stem cells and autopsied brains are all telling us the same story here, that this is a fundamental defect causing disease," says Rothstein.

In another set of experiments using the fly and human stem cells, the scientists added antisense oligonucleotides, bits of RNA designed to bind to the repetitive RNA strands, blocking them from interacting with the RanGAP protein. The jammed up nuclear pores reopened, they report, and key proteins once again moved into the nucleus.

Rothstein has launched a collaboration with California-based Isis Pharmaceuticals to pursue the development of a drug that could do the same for patients with ALS and FTD. He cautioned, however, that further studies must be done to confirm this potential, and a commercially available drug is many years off.

"We still don't know every step between the C9orf72 mutation and cellular death in the brain," says Rothstein. "But our belief is that this is what starts it off, and this is certainly a good therapeutic target."

Funding for the study was provided by grants from the National Institute of Neurological Disorders and Stroke (R01 NS085207, NS091046, R01 NS082563, R01 NS074324, NS089616, NS091486), the National Cancer Institute (CA009110), the Brain Science Institute, the Robert Packard Center for ALS Research at Johns Hopkins, the Muscular Dystrophy Association, the Alzheimer's Drug Discovery Foundation, the Judith and Jean Pape Adams Charitable Foundation, the Alzheimer's Disease Research Center - Johns Hopkins, Maryland TEDCO, the Target ALS Springboard Fellowship, the William and Ella Owens Foundation and the ALS Association.

Johns Hopkins Medicine

An in silico platform for predicting, screening and designing of antihypertensive peptides

High blood pressure or hypertension is an affliction that threatens millions of lives worldwide. Peptides from natural origin have been shown recently to be highly effective in lowering blood pressure. In the present study, we have framed a platform for predicting and designing novel antihypertensive peptides. Due to a large variation found in the length of antihypertensive peptides, we divided these peptides into four categories (i) Tiny peptides, (ii) small peptides, (iii) medium peptides and (iv) large peptides. First, we developed SVM based regression models for tiny peptides using chemical descriptors and achieved maximum correlation of 0.701 and 0.543 for dipeptides and tripeptides, respectively. Second, classification models were developed for small peptides and achieved maximum accuracy of 76.67%, 72.04% and 77.39% for tetrapeptide, pentapeptide and hexapeptides, respectively. Third, we have developed a model for medium peptides using amino acid composition and achieved maximum accuracy of 82.61%. Finally, we have developed a model for large peptides using amino acid composition and achieved maximum accuracy of 84.21%. Based on the above study, a web-based platform has been developed for locating antihypertensive peptides in a protein, screening of peptides and designing of antihypertensive peptides.

Gajendra P.S. Raghava et al., Scientific Reports 5, Article number: 12512 (2015) doi:10.1038/srep12512

A biomimetic approach for enhancing the *in vivo* half-life of peptides

The tremendous therapeutic potential of peptides has not yet been realized, mainly owing to their short in vivo half-life. Although conjugation to macromolecules has been a mainstay approach for enhancing protein half-life, the steric hindrance of macromolecules often harms the binding of peptides to target receptors, compromising the in vivo efficacy. Here we report a new strategy for enhancing the in vivo half-life of peptides without compromising their potency. Our approach involves endowing peptides with a small molecule that binds reversibly to the serum protein transthyretin. Although there are a few molecules that bind albumin reversibly, we are unaware of designed small molecules that reversibly bind other serum proteins and are used for half-life extension in vivo. We show here that our strategy was effective in enhancing the half-life of an agonist for GnRH receptor while maintaining its binding affinity, which was translated into superior in vivo efficacy.
Mamoun M Alhamadsheh et al. Nature Chemical Biology (2015) doi:10.1038/nchembio.1907

Improving on nature: making a cyclic heptapeptide orally bioavailable

The use of peptides in medicine is limited by low membrane permeability, metabolic instability, high clearance, and negligible oral bioavailability. The prediction of oral bioavailability of drugs relies on physicochemical properties that favor passive permeability and oxidative metabolic stability, but these may not be useful for peptides. Here we investigate effects of heterocyclic constraints, intramolecular hydrogen bonds, and side chains on the oral bioavailability of cyclic heptapeptides. NMR-derived structures, amide H-D exchange rates, and temperature-dependent chemical shifts showed that the combination of rigidification, stronger hydrogen bonds, and solvent shielding by branched side chains enhances the oral bioavailability of cyclic heptapeptides in rats without the need for N-methylation.
Fairlie, D. P. et al. , Angew. Chem. Int. Ed., 53: 12059–12063. doi: 10.1002/anie.201405364

Role of electrostatic interactions for ligand recognition and specificity of peptide transporters

Peptide transporters are membrane proteins that mediate the cellular uptake of di- and tripeptides, and of peptidomimetic drugs such as β-lactam antibiotics, antiviral drugs and antineoplastic agents. In spite of their high physiological and pharmaceutical importance, the molecular recognition by these transporters of the amino acid side chains of short peptides and thus the mechanisms for substrate binding and specificity are far from being understood.
The X-ray crystal structure of the peptide transporter YePEPT from the bacterium Yersinia enterocolitica together with functional studies have unveiled the molecular bases for recognition, binding and specificity of dipeptides with a charged amino acid residue at the N-terminal position. In wild-type YePEPT, the significant specificity for the dipeptides Asp-Ala and Glu-Ala is defined by electrostatic interaction between the in the structure identified positively charged Lys314 and the negatively charged amino acid side chain of these dipeptides. Mutagenesis of Lys314 into the negatively charged residue Glu allowed tuning of the substrate specificity of YePEPT for the positively charged dipeptide Lys-Ala. Importantly, molecular insights acquired from the prokaryotic peptide transporter YePEPT combined with mutagenesis and functional uptake studies with human PEPT1 expressed in Xenopus oocytes also allowed tuning of human PEPT1's substrate specificity, thus improving our understanding of substrate recognition and specificity of this physiologically and pharmaceutically important peptide transporter.
This study provides the molecular bases for recognition, binding and specificity of peptide transporters for dipeptides with a charged amino acid residue at the N-terminal position.
Dimitrios Fotiadis et al., BMC Biology 2015, 13:58 doi:10.1186/s12915

Self-sorting heterodimeric coiled coil peptides with defined and tuneable self-assembly properties

Coiled coils with defined assembly properties and dissociation constants are highly attractive components in synthetic biology and for fabrication of peptide-based hybrid nanomaterials and nanostructures. Complex assemblies based on multiple different peptides typically require orthogonal peptides obtained by negative design. Negative design does not necessarily exclude formation of undesired species and may eventually compromise the stability of the desired coiled coils. This work describe a set of four promiscuous 28-residue de novo designed peptides that heterodimerize and fold into parallel coiled coils. The peptides are non-orthogonal and can form four different heterodimers albeit with large differences in affinities. The peptides display dissociation constants for dimerization spanning from the micromolar to the picomolar range. The significant differences in affinities for dimerization make the peptides prone to thermodynamic social self-sorting as shown by thermal unfolding and fluorescence experiments, and confirmed by simulations. The peptides self-sort with high fidelity to form the two coiled coils with the highest and lowest affinities for heterodimerization. The possibility to exploit self-sorting of mutually complementary peptides could hence be a viable approach to guide the assembly of higher order architectures and a powerful strategy for fabrication of dynamic and tuneable nanostructured materials.
Daniel Aili et al., Scientific Reports 5, Article number: 14063 (2015) doi:10.1038/srep14063

Your Peptide needs, from R&D to GMP Manufacturing, PolyPeptide provides **Global Support** for a **Quality Solution**

GLOBAL SUPPORT FOR A QUALITY SOLUTION

At PolyPeptide, going the extra mile with our customers is a priority. Agility, global presence, flexibility, ability to create fast custom-tailored solutions, and exceeding the highest requirements, are all key benefits that you could only expect from a world leader in peptide manufacturing.

Our client's success is our primary goal, with a proven track record in producing cost-effective proprietary and generic GMP grade peptides for the pharmaceutical and biotechnology industries.

Our long term relationships with our customers are based on transparency and an approach to partnership which ensures that we provide **global support** for a **quality solution**!

PolyPeptide GROUP

THE ULTIMATE PEPTIDE PARTNER

www.polypeptide.com

Sales contacts: **France** +33 388 790 879 - **Sweden** +46 40 366 200 - **USA** +1 310 782 3569 DENMARK – FRANCE – INDIA – SWEDEN – USA

Pharmaceutical optimization of peptide toxins for Ion channel targets: potent, selective, and long-lived antagonists of Kv1.3

To realize the medicinal potential of peptide toxins-naturally occurring disulfide-rich peptides-as ion channel antagonists, more efficient pharmaceutical optimization technologies must be developed. Here we show that the therapeutic properties of multiple cysteine toxin peptides can be rapidly and substantially improved by combining direct chemical strategies with high-throughput electrophysiology. We applied whole-molecule, brute-force, structure-activity analoging to ShK, a peptide toxin from the sea anemone Stichodactyla helianthus that inhibits the voltage-gated potassium ion channel Kv1.3, to effectively discover critical structural changes for 15x selectivity against the closely related neuronal ion channel Kv1.1. Subsequent site-specific polymer conjugation resulted in an exquisitely selective Kv1.3 antagonist (>1000x over Kv1.1) with picomolar functional activity in whole blood and a pharmacokinetic profile suitable for weekly administration in primates. The pharmacological potential of the optimized toxin peptide was demonstrated by potent and sustained inhibition of cytokine secretion from T cells, a therapeutic target for autoimmune diseases, in cynomolgus monkeys.

Miranda LP et al., J Med Chem, 2015, 58(17):6784-802. doi: 10.1021/acs.jmedchem.5b00495

Blocking of the PD-1/PD-L1 interaction by a D-peptide antagonist for cancer immunotherapy

Blockade of the protein-protein interaction between the transmembrane protein programmed cell death protein 1 (PD-1) and its ligand PD-L1 has emerged as a promising immunotherapy for treating cancers. Using the technology of mirror-image phage display, we developed the first hydrolysis-resistant D-peptide antagonists to target the PD-1/PD-L1 pathway. The optimized compound D PPA-1 could bind PD-L1 at an affinity of 0.51 μM in vitro. A blockade assay at the cellular level and tumor-bearing mice experiments indicated that D PPA-1 could also effectively disrupt the PD-1/PD-L1 interaction in vivo. Thus D-peptide antagonists may provide novel low-molecular-weight drug candidates for cancer immunotherapy.

Gao YF et al., Angew Chem Int Ed Engl, 2015 doi: 10.1002/anie.201506225

Cross-linking strategies to study peptide ligand-receptor interactions

Experiments are described that allowed cross-linking of analogs of a 13-amino acid peptide into the binding site of a model G protein-coupled receptor. Syntheses of peptide analogs that were used for photochemical or chemical cross-linking were carried out using solid-phase peptide synthesis. Chemical cross-linking utilized 3,4-dihydroxy-l-phenylalanine-incorporated peptides and subsequent periodate-mediated activation, whereas photochemical cross-linking was mediated by p-benzoyl-l-phenylalanine (Bpa)-labeled peptides and UV-initiated activation. Mass spectrometry was employed to locate the site(s) in the receptor that formed the cross-links to the ligand. We also describe a method called unnatural amino acid replacement that allowed capture of a peptide ligand into the receptor. In this method, the receptor was genetically modified by replacement of a natural amino acid with Bpa. The modified receptor was UV-irradiated to capture the ligand. The approaches described are applicable to other peptide-binding proteins and can reveal the ligand-binding site in atomic detail.

Becker JM, Naider F, Methods Enzymol. 2015, 556:527-47. doi: 10.1016/bs.mie.2014.12.001

Predicting the sequence specificities of DNA- and RNA-binding proteins by deep learning

Knowing the sequence specificities of DNA- and RNA-binding proteins is essential for developing models of the regulatory processes in biological systems and for identifying causal disease variants. Here we show that sequence specificities can be ascertained from experimental data with 'deep learning' techniques, which offer a scalable, flexible and unified computational approach for pattern discovery. Using a diverse array of experimental data and evaluation metrics, we find that deep learning outperforms other state-of-the-art methods, even when training on in vitro data and testing on in vivo data. We call this approach DeepBind and have built a stand-alone software tool that is fully automatic and handles millions of sequences per experiment. Specificities determined by DeepBind are readily visualized as a weighted ensemble of position weight matrices or as a 'mutation map' that indicates how variations affect binding within a specific sequence.

Brendan J Frey et al., Nature Biotechnology 33, 831–838 (2015) doi:10.1038/nbt.3300


mRNA
Custom synthesis of research, diagnostic or therapeutic mRNA for discovery and early phase clinical trials
mRNA for gene replacement, immunotherapy and vaccines
Tools for genome editing and reprogramming
Reporter genes for delivery optimization
DIAGNOSTIC & THERAPEUTIC GMP QUALITY
ISO 9001
TriLink BIOTECHNOLOGIES
trilinkbiotech.com/mrna

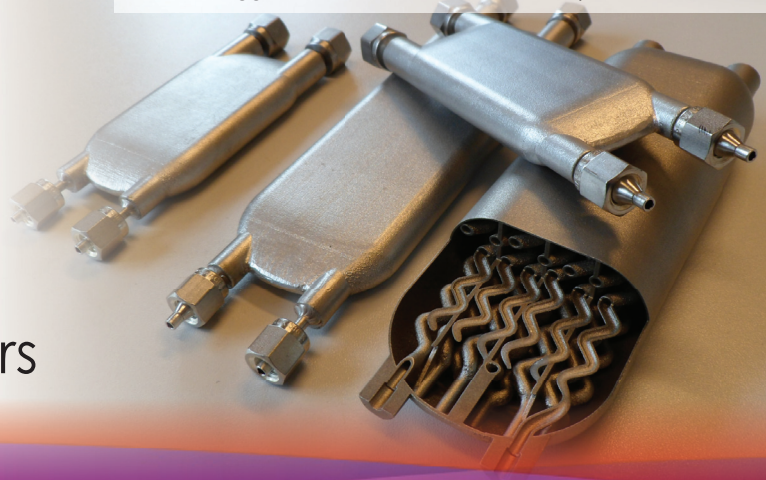

DSM InnoSyn®

3D printed Flow Reactors

ONE CONCEPT FROM LAB SCALE RESEARCH TO INDUSTRIAL PRODUCTION

MR module	Channel volume (ml)	Channel diameter (mm)	Channel length (cm)	Typical performance (@ visco 1mPa.s)		
				Pressure drop (bar)	Heat transfer coeff. (W/m^2K)	Output (ltr/h)
Flow 1	1.0	1.13	100	0.1 – 0.3	1000-2000	0.75 – 1.5
Flow 2	2.0	1.60	100	0.1 – 0.3	1000-2000	1.5 – 3.0
Flow 4	4.0	2.26	100	0.1 – 0.3	1000-2000	3.0 – 6.0
Flow 8	8.0	2.26	200	0.3 – 1.0	1000-2000	6.0 – 12.0

The continuous tubular reactor is a well-known concept, applied broadly in the bulk chemical industry. The micro reactor took its performance to the next level by offering improved control and unprecedented transfer rates. Nevertheless broad industrial application of micro reactor technology has been hampered by a relative high cost level arising from conventional manufacturing technologies.
DSM latest innovation in flow reactors tackles this poor manufacturability. The key to success is found in 3D metal printing - a new fast developing manufacturing technology - delivering full freedom of geometrical design and a magnitude lower cost level, combined with DSM's expertise in design. In short the latter is based on optimizing fluid dynamics in channels of 1-5 millimeters in diameter, rather than micrometer channels. Securing 'micro reactor level' productivity in these millimeter sized channels has been achieved by manipulating the shape, geometry, lay-out of the channel, and flow speed, creating so-called secondary flow phenomena and sufficient high Reynolds numbers (see Figure 1). Typical flow regimes are between laminar and turbulent whilst pressure drop is limited and the residence time distribution shifts to plug flow behavior.
Metal, such as stainless steel, as construction material is well known and accepted in the processing industry. Its properties provide: durability, pressure resistance, high heat conductivity, and easy connections with conventional equipment.
DSM now offers a six-pack of stainless steel flow reactor modules (any set or mix of 1, 2, 4, and 8 mL channel volume) that will facilitate fast process development and kg scale production. The modularity allows to set up swiftly any desired experimental configuration and required volume. If preferred, customized configurations can be designed as well, and 3D printed within weeks. At request we can also develop and manufacture 3D printed flow reactors prepared of better corrosion resistant materials such as titanium and hastelloy.
Since only limited parallelization is required for these 1-5 millimeter channel flow reactors, scale up to ton scale production has now become affordable. Kiloton per annum capacity can be obtained using only a small modular volume due to the very high productivity.
A single concept lifts your lab scale development into industrial production.

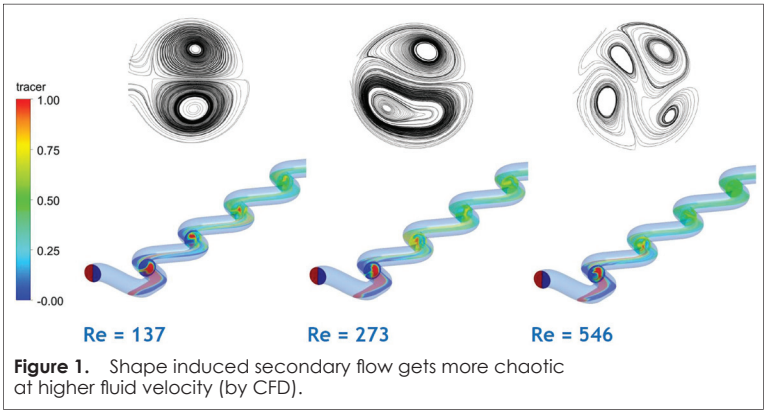

Figure 1. Shape induced secondary flow gets more chaotic at higher fluid velocity (by CFD).

DSM InnoSyn®
andre.vries-de@dsm.com
tel.: +31 46 4761573
www.innosyn.com

DSM
BRIGHT SCIENCE. BRIGHTER LIVING.


Dimitrios I. Gerogiorgis

DIMITRIOS I. GEROGIORGIS*, HIKARU G. JOLLIFFE

*Corresponding author

Institute for Materials and Processes (IMP), School of Engineering, University of Edinburgh, The King's Buildings, Mayfield Road, Edinburgh, EH9 3JL, United Kingdom

Continuous pharmaceutical process engineering and economics

Investigating technical efficiency, environmental impact and economic viability

KEYWORDS: Continuous Pharmaceutical Manufacturing (CPM), synthesis, design, separations, ibuprofen, economics.

Abstract Continuous Pharmaceutical Manufacturing (CPM) emerges as a ground-breaking technology which can invigorate the global pharmaceutical industry by sustainably fostering its agility and the affordability of healthcare for large populations. Continuous production methods feature numerous significant technical advantages, which however need be ensured by robust, scaleable chemistry, systematic process design and efficient Process Analytical Technology (PAT) for control. Quality by Design (QbD) must be achieved by a relentless pursuit of efficiency in energy and solvent use, but above all the business case for a product must be strong enough to cover both synthesis and process R&D against competition. Remarkable corporate investments in production-scale CPM facilities illustrate the value and promise of this paradigm. This paper focuses on applications of process systems engineering methodologies (flowsheet modelling and simulation) toward evaluating the technical efficiency, environmental impact and economic viability of two continuous processes. Original final upstream separation results for ibuprofen and recent ones for plantwide CPM economics are discussed.

INTRODUCTION

Pharmaceutical processes are broadly distinguished in batch (the overwhelming majority) and continuous (a growing minority): in either case, a process comprises a primary (upstream) and a secondary (downstream) part: the first addresses production of the Active Pharmaceutical Ingredient (API or Drug Substance, DS), while the latter focuses on mixing the API with excipients to manufacture the final marketed formulation (Drug Product, DP).

The incentive for technically sound and economically viable CPM (1) depends on each business case, but also on technical advances in organic synthesis, multiphase flow units and process automation (2). The business aspect has paramount importance for deciding if a CPM process should even be evaluated (3). The economic viability is determined using several factors: the total manufacturing cost comprising capital (CapEx) and operating (OpEx) expenditures, the product selling price, marketing costs, and often product and/or technology licensing costs (4).

Batch organic synthesis of API molecules at laboratory and production scale is an arduous procedure, in which long sequences of separate reactions are performed in large reactors, with purification steps conducted between successive stages. This normally effective procedure is also extremely wasteful: the E-factor (waste-to-product ratio) is as high as 25-100 for APIs, indicating that 25-100 kg of waste are generated for every 1 kg of API produced (petrochemical industries have E << 1). Reducing the manufacturing cost is possible via fewer reactions, fewer separations and more efficient unit operations. Disruptive microreactor technology enables previously unattainable syntheses, which are now possible via dramatic intensification (much higher concentration, pressure, temperature) and/or drastic reaction time reduction (flash chemistry), in which hazardous reactions can be safely performed and highly unstable intermediates can be used in flow (5-6). Precise reaction time control (< 1s) yields higher selectivity, economising on unit size (lower CapEx) and materials (lower OpEx). Microreactors facilitate rapid and efficient scaling up of flow syntheses, unleashing CPM potential due to several key advantages (7). Several continuous flow microreactors can accommodate catalyst immobilisation, gas handling and multiphase reactions, ensuring process intensification due to their high mixing efficiency, effective heat removal and low process inventories (8-10). Common pharmaceutical syntheses include hydrogenations, nitrations, fluorinations, oxidations and organometallic reactions.

The most important contributions which hold the promise to revolutionise the global pharmaceutical industry by facilitating the advent of CPM processes can thus be summarised in synthetic chemistry and process engineering, as:

- New, robust and more efficient chemical pathways are discovered and demonstrated for many APIs (5, 6, 11, 12).
- New miniaturised, multi-purpose reactors are developed and effective for a wide spectrum of conditions (8-10).
- New miniaturised separators are integrated in several pilot- and production-scale plant demonstrations (13-14).

Moreover, plantwide process modelling and simulation are instrumental toward CPM design, optimisation and control.

CONTINUOUS FLOW SYNTHESES

A rapidly growing body of literature details the quest for organic synthesis routes to replace batch with CPM processes. Continuous synthesis studies illustrate the production of ibuprofen (15), artemisinin (16) and 6-quinolone (17), and an extensive review covers a wide range of APIs (6). Process modelling, simulation (18-19) and optimisation (20) are key in CPM process analysis.

The flowsheet presented in Figure 1 considers a series of 3 plug flow reactors (PFRs) toward producing ibuprofen (15). Isobutylbenzene (IBB) is mixed with propanoic acid and neat triflic acid (TfOH): the mixture enters the first reactor (150 °C), where IBB undergoes Friedel–Crafts acylation to produce a ketone (2). The outlet stream is cooled (0 °C) and then reacts with a cold (0 °C) solution of diacetoxyiodobenzene, $PhI(OAc)_2$, in a mixture of trimethyl orthoformate (TMOF) and methanol (MeOH). The combined stream is fed to the second reactor (50 °C), where intermediate **2** undergoes $PhI(OAc)_2$-mediated 1,2-aryl migration to produce an ester (3). The outlet stream is mixed with a methanol-water KOH solution and fed into the third reactor, where **3** undergoes base hydrolysis and is converted to the salt form of the API, K-ibuprofen.

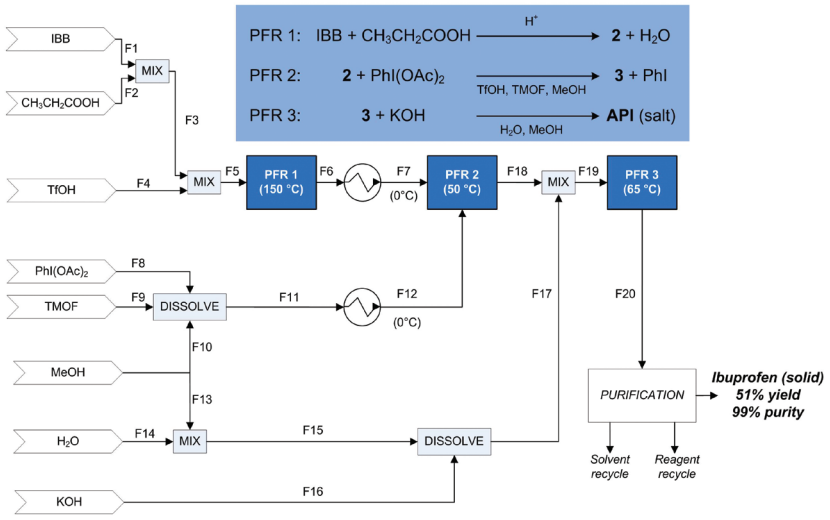

Figure 1. A continuous pharmaceutical process for ibuprofen (15, 19).

ENVIRONMENTALLY BENIGN, EFFICIENT SEPARATIONS

Efficient continuous separations which can achieve high API recovery and low waste generation are essential for CPM. Reactor effluent streams often carry large excess reagent quantities for recycling and by-products for elimination. Ensuring that a high-purity API stream can be fed to downstream processing is critical toward final dosage formation. Successful separation design must satisfy technical, regulatory but also environmental constraints, and the E-factor (ratio of API mass produced over total waste generated) is a convenient metric for evaluating how benign a process is.

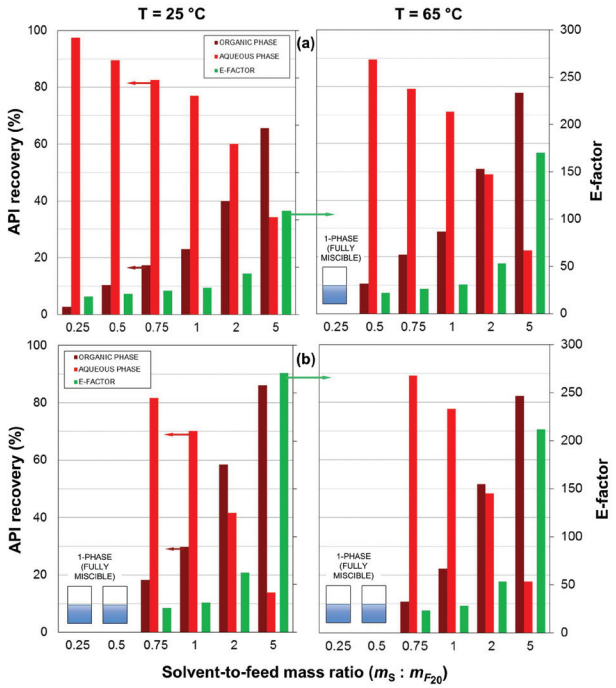

Figure 2. Solvent use and environmental efficiency in the continuous ibuprofen process: (a) n-hexane, (b) toluene.

Systematic unit operation modelling and simulation is very useful in designing and operating efficient separations: one of the several choices available is Liquid-Liquid Extraction (LLE), here explored in the context of ibuprofen CPM. Judicious selection of LLE solvents is key from a technical (efficiency) as well as an environmental (waste) viewpoint. For LLE design, stream F20 is assumed to be a binary (water-methanol) mixture which carries several solutes, and multicomponent thermodynamics (the UNIFAC method) have been used to compute effluent compositions upon solvent addition and phase separation at ambient (25 °C) as well as effluent (65 °C) temperature, to facilitate comparisons (18). Thermodynamic equilibrium between the aqueous and the organic phase is taken to be rapidly established in the unit, with crystallisation and precipitation phenomena negligible. The API distribution in effluent (organic/O, water/W) streams relies on assuming that the ibuprofen partition coefficient is equal to the ratio of corresponding solubilities in each phase. Technical (recovery) and environmental (E-factor) metrics for two solvents n-hexane and toluene are depicted in Figure 2.

Increasing solvent feed is technically and environmentally detrimental, inducing lower recoveries and higher E-factors.

Hexane is superior to toluene in terms of LLE operability, due to a wider immiscibility window at low solvent feed ratios; it also achieves higher, less wasteful API recovery than toluene in the entire solvent feed range at ambient temperature. Nevertheless, the trend is reversed for the higher (PFR3 effluent) temperature (65 °C), in which toluene is clearly more advantageous, as it offers consistently higher and marginally less wasteful API recovery, as long as phase immiscibility is ensured: the most technically efficient and environmentally benign LLE operation is achieved for ratios below 1 (0.75).

COST SAVINGS AND ECONOMIC BENEFITS

Numerous research studies highlight the incontrovertible technical advantages of CPM over batch processes, but to this day very few peer-reviewed publications have quantitatively evaluated the projected economic performance benefits. Envisaging that the promise of higher yields and selectivities will result in lower capital (CapEx) and operating (OpEx) costs as a result of continuous operation is plausible, but very few comparative evaluations of options have appeared. Roberge et al. (21) published a technoeconomic analysis of process alternatives for an annual capacity of 700 kg, identifying clear economic benefits (albeit without analysing the entire process, from raw materials to final product formulation).
Schaber et al. (22) investigated the economic impact of operating an integrated CPM plant using an organic key intermediate (KI) and three organic reactions to derive the API, toward subsequent tablet formation, at an annual blockbuster drug production scale (2000 tons) and for several design parameters. The batch process has been evaluated for a set of four key CPM process variants (roller compaction/RC or direct tablet formation/DTF, with/without recycle). Three pivotal sensitivity variables (Key Intermediate/KI cost, 100-3000 USD/kg; production yield, ±10% vs. batch; tablet API load, 10 and 50 wt%) are employed for each variant, indicating a strong incentive for CPM implementation. Process flow diagrams for both pharmaceutical processes considered are illustrated in Figures 3 and 4, respectively.
Seifert et al. (23) conducted an economic analysis of modular CPM in comparison to multi-product batch manufacturing plants, identifying that the former results in a 30% Net Present Value (NPV) increase over the latter: a further 35% NPV increase was obtained under the assumption that construction can be completed within one year.
The summary of CapEx, OpEx and total cost comparisons for all CPM cases considered by Schaber et al. (2011) is presented in Figure 5. The highest production cost reduction is obtained for a switch from batch to CPM with recycle (R) and tablet formation (TF), options; the alternative technology of roller compaction (RC) is also advantageous, but not in all cases without a recycle stream. Depending on KI production cost, total (CapEx+OpEx) cost savings range between 9-40% when batch and CPM yields coincide, but increase considerably (19-44%) if the latter exceeds the former. Total cost savings remain noteworthy even for a CPM yield lower than the corresponding batch, due to the enormous CapEx savings achieved when using smaller, cheaper units. OpEx savings are due to lower labour and water/solvent costs (61% and 21%, respectively), but they illustrate higher KI price sensitivity. Another detailed technoeconomic analysis for ibuprofen and artemisinin further corroborates the strong incentive for CPM processes due to the remarkable cost savings attainable by continuous flow synthesis and efficient separations (24).

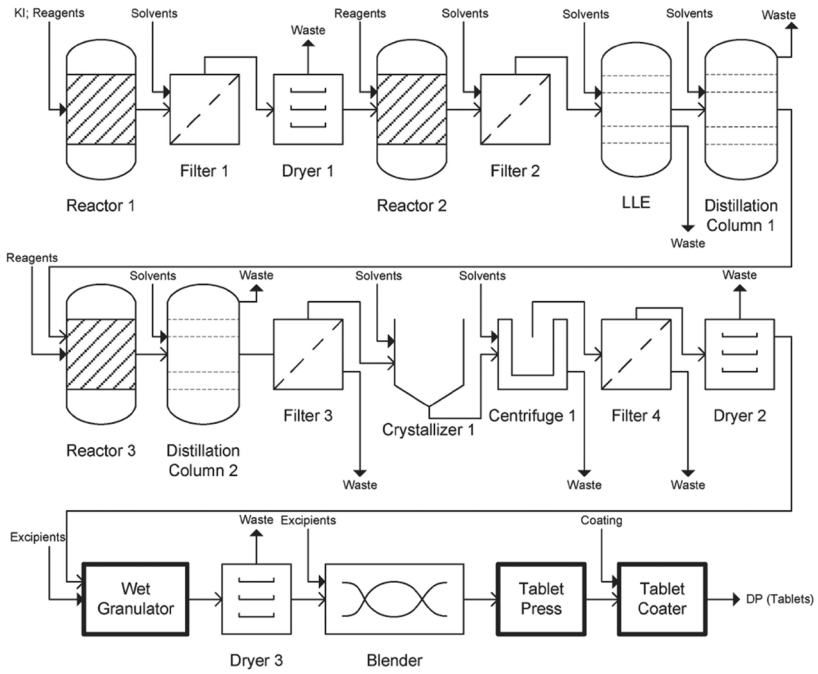

Figure 3. Process flow diagram for batch pharmaceutical manufacturing of an API (22).

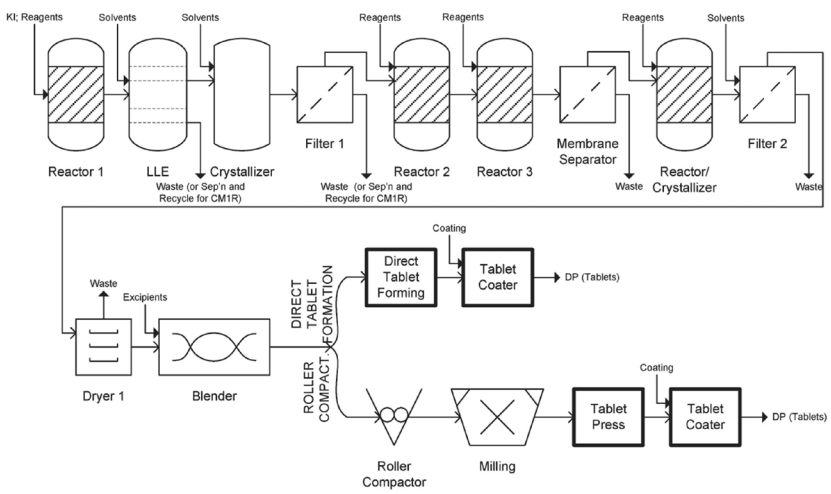

Figure 4. Process flow diagram for continuous pharmaceutical manufacturing of an API (22).

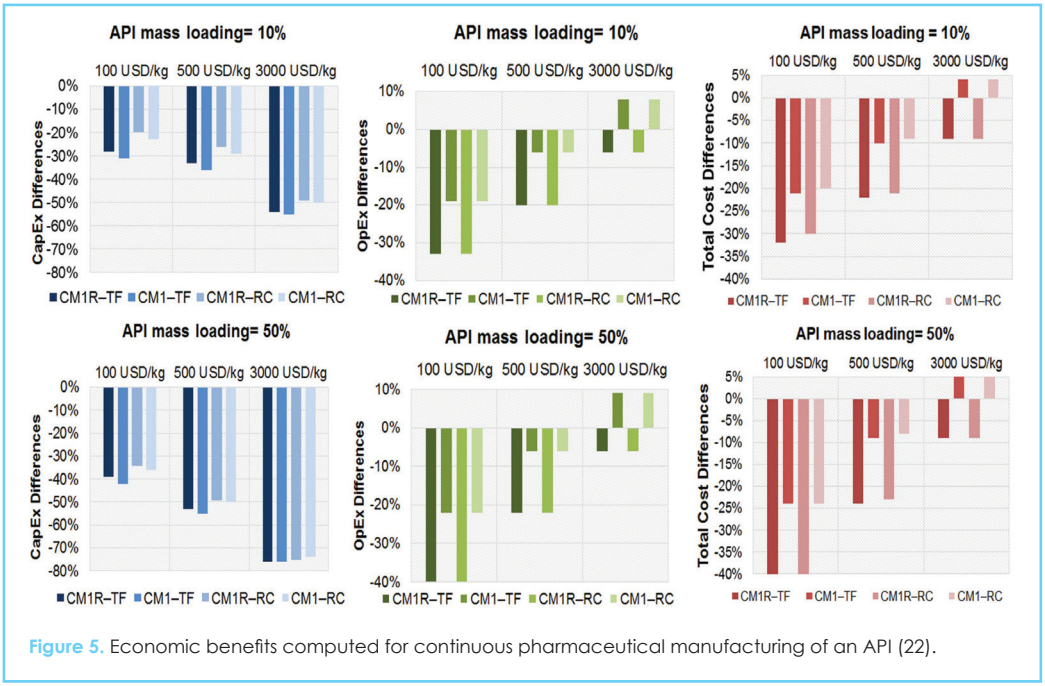

Figure 5. Economic benefits computed for continuous pharmaceutical manufacturing of an API (22).

CONCLUSIONS

The remarkable benefits of continuous over traditional batch processes for manufacturing APIs and organic intermediates are enormous and clearly documented, as the gradual adoption and industrial implementation of CPM concepts can result in significant technical as well as economic gains: CapEx savings are attainable via fewer unit operations and smaller footprint required, while OpEx savings emerge due to increased productivity (higher yield and selectivity), reduced materials, labour and waste. Microreactors improve heat and mass transfer rates spectacularly, enabling reaction intensification under reliable control. First-principles process modelling, simulation and optimisation (18-20) are pivotal enabling technologies toward rapid evaluation of process (flowsheet and unit operation topology) and operation (solvent selection) alternatives, and critical in accelerating R&D by systematic design of reactors and separators which demonstrably achieve optimal performance. Finally, this methodology can seamlessly accommodate detailed and comprehensive economic analyses (21-24) toward comparison with existing or potential batch counterparts, to investigate a priori the economic viability of CPM processes.

REFERENCES

1. Evans, J.M.B., "A paradigm shift", *The Chemical Engineer*, available online (02/2013).
2. Backx, I., "The key to continuous manufacturing", *PharmaAsia* 9-11, available online (03-04/2013)
3. Behr, A., et al., "New developments in chemical engineering for the production of drug substances", Eng. Life Sci. 4(1): 15-24 (2004).
4. Plumb, K., "Continuous processing in the pharmaceutical industry", *Chem. Eng. Res. Des.* 83(6): 730-738 (2005).
5. Yoshida, J. et al., "Flash chemistry: fast chemical synthesis by using microreactors", *Chem.-Eur. J.*, 14(25): 7450-7459 (2008).
6. Malet-Sanz, L. Susanne, F., "Continuous flow synthesis: A pharma perspective", *J. Med. Chem.*, 55(9): 4062-4098 (2012).
7. Kockmann, N. et al., "Scale-up concept of single-channel microreactors: from process development to industrial production", *Chem. Eng. J.* 167(2-3): 718-726 (2011).
8. Losey, M.W. et al., "Microfabricated multiphase packed-bed reactors: Characterization of mass transfer and reactions", *Ind. Eng. Chem. Res.*, 40(12): 2555-2562 (2001).
9. Burns, J.R., Ramshaw, C., "A microreactor for the nitration of benzene and toluene", *Chem. Eng. Commun.*, 189(12): 1611-1628 (2002).
10. Hartman, R. et al., "Deciding whether to go with the flow: evaluating the merits of continuous flow reactors for synthesis", *Angew. Chem. Int. Ed.* 50(33): 7502-7519 (2011).
11. Webb, D., Jamison, T.F., "Continuous flow multi-step organic synthesis", *Chem. Sci.*, 1(6): 675-680 (2010).
12. Gutmann et al., "Continuous flow technology – A tool for the safe manufacturing of active pharmaceutical ingredients", *Angew. Chem. Int. Ed.* 54(23): 6688–6728 (2015).
13. Kralj, J.G. et al., "Integrated continuous microfluidic liquid-liquid extraction", *Lab Chip*, 7(2): 256-263 (2007).
14. Heider, P. et al., "Development of a multi-step synthesis and workup sequence for an integrated continuous manufacturing process of a pharmaceutical", *Org. Process Res. Dev.*, 18(3): 402-409 (2014).
15. Bogdan, A.R., et al., "The continuous-flow synthesis of Ibuprofen", *Angew. Chem. Int. Ed.*, 48(45): 8547-8550 (2009).
16. Lévesque, F., Seeberger, H., "Continuous-flow synthesis of the anti-malaria drug artemisinin", *Angew. Chem. Int. Ed.* 51(7): 1706-1709 (2012).
17. Qian, Z. et al., "A flow process using microreactors for the preparation of a quinolone derivative as a potent 5HT1B antagonist", Synlett 4: 505-508 (2010).
18. Jolliffe, H.G., Gerogiorgis, D.I., "Process modelling and simulation for continuous pharmaceutical manufacturing of ibuprofen", Chem. Eng. Res. Des. 97: 175-191 (2015).
19. Jolliffe, H.G., Gerogiorgis, D.I., "Process modelling and simulation for continuous pharmaceutical manufacturing of artemisinin", Chem. Eng. Res. Des., in press (2015).
20. Gerogiorgis, D.I., Barton, P.I., "Steady-state optimization of a continuous pharmaceutical process", Comput. Aided Chem. Eng. 27: 927-932 (2009).
21. Roberge, D.M. et al., "Microreactor technology and continuous in the fine chemical and pharmaceutical industry: Is the revolution underway?",*Org. Proc. Res. Dev.* 12(5): 905-910 (2008).
22. Schaber, S.D., Gerogiorgis, D.I. et al., "Economic analysis of integrated continuous and batch pharmaceutical manufacturing: A case study", *Ind. Eng. Chem. Res.* 50(17): 10083-10092 (2011).
23. Seifert, T. et al., "Small scale, modular and continuous: A new approach in plant design", *Chem. Eng. Process.: Proc. Intensif.* 52(2): 140-150 (2012).
24. Jolliffe, H.G., Gerogiorgis, D.I., "Plantwide design and economic analysis of ocess modelling and simulation for continuous pharmaceutical manufacturing: Ibuprofen and artemisinin", Comput. Chem. Eng., under review (2015).

CAPSUGEL®
A record of excellence

Jan Vertommen

We offer a wide range of formulation options and technologies for compounds with low solubility or bioavailability. Jan Vertommen, PhD, Senior Director Product Development and Manufacturing, explains more about Capsugel's experience in liquid-filled hard and soft gelatin capsules.

What technologies can Capsugel provide for compounds with low aqueous solubility or poor permeability?
Lipid-based formulations based on oils, surfactants and co-solvents represent a good solution to improve bioavailability or reduce food effect for poorly soluble compounds. The fill technology options to encapsulate the lipid-based formulations include soft gelatin and liquid- and semi-solid filled hard capsules, and we have a full range of production capabilities appropriate for laboratories up to commercial scale.

What sealing technologies do you have available?
Formulations which are liquid at room temperature and filled in a hard capsule format require the capsule to be sealed using capsule banding, or Liquid Encapsulation Micro Spray (LEMS®) technology developed by Capsugel. The LEMS technology involves the application of a fine micro-spray of fusion solution around the join between the body and cap. With a choice of solutions available, we work with customers to select the optimal technology for each product.

How much experience does Capsugel have in softgels?
The site in Ploërmel, France has produced soft gelatin capsules for the past 18 years, across a number of markets including OTC, generics and NCE products containing oxygen-sensitive, high potency and hormonal compounds. Our operational excellence is now spread across three production and development units that are all working under cGMP environments.

Which selection considerations should be taken into account?
For many applications, the technologies are interchangeable but there are situations where one may be more appropriate. Both scientific as well as marketing considerations may guide the product development team towards a preferred dosage form for encapsulation of the lipid-based formulation.

www.capsugel.com
Tel: +33 3 89 20 57 25
Email: DFSinquiry@capsugel.com

YING ZHU
REACHLaw Oy, Vänrikinkuja 3, 02600 Espoo, Finland


Ying Zhu

Pre-emptive risk management
option analysis (PRMOA) under REACH

KEYWORDS: REACH, Substance of Very High Concern (SVHC), Risk Management Options Analysis (RMOA), Authorisation, Restriction, Pre-emptive Risk Management Options Analysis (PRMOA), strategic planning.

Abstract This article explains the process and estimated timetables related to the risk management option analysis (RMOA) and the two most important risk management options under REACH: authorisation and restriction. From a company's point of view, there is an imminent need to actively manage the regulatory risks, because any of the regulatory actions being decided can mean considerable investment for improving current operation conditions, significant obsolescence management and/or replacement cost, potential supply chain disruption, as well as dramatic market reactions. The pre-emptive risk management option analysis (PRMOA) and strategic planning offers a structured concept to safeguard the company's future business in the best possible way.

As part of the European Commission's SVHC Roadmap to 2020, the risk management option analysis (RMOA) has been introduced as a step in the decision-making process for the authorities, although there is no legal obligation for it. Associated with it, the Public Activities Coordination Tool (PACT) was published by ECHA, listing the substances for which a RMOA or an informal hazard assessment for PBT/vPvB (persistent, bioaccumulative and toxic/very persistent and very bioaccumulative) properties or ED (endocrine disruptor) properties is either under development or has been completed since the implementation of the SVHC Roadmap commenced in February 2013. The PACT list has been welcomed widely for increasing transparency, but it has also caused quite some confusion among the industry. This article aims to explain the processes and estimated timetables related to the RMOA and the two most important risk management options under REACH: authorisation and restriction; and introduces the concept of the pre-emptive regulatory risk management option analysis for individual companies.

SCREENING

In February 2013, the European Commission (Commission) published its "Roadmap on Substances of Very High Concern" and later that year, ECHA published the "SVHC Roadmap to 2020 Implementation Plan". The two papers describe the objectives, methodologies and processes for reaching the goal of including all currently known SVHCs in the Candidate List for Authorisation by 2020. The (main) substance groups for which screening activities have been carried out are:

- Carcinogenic, mutagenic and reprotoxic (CMR) substances (cat 1A/1B),
- Sensitisers (& substances with other human health related hazard profiles, which may give rise to equivalent level of concern),
- PBT/vPvBs,
- Endocrine disrupters (EDs),
- Petroleum/coal stream substances which are CMRs or PBTs.

The screening is carried out yearly, starting with an IT screening and followed by a manual screening, mainly based on registration information and CLP notification data available at ECHA. In addition, Member States (MSs) may have certain national priorities, for example based on observed safety concerns. The screening result is a list of potential SVHCs of the highest priority, for which RMOAs shall be conducted before any further regulatory decision is made. These substances should also be included in the PACT list at this stage.

RMOA

An RMOA is a case-by-case analysis conducted by a MS, the Commission or ECHA - at the request of the Commission - to conclude for an identified substance of concern, whether and which additional regulatory instrument(s) should be proposed to manage the risks from its use to human health or the environment. As such, the RMOA is not prescribed in the REACH legal text, but a main EU principle driving its use is the principle of proportionality.

Key questions that will be reflected in the RMO assessment phase for the SVHC prioritised from the screening step are: 1) the available information does not demonstrate that there is a risk that is not adequately controlled and needs to be addressed at EU level, otherwise a restriction process should be started; 2) the known uses of the substance are not exempted from the authorisation requirement and are not already regulated by specific EU legislation that provides a pressure for substitution, leading to the conclusion that no further regulatory action is needed under REACH. Exceptional cases include PBT, vPvB, and ED substances, where an SVHC identification process is considered necessary even if a restriction is foreseen.

The main conclusions that will be drawn are one or multiple choices of the following:

- Identification as SVHC (entering the Candidate List before prioritised for REACH authorisation)
- REACH restriction
- REACH substance evaluation
- CLP harmonized classification and labelling
- Other EU-wide measures
- No need for follow up regulatory action at EU level

There are no EU-wide harmonized rules for the gathering of industry input in the RMOA step. Some MSs have started conducting systematic public consultations on their webpages (e.g. Germany), which run for several weeks, to allow early participation of stakeholders and their input of substance-specific data.

According to some Member States, the RMOA should last 1-6 months. However, experience has shown that it could take much longer.

IDENTIFICATION AS SVHC AND AUTHORISATION

If in the RMOA conclusion the identification as SVHC (authorisation) is suggested, a MS or ECHA may prepare – in a subsequent step - an Annex XV dossier for identification as SVHC. The responsible authority should also inform its intention to do so to ECHA, so that it will be published in the Registry of Intentions list on ECHA's webpage. The preparation of the Annex XV dossier may take up to 6 months or a year.

Once the Annex XV SVHC dossier has been submitted to ECHA, third parties can view it and give comments during the public consultation which is organized by ECHA twice a year. The information most relevant at this point is: 1) the identity of the substance (i.e. substance name/EC number/CAS number/molecular structure etc.); 2) the reason for identification as SVHC, such as PBT or vPvB properties or properties giving rise to an equivalent level of concern. However, SVHC proposals based on harmonised classification included in Annex VI of the CLP Regulation (EC) No 1272/2008 cannot be challenged in the SVHC identification process, because those are legally binding. After the public consultation, the Member State Committee (MSC) will discuss and vote on the inclusion of the identified substance in the candidate list during its meeting. A unanimous decision must be made, otherwise the proposal will be referred to the Commission for further consideration.

The whole process takes around 6 months. So far ECHA has conducted a prioritization exercise on the candidate list substances once per year, using a scoring system that is based on the substances' inherent properties, volume and uses, as foreseen in REACH Article 58(3). The substances will then be ranked according to the sum of the scores and, in general, the highest scoring substances will be recommended to be prioritized to the Authorisation List (Annex XIV). The draft recommendation is then subjected to a public consultation. The information most relevant at this stage is: 1) information on the complexity of the supply chain; 2) comments on those uses that are believed to qualify for an exemption from authorisation; 3) information on volume, types of uses, and the potential that other substances on the Candidate List could substitute/be substituted by the substance in some uses. In September 2014, a parallel call for information on socio-economic elements was also initiated by ECHA on behalf of the Commission, allowing the Commission to consider socio-economic elements which are not mentioned as criterion for prioritisation in the legal text. The Commission announced recently that this practice will continue. After the public consultation, the MSC discusses and votes its opinion on the ECHA draft recommendation, based on which ECHA will make its final recommendation to the Commission. The whole process takes around half a year and is done on a yearly base.

The Commission will then follow the regulatory procedure with scrutiny for including SVHCs in Annex XIV, which has taken around 1 year in the past. However, due to a general reflection of the authorisation process there is currently a moratorium in place, which has lasted already more than one year and it is not clear when the moratorium will be lifted. This implies a delay of Annex XIV inclusions based on the existing 4th, 5th and 6th ECHA Annex XIV recommendations.

In total, the listing process may take altogether around 5 years from the screening stage to the point when a substance is included in the Annex XIV list.

RESTRICTION

If in the RMOA the need for a restriction is concluded, a MS or ECHA will prepare an Annex XV dossier for restriction. The responsible authority should also notify its

intention to do so to ECHA, so that it will be published in the Registry of Intentions list on ECHA's webpage. The restriction dossier shall be prepared within 12 months of the notification.

Interested parties will have an opportunity to comment on the restriction dossier for 6 months after the publication of the dossier. The ECHA Risk Assessment Committee (RAC) shall formulate an opinion within 9 months and the ECHA Committee for Socio-Economic Analysis (SEAC) shall formulate its opinion within 12 months. The public will have once again an opportunity to comment on the SEAC draft opinion. The relevant input for the public consultations are:

1. comments on dossiers and the suggested restriction;
2. a socio-economic analysis, or information which can contribute to one, of the suggested restrictions, examining the advantages and drawbacks of the proposed restrictions.

The Commission will then follow the regulatory procedure with scrutiny for updating the Annex XVII list (restrictions). Time wise the whole procedure could take about 2.5 years.

PRE-EMPTIVE RISK MANAGEMENT OPTION ANALYSIS AND STRATEGIC PLANNING

From companies' point of view, there is an imminent need to actively manage the regulatory risks, because any of the regulatory actions being decided can mean considerable investment for improving current operation conditions, significant obsolescence management and/or replacement cost, potential supply chain disruption, as well as dramatic market reactions. Therefore a strategy-level analysis and action plan is recommended to determine the potential risk management options that the authorities may apply and how to act accordingly. This exercise can be described in roughly four steps:

1. Monitoring
2. Analysing
3. Intervening
4. Strategic planning

Monitoring

The PACT list is the main list to be followed, which gives the first signal of which substances the authorities are working on, and whether there may be impact on the business. Knowing which authority is working on what subject is also important for potential intervention activities.

Analysing

Companies can try to put themselves into the authorities' shoes and make the RMOA themselves. It should be important to understand, that RMOAs for potential SVHC are normally looking at the full range of uses for a given substance. For individual companies or sector trade associations, it may be difficult to know this big picture. However, it should be understood that the main data source for the authorities, namely the registration information, is mostly available to the general public through ECHA's dissemination tool as well. In addition, it is important for the companies to understand the decision criteria and the related timelines.
The goal of the analysing step is to make a realistic prediction of the RMOA outcome and the associated timetable, which will be the input for the intervention and the strategic planning steps.

Intervening

The idea of intervention is to provide the right information to the right party at the right time. There are a few things that companies can do:

1. Keep the registration dossier up to date and reflecting the reality
   Updating the registration dossier to reflect the most current understanding is particularly important for information that is used as selection criteria, such as information on hazardous properties that may change the classification or qualification as PBT, vPvB and/or ED, as well as information on the uses and volumes. It is also important to coordinate this work with the Substance Information Exchange Forum under REACH, because every registrant needs to update in order for the change to be taken into consideration.
2. Participate in the public consultations with the most useful information
   The public consultation is the only official route to provide the decision makers with information that is not available in the registration dossier. The information concerning the use conditions, volumes, alternatives, as well as the socio-economic effects are all issues that may help authorities to make the most proportionate regulatory decisions.

In addition to individual companies' activities, the trade associations often play important roles in lobbying for a more appropriate regulatory option. For example, a use already regulated by specific EU laws aiming at the protection of human health or the environment may have the grounds for claiming inclusion of an exemption in Annex XIV based on REACH Article 58(2).

Strategic planning

In addition to the intervention activities, companies should develop a regulatory roadmap as part of their strategic planning. Such roadmap may address key issues such as

- processes to be designed or optimised on the substance and use information collection,
- mitigation of regulatory risks along the supply chain,
- timely obsolescence management,
- cost-effective replacement plan,
- portfolio optimisation,
- effective public communication.

CONCLUSIONS

Industry has now more possibilities than earlier to interact with the authorities during the RMOA and the subsequent regulatory decision making processes. Companies are advised to take a proactive approach to safeguard their future business in the best possible way. The pre-emptive risk management option analysis and strategic planning offers a structured concept to implement this approach.

ACKNOWLEDGEMENTS

The author would like to thank Mr. Tim Becker and Mr. Michel Vander Straeten for valuable discussions.

Intelligen Suite®

The Market-Leading Engineering Suite for Modeling, Evaluation, Scheduling, and Debottlenecking of Multi-Product Facilities

SuperPro®

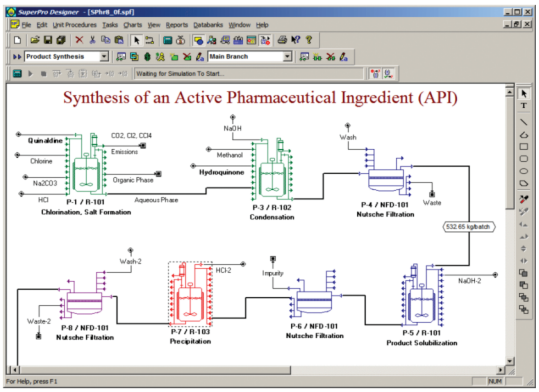

Use SuperPro Designer to model, evaluate, and optimize batch and continuous processes

Recipe DB

SchedulePro®

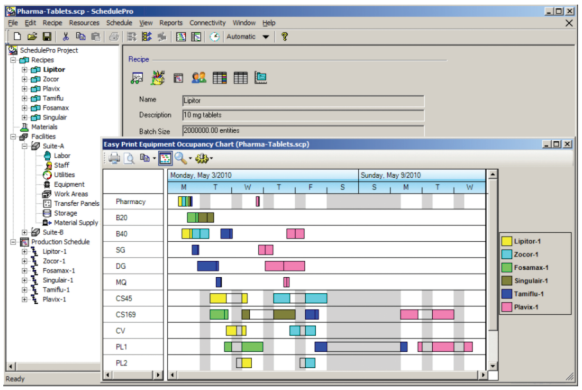

Migrate to SchedulePro to model, schedule, and debottleneck multi-product facilities

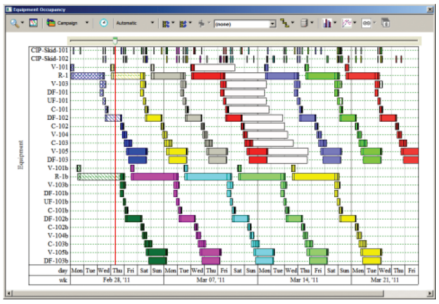

Easy production tracking, conflict resolution and rescheduling

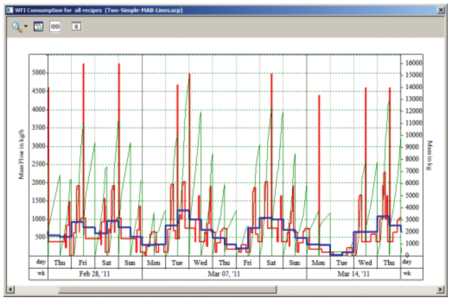

Tracking demand for resources (e.g., labor, materials, utilities, etc.)

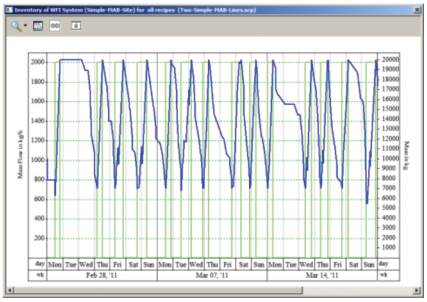

Managing inventories for input, intermediate, and output materials

SuperPro Designer is a comprehensive process simulator that facilitates modeling, cost analysis, debottlenecking, cycle time reduction, and environmental impact assessment of integrated biochemical, bio-fuel, fine chemical, pharmaceutical (bulk & fine), food, consumer product, mineral processing, water purification, wastewater treatment, and related processes. Its development was initiated at the Massachusetts Institute of Technology (MIT). SuperPro is already in use at more than 500 companies and 900 universities around the globe (including 18 of the top 20 pharmaceutical companies and 9 of the top 10 biopharmaceutical companies).

SchedulePro is a versatile production planning, scheduling, and resource management tool. It generates feasible production schedules for multi-product facilities that do not violate constraints related to the limited availability of equipment, labor, utilities, and inventories of materials. It can be used in conjunction with SuperPro (by importing its recipes) or independently (by creating recipes directly in SchedulePro). Any industry that manufactures multiple products by sharing production lines and resources can benefit from the use of SchedulePro. Engineering companies use it as a modeling tool to size shared utilities, determine equipment requirements, reduce cycle times, and debottleneck facilities.

Visit our website to download detailed product literature and functional evaluation versions of our tools

INTELLIGEN, INC. • 2326 Morse Avenue • Scotch Plains, NJ 07076 • USA
Tel: (908) 654-0088 • Fax: (908) 654-3866
Email: info@intelligen.com • Website: www.intelligen.com

Intelligen also has offices in Europe and representatives in countries around the world

MARCO PIUMETTI[1]*, NIK LYGEROS[2]
*Corresponding author
1. Department of Applied Science and Technology, Politecnico di Torino, Corso Duca degli Abruzzi 24, 10129 Turin, Italy
2. Université de Lyon, LGPC (UMR 5285), 69616, Villeurbanne, France

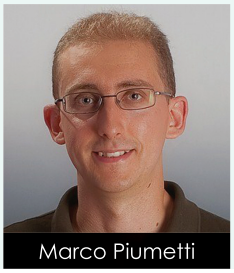
Marco Piumetti

From cooperative phenomena to synergetic hyperstructures in catalysis

KEYWORDS: Active sites, cooperation, game theory, hv-groups, hypergroups, hyperstructures theory, nash equilibrium, synergy.

Abstract Synergistic and cooperative phenomena in catalysis are defined here via a formal classification of the catalytic systems, using the combination of game theory and hyperstructure theory. Game theory is based on the idea that players are rational decision-makers; therefore, making a transposition is reported as rational, the chemical choice.
Three catalytic reactions are considered as characteristic examples: i) the degradation of an azo-dye (Acid Orange 7) with vanadium/hydrogen peroxide/ascorbic acid solutions (homogeneous catalysis); ii) the total oxidation of ethene and iii) the carbon monoxide oxidation over Cu-Ce mixed oxide catalysts (heterogeneous catalysis). According to the game theory, these reactions are paradigms of not-zero sum, asymmetrical and synchronous cooperative-games. The players (i.e. active phases/centres) exhibit a finite number of pure strategies, reflected by their concentrations, and play a strategic game. Moreover, there is the Nash equilibrium and even Pareto equilibrium in the synergistic case. Since the effects of the structural relations among players depend on the catalytic system, a scale of magnitude (in terms of catalytic benefits) is proposed: cooperation < synergetic hyperstructure << strong synergetic hyperstructure.

INTRODUCTION

In catalysis there are several characteristic examples in which the presence of two, or more, components may influence the catalytic activity of a catalyst by changing its solid-state chemistry (1). Many solid catalysts are multicomponent materials (e.g. bismuth molybdates, perovskites, heteropolyanions, vanadium phosphate, and so on) with active phases and promoters mutually-interacting each other over different domains (2-3). Thus, either cooperative or synergistic phenomena may appear and the catalytic behavior typically results in a non-linear combination of complexity structures of active sites (4-6). For instance, it has been shown through X-ray photoelectron spectroscopy (XPS) and electrical conductivity measurements that multicomponent catalysts, such as bismuth molybdates over Co(Fe)-molybdates, reveal synergistic effects due to the enhanced electrical conductivity of the Co(Fe)-molybdate support, attributable to the presence of both Fe^{2+} and Fe^{3+} in Co^{2+} molybdates, thus favouring the so-called Mars and van Krevelen (MvK) mechanism (7, 8). Similarly, the incorporation of isovalent non-reducible elements, such as Zr^{4+} ions into ceria lattice has a beneficial effect on the structural/electronic properties of CeO_2-based catalysts, thus improving their thermal stability, oxygen storage capacity (OSC) and oxygen mobility in the solid (9). These physico-chemical properties render the metal oxidation catalysts highly active in oxidation reactions kinetically modelled via a MvK-type mechanism (9, 10). Examples of such redox mechanisms are known also in homogeneous catalysis, *i.e.* in the Wacker process, consisting typically of the conversion of ethene into acetaldehyde by oxygen in water in the presence of catalytically active Pd^{2+} and Cu^{2+} reagents (11).
Synergies in catalysis typically arise through phase-cooperation (namely, the structural relations among atoms/ions/electrons) and spillover effects. Grasselli (12) first introduced the concept of "phase-cooperation" for oxidation and ammoxidation reactions. For instance, it has been observed that both α-$Bi_2Mo_3O_{12}$ and γ-Bi_2MoO_6 phases are needed to carry out the oxidation/re-oxidation functions, through their complementary properties.
It appears that two phases (*A* and *B*) of different properties, when brought into contact with each other (*AB phase*) may lead to better catalytic performances (i.e. in terms of reaction yield) than those that can be reached by the two phases acting separately and independently from each other (10). The magnitude of the phase-cooperation can be expressed as follows:

$$\Delta Y = Y_{AB} - (W_A Y_A + W_B Y_B)$$

Where Y_{AB}, Y_A and Y_B denotes the yields of the *AB* phase, phases *A* and *B*, respectively, measured under the same operating conditions; W_A and W_B are the weight percentages of the phases *A* and *B* in the binary phase (11, 12).

On the other hand, spillover phenomenon involves the transport of active species (e.g. oxygen, hydrogen, etc.) adsorbed on one phase (donor) onto a second phase (acceptor) which does not form the active species under the same conditions (13, 14). When the catalytic sites are "irrigated" by spillover species, the solid surface significantly improves its chemical reactivity (13-15); indeed, the presence of spillover phenomena allows the solid catalysts to act more effectively (16). Similar phenomena can be observed in enzymatic catalysis by the concept of allostery (17). Accordingly, Delmon et al. (18) proposed the "remote-control" concept to explain the fact that many industrial catalysts used for the partial oxidation of hydrocarbons are multiphasic, and that specific phase compositions lead to synergistic phenomena.
In the present work, we investigate synergistic and cooperative phenomena in both homogeneous and heterogeneous catalysis via a formal classification of the catalytic systems with the combination of game theory and hyperstructure theory. Game theory is based on the idea that players are rational decision-makers (18, 19), thus here we make a transposition and we consider the chemical choice as rational. Hyperstructure theory has recently been used as a model to describe the complexity of catalysts (5, 6). Three catalytic reactions, with different numbers of products, will be used as paradigms: the degradation of azo-dye (Acid Orange 7) with vanadium/hydrogen peroxide/ascorbic acid solutions (homogeneous catalysis), the total oxidation of ethene and the carbon monoxide oxidation over Cu-Ce mixed oxide catalysts (heterogeneous catalysis).

RESULTS AND DISCUSSION

Degradation of azo-dye using vanadium/H_2O_2/ascorbic acid systems (homogeneous catalysis)

Experiments were carried out with a 10^{-3} M solution of acid orange 7 (A07), a "probe molecule" for many azo-dyes. Tests were performed at room temperature in "dark" conditions with 10 mL total volume. The component concentrations in the aqueous solution were: 20 mM ammonium metavanadate (NH_4VO_3), 80 mM hydrogen peroxide (30% H_2O_2), 80 mM ascorbic acid ($C_6H_8O_6$).
At constant time intervals, aliquots of the solution were collected. After each sampling, the UV-Vis spectrum of the solution was analyzed in the 200-600 nm range by UV-Vis spectrophotometer. The concentration of AO7 in the solution was evaluated by the intensity of the band at 484 nm, related to the hydrazone form. Degradation (%) of AO7 was calculated as $100 \cdot (C_0 - C_f)/C_0$ where C_0 and C_f are the initial and the final dye concentration (mM), respectively.

Total oxidation of ethene/co oxidation using copper-cerium mixed oxide catalysts (heterogeneous catalysis)

Preparation of the catalysts

A set of Ce-Cu mixed oxide catalysts with different Ce/Cu-contents (denoted hereafter as Cu_xCe_{1-x} where x indicates the atomic ratios of Cu/Ce+Cu) were synthesized by means of solution combustion synthesis (SCS), as described elsewhere (21). Briefly, proper amounts of $Ce(NO_3)_3$, $Cu(NO_3)_2$ and urea (in stoichiometric conditions) were dissolved in 50 mL of deionized water and stirred at room temperature for 30 min. The homogeneous solution was then placed in the oven at 600°C for 20 min. The resultant powder was washed with deionized water to remove impurities and then dried at 90°C overnight.

Catalyst characterization

The powder X-ray diffraction patterns were collected on a X'Pert Philips PW3040 diffractometer using Cu Kα radiation (2θ range = 15°- 70°; step = 0.05° 2θ; time per step = 0.2 s). The diffraction peaks were indexed according to the Powder Data File database (PDF 2000, International Centre of Diffraction Data, Pennsylvania).
Specific Surface Area (S_{BET}) and total pore volume (V_p) were measured by means of N_2 physisorption at -196°C (Micrometrics ASAP 2020) on samples previously outgassed at 200 °C for 4 h to remove water and other atmospheric contaminants. The specific surface area of the samples was calculated using the BET method.
Sample morphology was studied by a field emission scanning electron microscope (FESEM Zeiss MERLIN, Gemini-II column). The Cu/Ce-content in the samples was determined through EDS analysis (Oxford X-ACT): 5 different spots with a 10–50 nm diameter were selected in representative zones of the sample, and the average Ce/Cu-content was then calculated.

Catalytic activity tests

Catalytic activity tests were performed in a continuous reactor that is a quartz U-tube with inner diameter = 4 mm, heated by an electric furnace; temperature was measured by means of a thermocouple placed approximately in the middle of the catalytic bed.

- *Total oxidation of ethene:* The catalyst (0.1 g) was pre-treated in He (flow rate = 100 $cm^3\,min^{-1}$) for 1 h at 150°C to remove any species adsorbed on the catalyst surface. The gas flow was then switched from helium to the reactive mixture: 500 ppm ethene and 10% O_2 were fed with N_2 to the reactor with a gas hourly space velocity (GHSV) of 19100 h^{-1}. The catalytic reaction was started when the temperature was stable at 100 °C. The temperature was then raised by 5 °C/min from 100 °C up to 700 °C.
- *Carbon monoxide oxidation:* The catalyst (0.05 g) was pre-treated in He (flow rate = 50 $cm^3\,min^{-1}$) for 1 h at 50 °C. Then, 1000 ppm CO and 10% O_2 were fed with N_2 to the reactor with a GHSV of 19100 h^{-1}. The reaction was started when the temperature was stable at 50 °C. The temperature was then raised by 5 °C/min in the range from 50 to 500°C.

The gaseous mixtures were analyzed via CO/CO_2 NDIR analyzers (ABB).

RESULTS AND DISCUSSION

Definition of synergetic hyperstructures

In classical algebraic structures, the notion of group ***G*** can be interpreted with the following necessary but not sufficient condition:

$$\forall\,(a,b) \in G^2 : |ab| = 1$$

in which *a* and *b* are two elements of *G*. Moreover, in a group there is an inner operation which means that:

$$\forall\,(a,b) \in G^2 \colon |ab| = G$$

In terms of cooperation, the elements *a* and *b* may cooperate to give a product. Thus, it is possible to generalize this concept to define the "synergetic hyperstructures" with the notion of hyperoperation. According to Marty's theory, a hyperstructure is every algebraic structure in which at least one hyperoperation is defined (22). In an algebraic structure the composition of elements is still an element, while in an algebraic hyperstructure the composition of elements is a set (22, 23). In a hypergroup *H*, according to the definition of Marty (22), we have:

$$\forall\,(a,b) \in H^2 \colon \;\; 1 \leq |a * b| \leq |H|$$

which is a consequence of the axioms of reproduction and associativity (5, 23-26).
In this context, we can give a more formal difference between cooperation and synergy. Specifically, the group operation is cooperation (C) but not synergy because we have only:

$$|a * b| = 1$$

On the other hand, synergy is more than cooperation, since it occurs when:

$$|a * b| > 1$$

According to the latter condition, we can define the synergetic hyperstructures (SH) as:

$$\forall\,(a,b) \in SH : |a * b| > 1$$

and strong synergetic hyperstructures (SSH) as:

$$\forall\,(a,b) \in SSH : |a * b| > 2$$

Therefore, a strong synergy has the following propriety:

$$a \cup b = \{a,b\} \subset a * b$$

These theoretical concepts may be applied to the science of catalysis, thus leading to a formal classification of the catalytic systems:

- *If there are ≥ two elements (i.e. active phases/centres) and one product can be obtained via catalysis, then it is cooperation (C).*
- *If there are ≥ two elements (i.e. active phases/centres) and two products can be obtained via catalysis, then it is a synergetic hyperstructure (SH).*
- *If there are ≥ two elements (i.e. active phases/centres) and at least three products can be obtained via catalysis, then it is a strong synergetic hyperstructure (SSH).*

Many catalytic reactions can be mentioned as characteristic examples, particularly for industrial and environmental catalysis where multicomponent catalysts are usually used. For instance, cooperation phenomena may appear in the CO oxidation over mixed oxides (e.g. ceria-doped catalysts) (27), as well as in the ammonia synthesis catalyzed by multicomponent catalysts (e.g. K-promoted iron oxides) (11, 28). Examples of synergetic hyperstructures can be observed in the total oxidation of Volatile Organic Compounds (VOC) over mixed oxide catalysts (e.g. Mn-Ce-O or Cu-Ce-O systems (10, 29)) when there are only the total oxidation products (CO_2 and H_2O). Similarly, strong synergetic hyperstructures may arise in the oxidative dehydrogenation (ODH) of light alkanes over multicomponent catalysts (e.g. V-Ti-O, V-Al-O, V-Mg-O, etc.), since several reaction products occur (e.g. alkenes, H_2, CO_x, etc.) (30, 31). It appears that the effects (e.g. catalytic benefits) of the structural relations among atoms/ions/electrons depend on the nature of catalytic system, and then a scale of magnitude should be proposed:

COOPERATION < SYNERGETIC HYPERSTRUCTURE << STRONG SYNERGETIC HYPERSTRUCTURE

This classification suggests that catalytic processes reflected by SSH and SH should exhibit better catalytic improvements, rather than reactions leading to one reaction product.

The concepts of relevance and strategic relevance
According to Hjørland and Sejer Christensen (32), something (A) is relevant to a task (T) if it increases the likelihood of accomplishing the goal (G), which is implied by T. This means that the concept of relevance is related to the task, but in strategy we need something more specific: it is necessary to codify the task as a strategic mix in order to be global and not only local. Thus, the relevance is close to the efficiency of contribution in this context. If the contribution of some elements in the strategic mix is negative (e.g. inerts, impurities, etc.) than it is not relevant. Conversely, the relevance is the positive contribution in the strategic mix, which can be passive and not active. In the last case, which means active, a strategic relevance appears in the frame of cooperation. Thus, the strategic relevance is related to the notion of cooperation. Moreover, we can make a distinction between a cooperative and a synergistic behavior: the former is a positive collaboration, whereas the latter is an efficient collaboration. The strategic relevance can be strong in the context of a synergistic behavior. Therefore, the concept of relevance, and even more of strategic relevance, is not independent of the task and it depends on the strategic mix. This means that in catalysis we have to consider the relevance as a condition and not as a result, to obtain a specific goal.

Degradation of azo-dye using vanadium (H_2O_2/ascorbic acid systems
In game theory, a game is cooperative when the players are able to form binding commitments; making a transposition we obtained the following results. The degradation of Acid Orange 7, a probe molecule for the several azo-dyes found as contaminants in both wastewater and groundwater, was examined, as in previous studies by Piumetti et al. (33, 34). The latter have shown that transition metals (i.e. V- and Fe-containing catalysts) strongly improve their oxidation activity in the presence of both H_2O_2 and ascorbic acid (HA), thus leading to effective degradation of A07 via complex redox

pathways, involving radical species (Fenton-like processes). In the present study, however, the A07 degradation was carried out using V species in homogeneous phase, with H_2O_2 and HA as oxidant/reductant agents. This catalytic system in normal form is a structure:

$G = \langle P, \mathbf{S}, \mathbf{F} \rangle$

where

$P = \{V, H_2O_2, HA\}$

is a set of players,

$\mathbf{S} = \{S_V, S_{H2O2}, S_{HA}\}$

is a 3-tuple of pure strategy sets, one for each player,

$\mathbf{F} = \{F_V, F_{H2O2}, F_{HA}\}$

is the 3-tuple of payoff functions.

Finally, we use the degradation ($= 100 \cdot (C_0 - C_f)/C_0$) as payoff function.

Figure 1 shows the Venn diagrams of $V/H_2O_2/HA$ and their initial concentrations in A07 solution. Thus, seven combinations are possible by considering the reactive components (players) in solution: V, H_2O_2 and HA (one component or player in the sense of decision theory); V/H_2O_2, V/HA and H_2O_2/HA (two components or players in the sense of game theory); $V/HA/H_2O_2$ (three components or players).
In this scenario, the catalytic reaction represents a synchronous game, since each player acts simultaneously over the reaction time (19). Moreover, it is a not-zero-sum game, since the outcome has net results greater (or lesser) than zero. The players have a finite number of pure strategies, reflected by their concentrations and play a strategic game (19, 20); moreover, they are in the Nash equilibrium (NE), since each player is making the best possible action in a cooperative-game, taking into account the actions of the other players (35). In other words, each strategy in NE is the best response to all other possible strategies in that equilibrium.

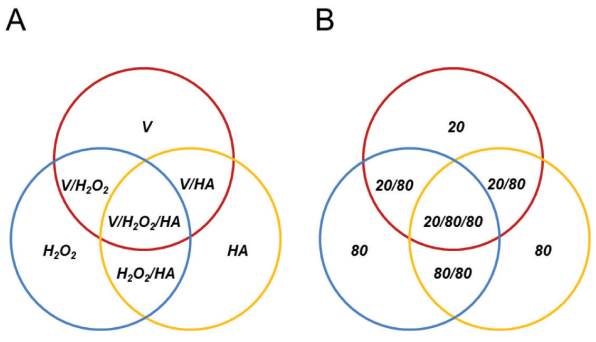

Figure 1. Venn diagrams of vanadium (V); hydrogen peroxide (H_2O_2); ascorbic acid (HA) and their initial concentration (mM) in A07 solution (Sections A and B, respectively).

As shown in Figure 2, the lowest A07 conversion values (%) as a function of time (namely 10, 20 and 30 min.) can be obtained

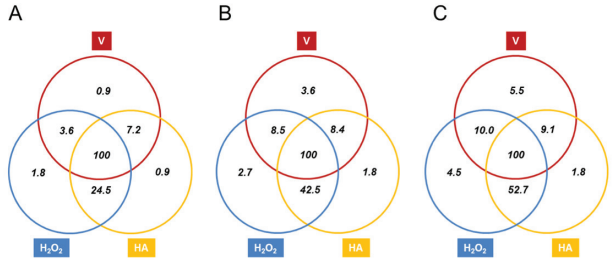

Figure 2. Venn diagrams of A07 conversion values (%) after 10, 20 and 30 min. (Section A, B and C, respectively).

for systems with just one player: the presence of either vanadium or hydrogen peroxide has a moderate effect on the degradation of A07 (around 5% degradation after 30 min.), whereas worse activity is obtained with ascorbic acid (1.8% degradation after 30 min.). Each player (V, H_2O_2 or HA) acts alone and thus its action is a pure strategy. Therefore:

$F_{HA} < F_{H2O2} < F_V$ (pure strategy)

However, with the presence of two players the A07 conversion increases slightly and the best results can be obtained with the HA/H_2O_2 system (degradation 52.7 % after 30 min.). In this case, two players (V/H_2O_2, V/HA or H_2O_2/HA) act together thus leading to a mixed strategy. Each player can choose his available pure strategies with certain probabilities, and hence there is a probability distribution to each pure strategy. J.F. Nash proved that if each player has a finite number of pure strategies, then there exists at least one equilibrium in mixed strategies (35). Thus, the payoff function of each player is maximized given the strategy of the other players, and the following order can be drawn:

$F_{V/HA} < F_{V/2O2} < F_{H2O2/HA}$ (mixed strategy)

Remarkable results may appear with vanadium in the presence of both HA and H_2O_2 (three players), thus confirming the beneficial effect of both oxidant and reductant agents in Fenton-like processes, as described elsewhere (33, 34). In this case, indeed, the presence of three active components in the systems leads to total conversion of the A07 in less than 10 min. (UV-vis spectra not reported for the sake of brevity).
The players act together with a totally mixed strategy and so it is possible to assign a strictly positive probability to every pure strategy. Therefore, the payoff function is also defined:

$F_{V/H2O2/HA}$ (totally mixed strategy).

As a result, the catalytic system is not a symmetric game, since the players cannot be changed without changing the payoff functions. The system is also in Pareto efficiency since it is not possible to improve any payoff function.
The players cooperate synergistically to decompose A07 into two reaction products, namely sulfanilic anion and 1-amino-2-naphtol (36). However, in either basic or acidic conditions, the amino group of the 1-amino-2-naphthol readily hydrolyzed to 1,2-dihydroxynaphtalene, which in turn is oxidized to o-naphthoquinone (37). As a whole, this complex process may produce several products (more than two) depending on the catalyst, pH and

reaction time. Therefore, the active components (players) cooperate synergistically in the framework of strong synergistic hyperstructures.

Total oxidation of ethene and co oxidation over copper-cerium mixed oxide catalysts

It is well-known that the oxidation of VOCs over transition metal oxides, such as CuO-CeO_2 catalysts, usually occurs via a MvK-type mechanism, and proceeds through lattice oxygens (nucleophilic attack) of the solid catalyst (37). This redox mechanism includes two steps: a hydrocarbon molecule (R-H) reacts by extracting lattice oxygen (O^{2-}) from the catalyst surface ($R\text{-}H + O^{2-} \rightarrow R\text{-}O^{-} + H^{+} + 2e^{-}$), thereby generating oxidized products and a reduced surface. Afterwards, the lattice oxygen is replenished by the reduction of gaseous oxygen ($½O_2 + 2e^{-} \rightarrow O^{2-}$) (38). Then, the molecular oxygen is only required to reoxidize the catalyst surface. The MvK-type mechanism has also been proposed for the CO oxidation over ceria-based catalysts: CO reacts with surface oxygen to form CO_2 and an oxygen vacancy (step I); then, a molecule of O_2 fills in this O vacancy (step II) (27).

In this scenario, Ce-Cu mixed oxides are effective catalysts for both VOCs total oxidation and CO oxidation reactions (27, 37, 39, 40). Therefore, a set of Ce-Cu oxide catalysts with different Cu/Ce contents was prepared to study the catalytic activity for both reactions. The high redox activity of Ce-Cu mixed oxides arises by the ability to reduce and re-oxidize of both Cu^{2+}/Cu^{+} and Ce^{4+}/Ce^{3+} couples, which is improved by the strong Cu-O-Ce interactions (27).

In the present study, the prepared Cu_xCe_{1-x} samples exhibit specific surface areas (SSA) and total pore volumes in the range of 3-31 m^2g^{-1} and 0.01-0.07 cm^3g^{-1}, respectively (Table 1). The highest surface area and pore volume are reached with the $Cu_{0.4}Ce_{0.6}$ catalyst, whereas further increases of Cu-contents lead to worse textural properties. Conversely, the SSA for pure CeO_2 and CuO are 21 $m^2\ g^{-1}$ and 3 $m^2\ g^{-1}$, respectively.

Catalyst	S_{BET}[a] (m^2g^{-1})	V_p[b] (cm^3g^{-1})	r_{C2H4}[c] (mmol $m^{-2}\ h^{-1}$)	r_{CO}[d] (mmol $m^{-2}\ h^{-1}$)
CeO_2	21	0.05	2.1	0.00
$Cu_{0.15}Ce_{0.85}$	24	0.06	5.5	23.2
$Cu_{0.40}Ce_{0.60}$	31	0.07	8.9	40.1
$Cu_{0.60}Ce_{0.40}$	25	0.06	10.3	24.9
$Cu_{0.85}Ce_{0.15}$	16	0.02	8.1	5.2
CuO	3	0.01	4.1	0.0

Table 1. Textural properties and specific oxidation rates of the Ce-Cu mixed oxide catalysts.

[a] S_{BET} = specific surface area.
[b] V_p = total pore volume.
[c] r_{C2H4} = Specific C_2H_4 oxidation rate (at 300 °C).
[d] r_{C2H4} = Specific CO oxidation rate (at 100 °C).

As a whole, a cubic fluorite lattice structure of ceria (*Fm3m* symmetry) appears for all Cu-Ce mixed oxide catalysts. Reflections of the copper oxide (CuO) phase can be observed in the addition to those of ceria, as the increase of copper leads to the formation of bulk CuO particles. Moreover, relatively uniform agglomerates of particles (diameter of ca. 100-150 nm) appear for all the prepared catalysts (XRD diffractograms and FESEM images not reported for the sake of brevity).

The conversion of ethene to CO_2 ($C_2H_4 + 3O_2 \rightarrow 2CO_2 + 2H_2O$) as a function of temperature over the Ce-Cu oxide catalysts is shown in Figure 3. All the catalysts display positive conversion trends for an increasing reaction temperature. However, different activity trends can be observed. The most active catalyst is the $Cu_{0.60}Ce_{0.40}$ (total conversion of ethene occurs below 450 °C), whereas higher Cu-contents reduce the catalytic performances. Conversely, the lowest conversion values are achieved for pure CeO_2 (total conversion obtained at 736°C). Indeed, Ce-Cu mixed oxide catalysts show better activities compared to either CuO or CeO_2, due to their easier reducibility and better redox properties (37, 39, 40), as revealed by H_2-TPR and XPS analysis (data not reported for the sake of brevity). On the other hand, the beneficial effect of the SSA on the overall oxidation activity may be also possible.

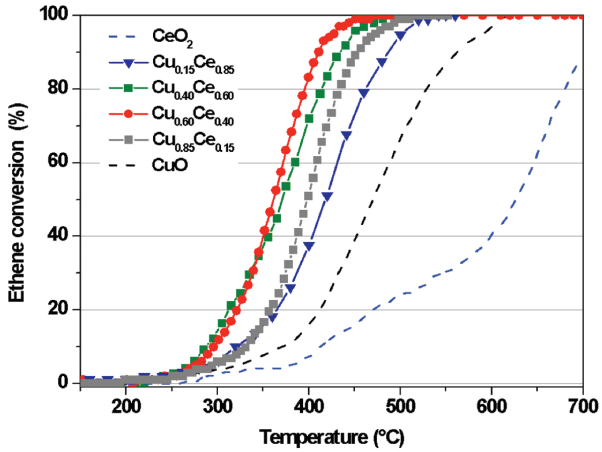

Figure 3. Conversion of ethene to CO_2 as a function of temperature over the Ce-Cu oxide catalysts.

These findings show that Ce-Cu mixed oxides (two players) cooperate synergistically to lead higher oxidation activities than those reached by either CuO or CeO_2 phase (one player). The magnitude of this synergy (payoff function) depends on the Cu/Ce ratio, which is the mixed strategy used to carry out the strategic game. The catalytic system displays the Pareto efficiency for each mixed strategy, although different payoff function values appear. Figure 4 show the temperature at which 50% ethene conversion to CO_2 (denoted as $T_{50\%}$) is attained over the Ce-Cu oxide catalysts. Since conversion values depend on GHSV, weight of catalyst and many other variable that make comparison with other systems a difficult task, it has been calculated the specific ethene oxidation rate for each catalyst under kinetic control (see Table 1). These results confirm that the co-presence of CeO_2 and CuO phases has a beneficial effect

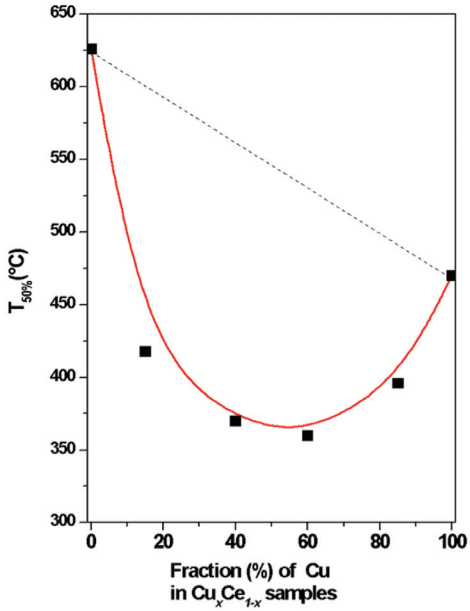

Figure 4. Temperature at which 50% ethene conversion is attained ($T_{50\%}$) as a function of the fraction of component Cu in the Cu_xCe_{1-x} catalysts.

on the structural and electronic properties of the catalysts, and the best catalytic performances can be obtained for intermediate compositions (Cu/Ce atomic ratio ~ 1.5). Since CeO_2 and CuO phases cooperate synergistically, giving rise to two oxidation products (CO_2 and H_2O), then this catalytic system is an example of synergetic hyperstructure. Likewise, the CO oxidation reaction over the same catalysts (Figure 5) shows the presence of a cooperative-game, in which the players act simultaneously to maximize the payoff function (here defined as "CO_2 production"). In the present case, however, the best mixed stategy is obtained for Cu/Ce atomic ratio ~ 0.7 ($T_{50\%}$ values and specific CO oxidation rates are reported in Figure 6 and Table 1, respectively) and this catalytic system reflects a cooperation among the players, since CO_2 is the only reaction product.

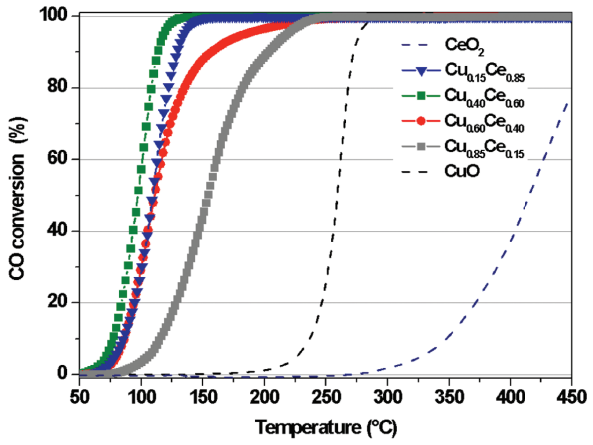

Figure 5. CO to CO_2 conversion as a function of temperature over the Ce-Cu oxide catalysts.

CONCLUSIONS

We have considered the synergistic and cooperative phenomena that may occur in catalytic reactions, introducing a formal classification of the catalytic systems, via the combination of game theory and hyperstructure theory. Three catalytic reactions have been considered:

- The degradation of Acid Orange 7 with V/H_2O_2/HA (= strong synergetic hyperstructure);

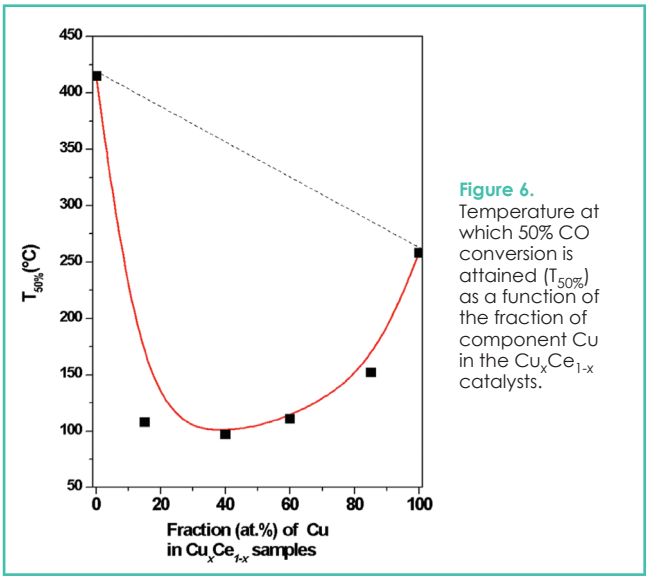

Figure 6.
Temperature at which 50% CO conversion is attained ($T_{50\%}$) as a function of the fraction of component Cu in the Cu_xCe_{1-x} catalysts.

- The total oxidation of ethene over Cu-Ce mixed oxide catalysts (= synergetic hyperstructure);
- The carbon monoxide oxidation over Cu-Ce mixed oxide catalysts (= cooperation).

According to the game theory, these reactions are characteristic examples of not-zero sum, asymmetrical and synchronous cooperative-games. The players (i.e. active phases/centres) exhibit a finite number of pure strategies, reflected by their concentrations, and play a strategic game. Moreover, there is the Nash equilibrium and even Pareto equilibrium in the synergistic case. Since the effects of the structural relations among players depend on the system, a scale of magnitude (in terms of catalytic benefits) has been proposed: cooperation < synergetic hyperstructure << strong synergetic hyperstructure. This means that multicomponent systems may operate through sophisticated self-organizing phenomena taking place on the catalyst surface, in which both structural and chemical complexity play a role. This suggests that catalytic processes reflected by SSH and SH should exhibit better catalytic improvements over multicomponent catalysts, rather than reactions leading to one reaction product. However, experimental studies are still necessary to provide evidence of these concepts and reveal the benefits for applied catalysis.

REFERENCES

1. R.A. Van Santen, M. Neurock M., Molecular Heterogeneous Catalysis, Wiley-VCH, Weinheim (2006) pp. 61-62.
2. O. Deutshmann, H. Knözinger, K. Kochloefl, T. Turek, Heterogeneous Catalysis and Solid Catalysts, 7th ed., Weinheim, Wiley-VCH, 2009.
3. J.C. Vedrine, Appl. Catal. A 474, pp. 40-50 (2014).
4. M. Piumetti, N. Lygeros, Chem. Today 31, pp. 48–52 (2013).
5. M. Piumetti, N. Lygeros, Hadronic J. 36, pp. 177-195 (2013)
6. M. Piumetti, N. Lygeros, Chem. Today 33, pp. 48-52 (2015)
7. G. Carson, J.C. Coudurier, A. Védrine, F. Laarif, Theobald, J. Chem. Soc. Faraday Trans. I 79, pp. 1921-1929 (1983).
8. J.M.M. Millet, H. Ponceblanc, G. Coudurier, J.M. Herrmann, J.C. Védrine, J. Catal.142, pp. 381-391 (1993).
9. M. Piumetti, F.S. Freyria, B. Bonelli, Chem. Today 31, pp. 55–58 (2013).
10. A. Trovarelli, P. Fornasiero, Catalysis by Ceria and Related Materials (2nd ed.), Imperial College Press, London (2013) pp. 565-621.
11. G. Ertl, H. Knözinger, F. Schüth, J. Weitkamp, Handbook of Heterogeneous Catalysis, 2nd ed., Weinheim, Wiley-VCH (2008) pp. 3684-3700.
12. R. K. Grasselli, Top. Catal. 15, 93-101 (2001)
13. M. Boudart, J. Mol. Catal. A 138, pp. 319-321 (1999).
14. W. Curtis Conner, J.L. Falcone, Chem Rev. 95, pp. 759-788 (1995)
15. E.M. Gaigneaux, H.M. Abdel Dayem, E.Godard, P. Ruiz, Appl. Catal. A 2002, pp. 265-283 (2000).
16. G.M. Pajonk, Appl. Catal. A 202, pp. 157-169 (2002)
17. B. Delmon, Heterog. Chem. Rev. 1, pp. 219-230 (1994).
18. L.-T. Weng, B. Delmon, Appl. Catal. A 81, pp. 141-213 (1992).
19. D. Fudenberg, J. Tirole, Game Theory, MIT Press (1991)
20. J. von Neumann, O. Morgenstern, Theory of games and Economic Behavior, John Wiley Science Ed. (1964).
21. D. Delimaris, T. Ioannides, Appl. Catal. B 89, pp. 295-302 (2009).
22. F. Marty, Sur une généralisation de la notion de groupe, 8th Congress Math. Stockholm, pp. 45-49 (1934).
23. T. Vougiouklis, New Frontiers in Hyperstructures, Hadronic Press, Palm Harbor, 48 (1996).
24. T. Vougiouklis, Hyperstructures and their representations, Hadronic Press Inc., Florida (1994).
25. N. Lygeros, T. Vougiouklis, Ratio Math., 25, pp. 59-66 (2013).
26. B. Davvaz, R.B. Santilli, T. Vougiouklis, Proc. 3th Int. Conf. Treat. Irrev. Proc.. (Kathmandu University, Nepal), 1-12 (2011).
27. S. Royer, D. Duprez, ChemCatChem 3 pp. 24-65 (2011).
28. G. Ertl, Reactions at Solid Surfaces, Ed. Wiley-VCH, Hoboken, 2009.
29. D. Duprez, F. Cavani, Handbook of Advanced Methods and Processes in Oxidation Catalysis, Imperial College Press, 2014.
30. F. Cavani, F. Trifirò, Catal. Today 24, pp. 307-313 (1995)
31. F. Cavani, N. Ballarini, A. Cericola, Catal. Today 127, pp. 113–131 (2007).
32. B. Hjørland, F. Sejer Christensen, JASIST 53(11), pp. 960-965 (2002)
33. M. Piumetti, F. S. Freyria, M. Armandi, F. Geobaldo, E. Garrone, B. Bonelli, Catal. Today 227, pp. 71-79 (2014)
34. M. Piumetti, F. S. Freyria, M. Armandi, G. Saracco, E. Garrone, B. Bonelli, Chem. Today 33(3), pp. 40-45 (2015).
35. J. Cao, L. Wei, Q. Huang, L. Wang, S. Han, Chemosphere 38, pp. 565-571 (1999)
36. F.S. Freyria, B. Bonelli, R. Sethi, M. Armandi, E. Belluso, E. Garrone, J. Phys. Chem. C 115, pp. 24143-24152 (2011)
37. V. Balcaen, H. Poelman, D. Poelman, G.B. Marin, J. Catal. 283, pp. 75-88 (2011).
38. M. Piumetti, D. Fino, N. Russo, Appl. Catal. B 163, pp. 277-287 (2015).
39. P.M. Heynderickx, J.W. Thybaut, H. Poelman, D. Poelman, G.B. Marin, J. Catal. 272, pp. 109-120 (2010).
40. U. Menon, V.V. Galvita, G.B. Marin, J. Catal. 283, pp. 1-9 (2011)


Irina Yu. Chukicheva

IRINA YU. CHUKICHEVA*, ALLA A. KOROLEVA, OLGA A. SHUMOVA,
SVETLANA A. POPOVA, ALEXANDR V. KUTCHIN
*Corresponding author
Russian Academy of Sciences, Ural division, Komi Scientific Center, Institute of Chemistry
48 Pervomaiskaya Str., 167982, Syktyvkar, Republic of Komi, Russia

Alkylation of phenol with β-pinene over heterogeneous acid catalysis

KEYWORDS: Phenol, β-pinene, alkylation, heteropolyacids, terpenophenols, FIBAN K-1, KSF.

Abstract Alkylation of phenol with β-pinene at presence of heterogeneous acid catalysts FIBAN K-1, KSF, ZrO2/ SO42-, H3PW12O40/TiO2 (HPWO/TiO2) is carried out for the first time. The influence of catalysts nature and reaction temperature upon the structure and composition of products is studied. It has been found, that alkylation at 40°C at the presence of FIBAN K-1 and KSF leads to formation of the optically active para-menthene-phenylic ether with high selectivity (100 and 76 % correspondingly). The reaction under the same conditions at the presence of ZrO2/ SO42- and HPO/TiO2 passes with formation of a significant amount of phenyl-isobornylic ether. The rise of temperature up to 70-100 °C gives an increase in C-alkylated phenol derivatives. KSF is a suitable catalyst for the isocamphyl phenols formation at 100°C. At the presence of all the investigated catalysts at the range of temperatures 40-100°C the formation of para-alkylated derivatives of phenol doesn't occur.

INTRODUCTION

Alkylphenols are widely used compounds. They apply as inhibitors of thermopolymerization and stabilizers of polymers (1), antioxidants (2-5). Terpenephenols, concerning the same class of compounds, are still insufficiently studied. Meanwhile, isomerization of terpenes at presence of some catalysts (6) opens prospect of obtaining the compounds with various structure depending on conditions of synthesis of terpenephenols. Tests have shown, that mono- and di-substituted *orto*-terpenephenols are effective as stabilizers of sindyotaktic polystyrenes and elastomers (7) inhibitors of olefin thermopolymerization (8, 9) accelerators of epoxy resin cure (10). Addition of these terpenephenols in polymeric mixes promotes rise in temperature of the beginning of disintegration of polymers (11) to decrease in speed of PVC dehydrochlorination in conditions of thermo-oxydative destruction (12-14); to increase in building tack with preservation of high stability ageing a rubber mix (15-16). Researches of biological activity and toxicity of the given compounds have shown, that terpenephenols possess low toxicity (LD_{50}> 5g/kg), membrane-protective properties (17-18) and can be considered as medical antioxidants (19-21). Terpenephenolic ethers are analogues of natural compounds (22-25) and also can be applied in medicine.
The structure of terpenephenols synthesized depends on the used catalyst. It is known, that the some aluminium-containing homogeneous catalysts possess high selectivity in *orto*-alkylation of phenols (26-27) However, the use of the homogeneous catalyst demands an additional stage for processing a reactionary mix leads to corrosion of the equipment. Besides, homogeneous catalysts cannot be used repeatedly. In this connection interest to recycled ecologically safe heterogeneous catalysts (28-30) recently increases. Thus, search of effective heterogeneous catalysts for selective synthesis of terpenephenols is an actual problem.
The purpose of the given work is research of influence of the heterogeneous catalyst nature on structure of products of alkylation of phenol with β-pinene. For achievement of an object in view: the alkylation of phenol with β-pinene at presence of acid heterogeneous catalysts FIBAN K-1, KSF, ZrO_2/SO_4^{2-}, $H_3PW_{12}O_{40}/TiO_2$ and $(HPWO/TiO_2)$ is lead in various reactionary conditions; individual compounds from a reactionary mix are isolated by column adsorption chromatography. Structures of compounds obtained are characterized by spectral methods of the analysis

EXPERIMENTAL

The ^1H and ^{13}C NMR spectra were measured on Bruker Avance II 300 (300 MHz and 75 MHz) in $CDCl_3$. Chloroform shifts (δ_H 7.26, δ_C 76.90) were used as an internal standard. The assignment of the ^{13}C NMR signals was carried out using JMOD experiments. Specific rotations were measured on Kruss Optronic P3002RS polarimeter. The analysis of the volatile

products of reactions was performed on Shimadzu GC-2010AF chromatograph equipped with a flame-ionization detector and a capillary column HP-1 (60m×0.25mm×0.25μm at temperature mode 100 - 240°C, heating 6°C in a minute; gas-carrier – helium). The course of the reactions was monitored by thin-layer chromatography (TLC) on Sorbfil plates using hexane–Et_2O solvent systems. To detect the compounds the plates were treated with $KMnO_4$ solution (15g of $KMnO_4$, 300 mL of H_2O, and 0.5 mL of concentrated H_2SO_4). Column chromatography used silica gel (70-230 μ, wet packed). (1S)-(-)-â-pinene (99%) $[\alpha]_D^{20}$ = -21° (pure) and phenol were purchased from Alfa Aesar. The catalyst FIBAN K-1 was provided by scientists of the Institute of Physical Organic Chemistry, NAS of Belarus; KSF (with 8-12% free acid) – was provided by the company Acros Organics. $H_3PW_{12}O_{40}\cdot xH_2O$ was from the Acros. The titanium-supported catalyst was prepared by the impregnation of TiO_2 (Degussa Aerolist S=260 m^2/g) with aqueous solution of the corresponding HPA. The loading of HPA was 20 wt. % of the support mass. The sample was dried at 100°C for 4 h and calcined in air-flow at 400°C for 2 h. Sulphated zirconia (SO_4^{2-}/ZrO_2) was prepared by the known method(31). The cristallographic phase structure of the catalyst was defined using the X-ray SHIMADZU XRD-6000 diffractometer with Cu K_α radiation. The sample had only the tetragonal crystalline phase of ZrO_2. The surface area and the porosity of the catalyst were measured by the N_2 physical sorption method on ASAP 2400 V3.07 device. The BET surface area was 126 m^2/g and the pore volume was 0.11 cm^3/g. The sample had the total acidity of 375 μmol/g. The sulfur content was 7 wt. %.

Alkylation of phenol with (-)-β-pinene (general procedure)

The reaction was carried out in a glass reactor equipped with a magnetic stirrer at 40, 69 and 100°C. A mixture of phenol 1 (2g, 21 mmol), (-)-â-pinene (3mL, 21 mmol) and ZrO_2/SO_4^{2-} (10% w/w based on 1) or KSF (100% w/w base on **1**) or FIBAN K-1 (10% w/w based on 1) or $HPWO/TiO_2$ (10% w/w based on 1) was refluxed in a solvent (CH_2Cl_2, C_6H_{14}, C_7H_{16}) at intensive stirring in Ar atmosphere. After 6h the reaction mixture was cooled to room temperature, and the catalyst was filtered and washed with Et_2O (2x30 mL). The solvent was removed under reduced pressure. The reaction products were separated by column chromatography (silica gel, 70-230 mesh) using n-hexane – diethyl ether mixture as an eluent. The selectivity of the reaction products is presented in Table 1. The structure of the compounds obtained was confirmed by NMR spectrometry.

Spectral characteristics of the obtained compounds 3 a-c, 4, 5, 6 a-c, 7a correspond to the published data(32,33).

2-(1,7,7-Trimethylbicyclo[2.2.1]hept-*endo*-2-yl) phenol (3c): $[\alpha]_D^{23}$ = +43.1(c 0.7; $CHCl_3$). 2-(1-isopropyl-4-methylcyclohexyl-3-enyl) phenol (3e): viscous oily light brown liquid. Found, %: C, 83.15, H, 9.52. $C_{16}H_{22}O$. Calculated, %: C, 83.43, H, 9.63. ^{1}H NMR spectrum (300 MHz, $CDCl_3$, δ, ppm, J/Hz): 1.26 (d, 6H, 3Hz, CH_3-8, CH_3-9), 1.41-1.47 (m, 1H, H-5), 1.72 (s, 3H, CH_3-10), 1.87-2.20 (m, 6H, H-3, H-5, H-6, H-7), 5.46 (m, 1H, H-2), 5.29 (s, 1H, OH), 7.00 (d, 2H, J = 9 Hz, H-12, H-16), 7.09 (m, 1H, J = 9 Hz, H-14), 7.29 (m, 2H, J = 9 Hz, H-13, H-15). ^{13}C NMR spectrum (75 MHz, $CDCl_3$): 23.38 (C-8, C-9), 24.17 (C-5), 24.51 (C-10), 27.14 (C-3), 31.7 (C-6), 43.93 (C-7), 82.66 (C-4), 120.73 (C-14), 123.05 (C-2), 124.16 (C-12, C-16), 128.83 (C-13, C-15), 134.11 (C-1), 155.48 (C-11).

2-(3-Isopropyl-6-methylcyclohexyl-2-enyl)phenol (3f): viscous oily light brown liquid. Found, %: C, 83.01, H, 9.00. $C_{16}H_{22}O$. Calculated, %: C, 83.43, H, 9.63. ^{1}H NMR spectrum (300 MHz, $CDCl_3$, δ, ppm, J/Hz): 0.75 (m, 3H, CH_3-10), 0.90 (d, 6H, CH_3-8, CH_3-9), 1.27-1.32 (m, 1H, H-5), 1.39-1.43 (m, 3H, H-4, H-5, H-6), 1.75 (m, 1H, H-6), 2.17-2.27 (m, 1H, H-7), 2.86 (m, 1H, H-3), 5.49 (m, 1H, H-2), 5.74 (s., 1H, OH), 6.81-6.85 (m, 1H, H-13), 7.06-7.12 (m, 2H, H-14, H-15), 7.20-7.29 (m, 1H, H-16). ^{13}C NMR spectrum (75 MHz, $CDCl_3$): 16.54 (C-10), 20.08 (C-8, C-9), 24.51 (C-10), 25.56 (C-6), 30.32 (C-5), 33.85 (C-4), 35.02 (C-7), 37.19 (C-3), 115.03 (C-13), 117.97 (C-15), 122.78 (C-2), 127.35 (C-14), 129.69 (C-16), 138.86 (C-11), 143.46 (C-1), 153.73 (C-12).

1,3,3-Trimethyl-2-phenoxybiciclo[2.2.1]heptane (6d): colorless oily liquid. Found, %: C, 83.67, H, 8.86. $C_{16}H_{22}O$. Calculated, %: C, 83.43, H, 9.63. ^{1}H NMR spectrum (300 MHz, $CDCl_3$, δ, ppm, J/Hz): 0.93 (s, 3H, CH_3-9), 1.03-1.09 (m, 2H, H-5, H-7), 1.14 (m, 1H, H-6), 1.17 (s, 3H, CH_3-8), 1.24 (s, 3H, CH_3-10), 1.40-1.45 (m, 1H, H-6), 1.50-1.59 (m, 2 H, H-6, H-7), 1.80-1.88 (m, 1H, H-4), 2.09-2.13 (m, 1H, H-5), 3.93 (s, 1H, H-2), 6.95 (d, 2H, J = 9 Hz, H-12, H-16), 7.30 (m, 3H, H-13, H-14, H-15). ^{13}C NMR spectrum (75 MHz, $CDCl_3$): 19.96 (C-8), 20.49 (C-10), 25.93 (C-5), 26.44 (C-6), 30.57 (C-9), 33.53 (C-3), 41.47 (C-7), 49.16 (C-4), 49.62 (C-1), 90.11 (C-2), 115.86 (C-12, C-16), 120.08 (C-14), 129.32 (C-13, C-15), 151.66 (C-11).

(1-Isopropyl-4-methylcyclohexyl-3-eniloxy)benzene (6e): colorless oily liquid. Found, %: C, 83.84, H, 8.90. $C_{16}H_{22}O$. Calculated, %: C, 83.43, H, 9.63. $[\alpha]_D^{23}$ = -43.1 (c 0.7; $CHCl_3$). ^{1}H NMR spectrum (300 MHz, $CDCl_3$, δ, ppm, J/Hz): 1.27 (d, 6H, J = 3 Hz, CH_3-8, CH_3-9), 1.44-1.48 (m, 1H, H -5), 1.73 (s, 3H, CH_3-10), 1.88-2.18 (m, 6H, H-3, H-5, H-6, H-7), 5.46 (m, 1H, H-2) , 7.01 (m, 2H, H-12, H-16), 7.28 (m, 2H, H-13, H-14, H-15). ^{13}C NMR spectrum (75 MHz, $CDCl_3$): 23.39 (C-8, C-9), 24.19 (C-6), 24.52 (C-10), 27.16 (C-5), 31.9 (C-3), 43.95 (C-7), 82.64 (C-4), 120.75 (C-12, C-16), 123.06 (C-2), 124.17 (C-14), 128.84 (C-13, C-15), 134.09 (C-1), 155.49 (C-11).

Reaction conditions	Conversion, %	Products relationship, %												
		3a	3b	3c	3e	3f	4	5	6a	6b	6c	6d	6e	7a
ZrO_2/SO_4^{2-}														
40°C, 24h	57	-	-	9	-	6	13	-	11	59	2	-	-	-
100°C, 2h	81	17	2	5	-	17	10	8	10	23	8	-	-	-
FIBAN K-1														
40°C, 6h	56	-	-	-	-	-	-	-	-	-	-	-	100	-
70°C, 6h	96	34	4	-	-	-	4	5	-	40	2	11	-	-
$HPWO/TiO_2$														
40°C, 24h	34	-	-	-	5	-	-	43	4	43	5	-	-	-
100°C, 12h	82	-	7	4	26	30	-	18	8	4	-	-	-	-
KSF														
40°C, 6h	59	24	-	-	-	-	-	-	-	-	-	-	76	-
70°C, 6h	93	21	7	36	-	-	5	1	-	17	7	-	-	12
100°C, 3h	100	45	4	-	-	6	7	4	-	-	19	-	-	15

Table 1. Reaction conditions and products of phenol alkylation with β-pinene at heterogeneous catalysis.

RESULT AND DISCUSSION

The catalytic activity and the selectivity for the phenol alkylation with (-)-β-pinene are demonstrated in Table 1. The products structure and composition are presented on Figure 1. The experiments were carried out in boiling dichloromethane (at 40°C), in boiling hexane (at 70°C) and in some cases in boiling heptane (at 100°C) at equimolecular ratio of phenol and (-)-β-pinene. The general tendency of this reaction is the conversion increase and selectivity decrease with the rise of temperature. Ethers of phenol are formed at temperature 40° in most cases.

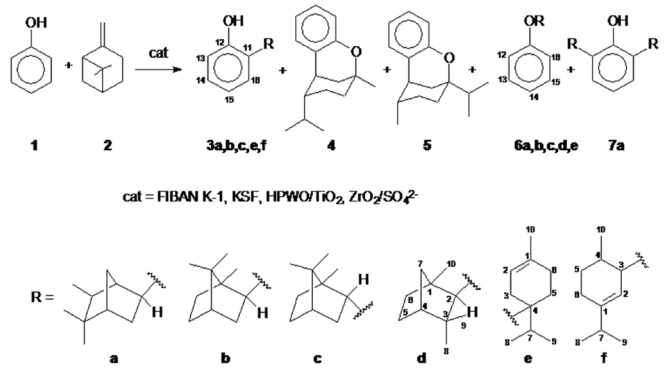

Figure 1. Products structure and composition.

The structure of the terpenic substituent depends on the applied catalyst. At the presence of FIBAN K-1 and KSF the *p*-menthylic ether of phenol 6e with the selectivity of 100 and 76% was obtained respectively. At the presence of ZrO_2/SO_4^{2-} and $HPWO/TiO_2$ at 40°C the isobornylphenylic ether 6b is mainly formed (with the selectivity of 59 and 43% respectively).

The interaction of phenol with (-)-β-pinene at 70 and 100°C gives a set of C- and O-alkylated products with various structures of terpenic substituent. The reaction over FIBAN K-1 leads to the formation of 2-isocamphyl phenol 3a (34%) and isobornylphenylic ether 6b (40%). Alkylation with KSF at 70°C gives 2-bornyl phenol 3c (36%) while at 100°C it gives 2-isocamphyl phenol 3a (45%). The interaction of phenol with (-)-β-pinene at the presence of supported heteropolyacid $HPWO/TiO_2$ at 100°C results in 2-terpenophenols 3e and 3f with the *p*-menthenic structure of the substituent (26 and 30% respectively). The under the same conditions reaction with use of ZrO_2/SO_4^{2-} passes with a low selectivity.

The structural variety of the terpenophenols obtained is the consequence of intermolecular rearrangements of

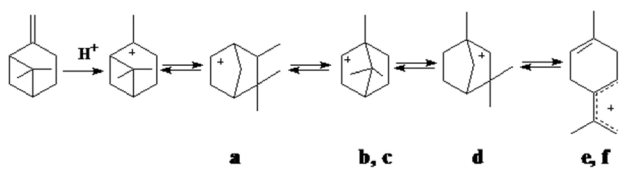

Figure 2. Structure of obtained terpenophenols.

(-)-β-pinene and its four-member cycle disclosing. These rearrangements can be presented as equilibrium between classical cations (Figure 2).

It should be noted that 2-isobornyl phenol 3b which is formed by intermolecular rearrangements of (-)-β-pinene does not possess optical activity in contrast to 2-bornyl phenol 3c. This fact is explained in Figure 3 showing the interaction of phenol with a non-classical cation formed from (-)-β-pinene.

Figure 3 shows that the coordination of phenol with this ion from the opposite side of the terpenic bridge is preferable and therefore leads to 2-bornyl phenol 3c.

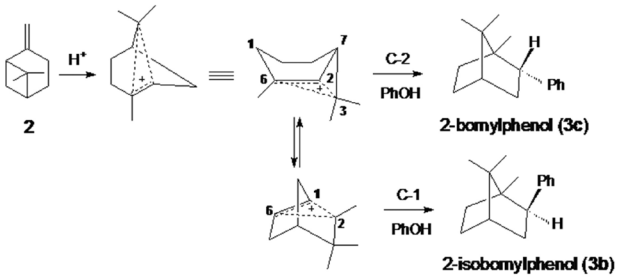

Figure 3. Interaction of phenol.

It is interesting that the alkylation of phenol with β-pinene over FIBAN K-1 leads to the formation of optically-active *p*-menthylic ether of phenol 6e with the selectivity of 100%. The addition of terpene to phenol oxygen corresponds to the mechanism proposed for the interaction of phenols with olefins(34, 35). However, considering the nature of the catalyst (FIBAN K-1) and alkylant ((-)-β-pinene) it is possible to offer an explanation for the formation of optically-active ether 6e (Figure 4).

FIBAN K-1, a fibrous sulphuric cation exchanger, is a sulphurated copolymer of styrene and divinylbenzene. First, (-)-β-pinene interacts with the sulphuric group of the catalyst. The research of the thermal stability of FIBAN K-1 has shown the presence of H_2O^+ ions in the reaction media at 40-50°(36). Therefore the next step is the disclosing of β-pinene minor cycle under the influence of H_2O^+ ions. Finally, the O-alkylation occurs. Possibly, the spatial orientation of the isopropylic fragment of *p*-menthene allows the phenol attack only from the less hindered side that leads to the formation of the optical-active ether 6e.

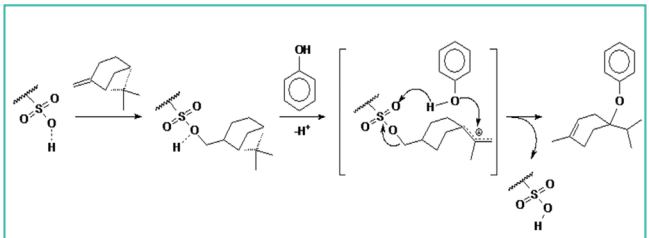

Figure 4. Formation of the optically-active ether 6e.

Most likely the reaction at 70°C occurs by the ionic pathway that explains the isomerization of the terpenic substituent in alkylated products.

The formation of *p*-alkylated derivatives of phenol doesn't occur at 40-100°C in the presence of all the investigated catalysts.

CONCLUSIONS

Heterogeneous acid catalysts (KSF, FIBAN K-1, HPWO/TiO_2, ZrO_2/SO_4^{2-}) were studied during phenol alkylation with (-)-β-pinene at 40°C, 70°C and 100°C.
The following observations were made.
The alkylation of phenol with (-)-β-pinene at the presence of all the investigated heterogeneous acid catalysts passes with greater selectivity at 40°C, than at 70 and 100°C.
(β)-Pinene undergoes various rearrangements in acid media. Isomerization of (-)-β-pinene depends on the type of a catalyst and the reaction conditions. In particular, ethers with *p*-menthene fragment 6e are the main products at 40°C at the presence of FIBAN K-1 and KSF; at the presence of $ZrO_2/SO_4^{2-}$and HPWO/TiO_2 at the same temperature the main products is phenylisobornyl ether.
KSF is a suitable catalyst for the isocamphyl phenols 3a and 7a formation at 100°C.
The formation of *p*-alkylated derivatives of phenol doesn't occur at 40-100°C in the presence of all investigated catalysts.

ACKNOWLEDGEMENTS

The research was executed due to the financial support of the Russian fund of the basic researches. (Grants № 10-03-31577; № 12-03-00900)

REFERENCES AND NOTES

1. Nikulicheva, O.N., Fadeeva, V.P., Logvinenko, V.A. Estimation of thermal stability of phenol stabilizers, by means of thermogravimetric analysis, *Journal of Thermal Analysis*, 44 (2), 332-336 (1995)
2. Harlampovich, G.D., Churkin, I.V. *Fenoly*. Khimia, Moscow, USSR (1974)
3. Menshchikova, E.B. Lankin, V.Z. Kandalitseva, N.V. *Fenolnye antioksidanty v biologii i meditsine*. LAP LAMBERT Academic Publishing, Moscow, Russian Federation (2012)
4. Zhang, Y., Shen, Y., Zhu, Y., et al. Assesment of the correlations between reducing power, scavenging DPPH activity and anti-lipid-oxidation capability of phenolic antioxidants, *Food Science and Technology*, 63 (1), 570-573 (2015)
5. Mateos, R., Madrona, A., Pereira-Caro, G., et al. Synthesis and antioxidant evaluation of isochroman-derivatives of hydroxytyrosol, *Food Chemistry,* 173, 313-320 (2015)
6. Gusevskaya, E. V. Reactions of Terpenes Catalyzed by Heteropoly Compounds: Valorization of Biorenewables, *ChemCatChem,* 6 (6), 1506-1515 (2014);
7. Novakov, I.A., Novopoltseva, O.M., Solovieva, Yu.D., Kutchin, A.V., Chukicheva, I. Yu.: Techlologia Polymerov, *Khimicheskaya promyshlennost segodnya,* 12, 25—31 (2012)
8. Batura, I.I., Chukicheva, I. Yu., Gogotov, A.F., et al. *Patent RU 2375342* (2009)
9. Batura, I.I Gogotov, A.F., Levchuk, A.A Shaganskaya, et al. *Patent RU 2387631* (2010)
10. Fedoseyev, M.S., Tereshatov, V.V., Strelnikov, V.N., et al. *Technical Chemistry: From Theory to Praxis,* Edited by Vladimir N. Strelnikov and Viktor A. Valtsifer. Cambridge Scholars Publishing, Newcastle upon Tyne, United Kingdom (2011)
11. Novakov, I.A., Novopoltseva, O.M., Solovieva, Yu.D., et al. Assessment of stabilizing action of terpenophenols on thermooxidative destruction of rubber mixtures on base of butadiyen-styrene rubbers, *Izvestia Vuzov Khimia i Khimicheskaya Tekhnologia,* 12, 90-96 (2012)
12. Ahmetkhanov, R.M., Kolesov, S.V., Kuchin, A.V., et al. *Patent RU 2458948* (2012).
13. Gabitov, I.T., Ahmetkhanov, R.M., Kolesov, S.V., et al. 4-metyl-2,6-diisobornylphenola na termoystoychivost' polyvinilchlorida, *Vestnik Bashkirskogo universiteta,* 17 (1), 48-52, (2012)
14. Gabitov, I.T., Astafurova, E.A., Ahmetkhanov, R.M., et al. Termookislitelnii raspad polyvinilchlorida v prisutstvii 4-metil-2,6-diisobornilphenola, *Enziklopediya ihzhenera-khimika*, *7*, 9-15 (2012)
15. Novakov, I.A., Novopoltseva, O.M., Soloviova, Yu.D., et al. *Patent RU 2507225* (2014).
16. Novakov, I.A., Novopoltseva, O.M., Soloviova, Yu.D., et al. *Patent RU 2516644* (2014).
17. Shishkina, L.N., Shevchenko, O.G., Chukicheva, I.Yu., et al. *New Steps in Physical Chemistry, Chemical Physics and Biochemical Physics,* Edited by Gennady E. Zaikov, Eli M. Pearce, Gerald Kirshenbaum, NOVA Publishers, New York, USA (2013)
18. Marakulina, K.M., Kramor, R.V., Lukanina, Yu.K., et al. *The Science and Engineering of Sustainable Petroleum,* Edited by Rafiq Islam. NOVA Publishers, New York, USA (2013)
19. Shevchenko, O.G., Plusnina, S.N., Shishkina, L.N., et al. The Membrane Protective Properties of Isobornylphenols – New Class of Antioxidants, *Biologicheskie membrany,* 30 (1), 40-51 (2013)
20 Plotnikov, M.B., Smolyakova ,V.I., Ivanov, I.S., et al. Synthesis and biological activity of O-isobornylphenol derivatives, *Pharmaceutical Chemistry Journal,* 44 (10*),* 530-533 (2011)
21. Logvinov, S.V., Plotnikov, M.B., Zdankina, A.A., et al. Morphological changes in retinal neurons in streptozotocin-induced Diabetes Mellitus and their correction with an isobornylphenol derivative, *Neuroscience and Behavioral Physiology*, 40 (7), 779-782 (2010)
22. Semenov, A.A. *Ocherk khimii prirodnykh soedineniy,* Nauka, Novosibirsk, Russian Federation (2000)
23. Plemenkov, V.V. *Vvedenie v khimiyu prirpdnykh soedineniy,* Khimia, Kazan, Russian Federation (2001)
24. Kukovinets, O.S., Zainullin, R.A., Kislitsyn, M.I. Natural arylterpenes and their biological activity, *Chemistry of Natural Compounds,* 42 (1), 1-7 (2006)
25. Devinsky, O., Cilio, M. R., Cross, H., et al. Cannabidiol. Pharmacology and potential therapeutic role in epilepsy and other neuropsychiatric disorders, *Epilepsia,* 55(6), 791-802 (2014)
26. Kolka, A. J., Napolitano, J. P., Ecke, G. G. The ortho-Alkylation of Aromatic Amines*, The Journal of Organic Chemistry*, 22(6), 639-642 (1957);
27. Chukicheva, I.Yu., Kutchin, A.V. Prirodnye I sysnteticheskye terpenophenoli, *Rossiiskyi Chimicheskyi Zhurnal* 48(3) 21-25 (2004)
28. Kaur, M., Sharma, S., Bedi, P. M. S.: Silica supported Brönsted acids as catalyst in organic transformations: A comprehensive review, *Chinese Journal of Catalysis,* 36 (4), 520-549 (2015)
29. Hajipour, A. R., Karimi, H. Zirconium phosphate nanoparticles as a remarkable solid acid catalyst for selected solvent-free alkylation of phenol, *Chinese Journal of Catalysis,* 35 (7), 1136-1147 (2014)
30. Jiang, T., Cheng, J., Liu, W et al. Sulfuric acid functional zirconium (or aluminum) incorporated mesoporous MCM-48 solid acid catalysts for alkylation of phenol with tert-butyl alcohol, *Journal of Solid State Chemistry,* 218, 71-80 (2014)

Readers interested in a full list of references are invited to visit our website at **www.teknoscienze.com**

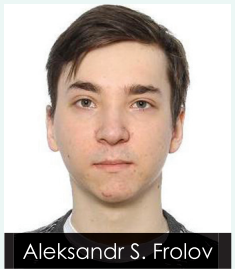
Aleksandr S. Frolov

ALEKSANDR S. FROLOV[1]*, EKATERINA A. KURGANOVA[1], GEORGIY N. KOSHEL[1], VALENTIN N. SAPUNOV[2]
*Corresponding author
1. Yaroslavl state technical university, Yaroslavl, Russia
2. D.I. Mendeleev Russian Chemical-Technological University, Moscow, Russia

Preparation of dimethyl-substituted cumene hydroperoxides

KEYWORDS: N-hydroxyphthalimide, catalysis, oxidation, hydroperoxides of aromatic compounds, dimethyl-substituted cumene, mathematical modeling, decomposition.

Abstract The article investigates the kinetics of the oxidation reaction of dimethyl cumene to hydroperoxides with molecular oxygen in the presence of N-hydroxyphthalimide.. In order to obtain information on the kinetic laws related to the process of dimethyl cumene oxidation in the presence of N-hydroxyphthalimide, a series of experiments was conducted. The experimental data related to the kinetics of hydroperoxides and non-reaction products formation provided the mathematical model that adequately describes the change of all components of the reaction at the time.
It was established that the role of N-hydroxyphthalimide as the initiator of the process is determined by the fact that its interaction with oxygen results in the stationary concentration of N-phthalimide radicals, which initiate oxidation process in their interaction with hydrocarbon.
The experimentally tested high-selective method used for the synthesis of hydroperoxides by liquid-phase catalytic dimethyl cumene oxidation can become the basis of a single universal method for producing xylenols that meets the latest environmental and economic requirements. The suggested mathematical model of the dimethyl cumene oxidation to hydroperoxides in the presence of NHPI is original and may be of interest for calculating the kinetics of similar reactions involving other alkylaromatic hydrocarbons.

INTRODUCTION

The liquid phase oxidation of alkylaromatic hydrocarbons serves as the basis for constant development of the new methods for producing various oxygenated compounds, which are widely used in the synthesis of polymeric materials. The production sector is familiar with such processes as the "cumene" method of preparation of phenol and acetone or joint synthesis of styrene and propylene oxide (the "chalcone" process) (1). These processes are based on the selective preparation of the corresponding hydroperoxides. The appearance of the new method of selective production of hydroperoxides using N-hydroxyphthalimide (NHPI) significantly expands the range of refinable raw materials and, consequently, the resulting products of petrochemical synthesis (2, 3). In particular, this method provides synthesis of valuable organic products by obtaining various alkylaromatic hydroperoxides, which is practically impossible by using conventional methods (4). Thus, for example, one of the promising methods is the method used for producing xylenes from xylenols through preparing by-products - isopropyl derivatives, and the corresponding hydroperoxides (5).

The use of NHPI for the selective oxidation of various radical reactions is well known (6). Despite the great scientific and practical importance of these processes, including aerobic oxidation of arenes to the HP, the mechanism of these processes is little studied.

Along with studies related to the oxidation of alcohols, they dealt with issues related to the use of NHPI in combination with metal salts of mixed valence in the oxidation of adamantans to alcohols and ketones (2).
One of the first studies on the use of NHPI in the oxidation of benzyl hydrocarbon oxidation was devoted to fluorene oxidation (7). The studies (2, 8, 9) present data on the oxidation of alkylaromatic compounds to carbonyl compounds in the presence of NHPI. The research paper (9) provides detailed study of the preparation of 1,3,5-triacetoxybenzol from 1,3,5-triisopropylbenzol by oxidation of the latter with the use of NHPI and the initiator in the solvent.
Studies, devoted to direct oxidation of cyclohexane to hexandioic acid are of particular interest. It was established that introducing NHPI together with salts of cobalt and manganese allows direct oxidizing of cyclohexane to hexandioic acid. It was shown that by using the catalyst system NHPI / Mn $(acac)_2$ adipic acid yield made approximately 73% (2, 10). In (2, 11) the authors suggested using NHPI as a catalyst for the oxidation of alkenes and alkynes to carbonyl compounds.
The research provided by the Italian scientists Francesco Recupero and Carlo Punta with their colleagues was devoted to the study of aerobic oxidation of alkyl benzenes with NHPI in combination with salts of mixed valency(3). In (12), the authors examined the use of NHPI in the oxidation of cumene

for industrial purposes, as well as the ways of regeneration of this catalyst. The authors also discussed the possibility of using NHPI in processes of liquid phase oxidation of tertiary alkylaromatic hydrocarbons to hydroperoxides in combination with various solvents (acetaldehyde diethyl acetaldehyde, 2,2-dimetilpropanal etc.) (13). Thermochemical and kinetic aspects related to oxidation of alkylaryl ketones to aromatic carboxylic acids, alkyl cyclopropyl ketones to cyclopropane carboxylic acids and cycloalkanones to dicarboxylic acids, occurring in the presence of phthalimide catalysts and salts of Mn (II), Co (II), Cu (II), were discussed in detail in (14). Study of the catalytic activity of nitroxide radicals having various substituents on the nitrogen atom, as well as the study of the oxidation mechanism in the presence of phthalimide compounds was discussed in (15).
Research works carried out by Opeida and his staff deal with the mechanism of oxidation of alkylaromatic hydrocarbons (16) to hydroperoxides. Recent studies established (17) that the interaction of NHPI molecule with the initiator radical or peroxide radical (ROO ●) of the oxidizing agent results in the formation of the N-oxyl phthalimide radical (PINO ●), which is capable to tear off a hydrogen atom from the C-H bonds of alkyl arenes (RH) with high selectivity to form the corresponding alkyl radicals (R ●). The resulting C-centered radical in the presence of oxygen is converted into a peroxyl radical, which in turn reacts with NHPI and forms PINO ● and HP (ROOH).

The studies (18-20) proposed to carry out the oxidation in the presence of NHPI, in a polar solvent. For example, the oxidation of cumene in acetonitrile in the presence of N-GPI together with an initiator at 60°C in 3 hours provides hydrocarbon conversion at a rate of 40% and HPA selectivity at a rate of 100% (19). Another method of increasing the efficiency of cumene oxidation to the HP is the modification of the original N-GPI. The use of lyotropic N-GPI derivatives (4-hexyloxycarbonyl, 4-dodecyloxycarbonyl, 4-hexadecyloxycarbonyl) in the absence of solvent provided approximately three-fold increase in the rate of cumene oxidation (18).
The analysis of research works shows that a large number of works (21) are devoted to studies related to the use of NHPI as a catalyst for various processes, and the interest in these issues is increasing every year, however, the information on the liquid-phase oxidation of alkyl aromatic hydrocarbons to hydroperoxides and mechanisms of this process is quite limited, and the issues of isopropyl xylene oxidation were not studied. In this regard, a large number of studies were carried out by G.N. Koshel' and his co-workers (22-26). Therefore, research in this field is important and relevant, as it allow clarifying the questions related to kinetics and mechanism of reactions involving NHPI, and the oxidation of hydrocarbons is the basis of long-term method of obtaining xylenols.

METHODS AND MATHERIALS

Materials

DMCs were prepared through alkylation of o-, m-, p-xylenes by isopropyl alcohol in the presence of concentrated sulfuric acid (20° C, the molar ratio of xylene: IPA: sulfuric acid made 3: 1: 3, the reaction time made 4 hours). After this reaction, the hydrocarbon layer was separated from the aqueous sulfuric acid solution, washed with water until neutral reaction, dried over calcium chloride. The resulting alkylate was subjected to distillation in vacuo. The DMC composition was confirmed by the GLC, IR and NMR ^{1}H (Table 1). The purity of 2.5 dimethyl cumene (2,5-DMC, 3-isopropyl-1,4-dimethylbenzene) and 3,4-dimethyl cumene (3,4-DMC, 4-isopropyl-1,2-dimethylbenzene) made > 99% wt. 3,5-DMC consisted of two isomers: 92% of 5-isopropyl-1,3-dimethylbenzene and 8% of 4-isopropyl-1,3-dimethylbenzene. The results of physical-chemical analysis of the samples are shown in Table 1.

Substance	T_{BP},°C	d_4^{20}	n_D^{20}	IR-spectum (KBr), cm^{-1}	NMR ^{1}H (400 Mhz), δ, ppm.
2- isopropyl-1,4-dimethylbenzene (2,5-DMC)	195	0.869	1.4962	2961, 2924, 2890, 2870 (ν CH_3); 1382, 1362 (δ -$CH(CH_3)_2$); 3099, 3006, (=CH arom.); 1505, 1578, 1505 (aromatic ring); 818, 879 (substitution 1,2,4).	7.02 m (1H, H-3, ^4J = 1.25), 6.98 m (1H, H-6, ^3J = 6.71), 6.85 m. (1H, H-5, ^3J = 6.71, ^4J = 1.25), 3.11-2.99 m (1H, H-2), 2.24 s (3H, 1-CH_3), 2.23 s (3H, 4-CH_3), 1.19-1.14 m (6H, 2'-CH_3, 2''-CH_3)
4-isopropyl-1,2-dimethylbenzene (3,4-DMC)	202	0.880	1.5034	2962, 2925, 2869, (ν CH_3); 1383, 1362 (δ -$CH(CH_3)_2$); 3041, 3017, (=CH arom.); 1502, 1459 (aromatic ring); 806, 880 (substitution 1,2,4).	7.02 m (1H, H-6, ^3J = 7.68), 6.98 m (1H, H-3, ^4J = 1.33), 6.92 m (1H, H-3, ^3J = 7.68, ^4J = 1.33), 2.82-2.75 m (1H, H-4), 2.18 s (3H, 2-CH_3), 2.16 s (3H, 1-CH_3), 1.19-1.13 m (6H, 4'-CH_3, 4''-CH_3)
3,5-DMC	194	0,865	1,4955	2960, 2922, 2869, (ν CH_3); 1382, 1362 (δ -$CH(CH_3)_2$); 3016 (=CH arom.); 3015, 1605, 1502, 1459 (aromatic ring); 883, 816 (substitution 1,2,4); 883, 846 (substitution 1,3,5).	6.82 д (2H, H-4, H-6, ^4J = 1.26), 6.78 т (1H, H-2, ^4J = 1.26), 2.85-2.71 м (1H, H-5), 2.28 м (6H, 1-CH_3, 3-CH_3), 1.21-1.12 м (6H, 5'-CH_3, 5''-CH_3)

Table 1. Results of dimethyl cumene identification according to IR and NMR^{1}H analysis

NHPI was synthesized by reaction of hydroxylamine hydrochloride in pyridine with phthalic anhydride. The flask equipped with a stirrer, reflux condenser and thermometer was charged with 0.11 mol of NH_2OH * HCl and 150 ml of pyridine. 0.1 mole of phthalic anhydride was rapidly added at 30 ° C, and stirring continued until a clear solution (42°C). Pyridine was distilled off from the solution using the rotary evaporator under water pump vacuum; the hot viscous residue was quickly poured into 200 mL of acetic acid. NHPI precipitate was separated, washed on the filter with 0.01 n with acetic acid and dried in vacuo. The NHPI melting point made 231.5°C (according to the reference data T mp = 233 °C).
The structure of NHPI was confirmed by IR spectroscopy.

Testing apparatus

Analysis of the starting materials and products of oxidation was performed by GLC, IR and ^{1}H NMR spectroscopy. Chromatographic analysis was performed on a chromatograph "Chromatek-crystal 5000.2" with a plasma-ionization detector. The capillary column SC-5, length 30 m, diameter 0.32 mm, was filled with (5%) phenyl (95%) dimethylpolysiloxane. Nitrogen was chosen as carrier gas; its flow rate made 2 cm^3 / min. Programmed temperature rise - from 80 to 200°C at a rate of 8°C per minute. The infrared spectroscopic analysis was performed on the IR RX-1 equipment. Spectrum processing was carried out under the program «Spectrum», provided by PerkinElmer. The spectra were recorded within the range of 4000 - 400 cm^{-1} as a microlayer between the panes of potassium bromide and potassium bromide cuvette with d = 0.0011 cm. ^{1}H NMR spectra were recorded on a Bruker DRX400 spectrometer (400 MHz). Solvent: DMSO-d_6, internal standard - TMS (27).

Experimental

In order to obtain information on the kinetic mechanisms of DMC oxidation in the presence of oxidation catalyst - NHPI,

a series of experiments were carried out for obtaining isopropyl hydroperoxide derivatives of ortho-, meta- and para-xylene mentioned above. Reactions were carried out at constant temperature, changing it in the range of 110 - 140° C. The concentration of NHPI remained constant and made 2.0% wt. The DMC oxidation was carried by the atmospheric oxygen in a glass reactor with a capacity of 10 cm^3 using the flow-closed type of equipment with constant and intensive stirring in the presence of N-hydroxyphthalimide catalyst in an amount of 2-2.5 wt% of the hydrocarbon load (0.1656 mol / kg of hydrocarbon). The reaction was monitored by the absorption of oxygen; the oxidation was conducted in a kinetic mode where the rate of reaction was not dependent on the stirring intensity.

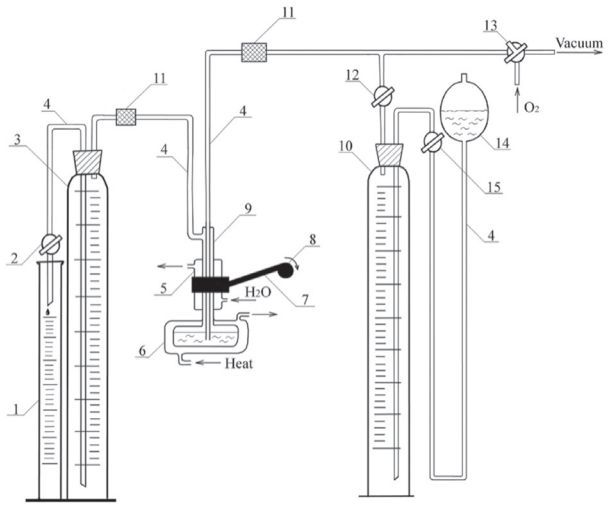

Figure 1. The scheme of kinetic installation for liquid-phase DMC oxidation.

1 - graduated cylinder; 2, 12, 15 - valves; 3, 10 - gas burettes; 4 – joining vacuum hose; 5 - holder of the reactor; 6 - reactor; 7 - motor pulley; 8 - rod; 9 - fridge; 11 - calcium chloride tube; 13 - three-way valve; 14 - pressurized bottle.

The installation was used in the following way (Figure 1): 3 cm^3 hydrocarbon and a calculated amount of catalyst or initiator were introduced into the reactor-oxidant (6) via dropping funnel. The reactor was connected to gas burettes via the vacuum hose (all valves closed), then the cooled water was turned on. Then the installation (using valve 13) was repeatedly and sequentially joined with a vacuum pump and with a balloon filled with oxygen to remove the air and then the burette was filled with oxygen by opening the valves. After the installation was filled with oxygen, it was disconnected from the external environment by turning the valve 13, the oxidation reactor was supplied with water heated to the desired temperature, from the thermostat. By using the pressurized bottle (14), slight overpressure was created in the system (20-40 Mmhg). The exhaust gases from the reaction zone were tapped by opening the valve 2. The gas tapping rate was set so that its further increase did not increase the rate of oxygen absorption. At the same time the amount of oxygen in the burette 10 and the graduated cylinder 1 was measured and then the shaker was turned on. The volume of exhaust gases in burette (13) was determined by the volume of fluid displaced in a graduated cylinder 1. At regular intervals using pressurized bottle 14, the system pressure was equalized with the atmospheric pressure and the amount of gas in both burettes was measured. After the required amount of oxygen was absorbed, valves 12, 2 and 15 were closed, and the reactor was disconnected from the system. After each experiment the oxidant was analyzed as regards the content of hydroperoxide and organic acids, and the process selectivity was calculated as the ratio of oxygen required for obtaining the specified amount of HP to the total amount of absorbed oxygen. The analysis of primary and secondary products of DMC oxidation indicates predominant oxidation of isopropyl group. Products of methyl groups' oxidation were not detected.

The mathematical model and justification of calculation methods

In order to analyze the patterns of the studied process, the authors modified the well-known kinetic model of oxidation of alkyl aromatic hydrocarbons, which has been successfully tested by several authors (28-30). This model includes equations related to the consumption rate of source hydrocarbon [RH] (Eq. 1), the formation of hydroperoxide [ROOH] (Eq. 2) and the expression for the concentration of peroxyl radicals [ROO ●] (Eq. 3) obtained given the equality of initiation rate of (r_0) and chain termination.

$$-d[RH]/dt = (k_0[RH] + k_{01}[NHPI]) \cdot [ROO^*] + f \cdot k_1[ROOH] + r_0 \quad (1)$$

$$d[ROOH]/dt = (k_0[RH] + k_{01}[NHPI]) \cdot [ROO^*] - k_1[ROOH] \quad (2)$$

$$[ROO^*] = \sqrt{r_0 + f \cdot k_1[ROOH]}/\sqrt{2k_t} \quad (3)$$

where [ROO●] – peroxide radical,

r_0 – initiation rate.

k_0 – interaction rate of peroxide radicals with hydrocarbon.

k_{01} – interaction rate constant of the peroxide radical to NHPI.

k_1 – rate constant of the hydroperoxide decomposition.

k_t – Quadratic termination constant.

f – proportion of radicals formed from one molecule of hydroperoxide and initiate a chain reaction.

The equation (Eq. 1) was supplemented by a therm that takes into account the consumption rate of [RH] in its interaction with the radicals formed during initiation (i.e., consumption rate of hydrocarbon). Earlier, in the oxidation of p-cymene, the authors showed the need to include this therm into the general kinetic scheme of oxidation processes in the presence of NHPI (24).

Besides the peroxyl radical, the PINO ● radical was also engaged in the development of chain process in the presence of NHPI. Therefore, the equations of [RH] consumption and the [ROON] formation (Eqs. 1 and 2, respectively), include the new component that reflects the new route of the reaction (24).

Due to the fact that the selectivity of [ROOH] formation was quite high and is within 87% (28) - 90% (31) and in

the presence of NHPI exceeds 92.3% (28) , even at 40% conversion, the analysis of [RH] consumption and the [ROOH] formation is complicated by the statistical error in the determination of their concentrations. In other words, the therms in equations (Eq. 1) and (Eq. 2), which did not include dependence on peroxide radical largely correlated with each other. For example, the correlation coefficient (R^2) indicating experimental values of *n*-cymene consumption and the hydroperoxide formation is almost equal to 1 (24). In this regard, the most informative data include formation patterns of by-products and not hydroperoxide reaction products (Pr). It is clear that the change in the source hydrocarbon or hydroperoxide approximately by 1% given such a high selectivity rate (approximately 90%) corresponds to the change in the concentration of by-products, almost by an order of magnitude (approximately by 10%), thereby increasing the informativity of the obtained data.
The kinetic equation for the formation of non-target, "side" products ([Pr]) is derived from a mass balance, i.e., from the equation:

$$[RH]_0 = [RH] + [ROOH] + [Pr] \quad (4)$$

where $[RH]_0$ - the initial concentration of hydrocarbon, $[RH]$, $[ROOH]$ and $[Pr]$ - present concentrations of reactive chemicals.

After differentiating the equation (4) by time and with regard to equations (Eq. 1) and (Eq. 2) one can determine the formation rate of the mentioned reaction products:

$$d[Pr]/dt = r_0 + (f+1)\cdot k_1[ROOH] \quad (5)$$

Using the differential method for analyzing kinetic curves (32) of [Pr] formation, one can determine values of certain constants of the mathematical model (Eq. 5) and further use the obtained data for the mathematical description of the whole process.

RESULTS

Preliminary studies

In order to determine the diffusion impact on the rate of aerobic oxidation of isopropyl dimethylbenzene (i.e., to determine the reaction site), the authors conducted a series of experiments at a temperature of 140 C in the presence of [NHPI] = 2.0% wt. with different stirring intensity. Control over the progress of the reaction was performed by the analysis of hydroperoxide concentration increase. Analysis of the obtained data showed that all the kinetic curves completely coincided with each other at the stirring intensity corresponding to the number of wobble > 200 min^{-1}. This fact showed that further change in the stirring intensity, i.e. further change in the reaction mass hydrodynamics did not affect the rate of the reaction and indicated the absence of diffusion resistance. Therefore, it could be argued that the reaction proceeds in the kinetic site.

Experimental results

The terms of dimethylbenzene oxidation to hydroperoxide are given above (see Section 2). It should be noted that at the end of the reaction the reaction mass was cooled and the source catalyst was almost quantitatively taken from it. Additional experiments showed practical absence of the initial hydroperoxides at the selected temperatures. Results of the reaction mixture analysis in the above series of experiments are presented in Tables 2 - 4.

Time, (min)	Temperature, °C							
	110	120	130	140	110	120	130	140
	Concentration of tertiary hydroperoxide of 3,4-DMC, % wt.				3,4-DMC concentration, % wt.			
0	0.0	0.0	0.0	0.0	100.0	100.0	100.0	100.0
10	0.9	2.9	4.4	8.1	99.1	97.0	95.4	91.5
20	2.4	5.5	10.2	15.3	97.5	94.3	89.1	83.8
30	3.6	8.7	15.4	21.8	96.3	91.0	83.5	76.8
40	4.1	11.1	20.2		95.8	88.4	78.2	
50	4.8	12.8	23.7		95.0	86.6	74.3	
60	6.3	14.9	26.2		93.5	84.2	71.4	

Table 2. Change in the concentration of isopropyl-ortho-xylol and relevant hydroperoxide during oxidation in the presence of NHPI (2% wt.).

Time, (min)	Temperature, °C							
	110	120	130	140	110	120	130	140
	Concentration of tertiary hydroperoxide of 3,5-DMC, % wt				3,4-DMC concentration, % wt.			
0	0.0	0.0	0.0	0.0	100.0	100.0	100.0	100.0
10	0.7	1.9	3.9	5.2	99.3	98.1	96.0	94.6
20	1.3	2.7	6.2	8.9	98.7	97.2	93.6	90.7
30	1.9	4.7	8.5	12.3	98.1	95.1	91.1	86.9
40	2.4	6.1	11.0	15.5	97.5	93.7	88.4	83.3
50	2.9	7.3	13.7	19.6	97.0	92.4	85.5	78.8
60	3.3	8.3	15.5	21.1	96.6	91.3	83.4	76.9

Table 3. Change in the concentration of isopropyl-meta-xylol and relevant hydroperoxide during oxidation in the presence of NHPI (2% wt.).

Time, (min)	Temperature, °C							
	110	120	130	140	110	120	130	140
	Concentration of tertiary hydroperoxide of 2,5-DMC, % wt				2,5-DMC concentration, % wt			
0	0.0	0.0	0.0	0.0	100.0	100.0	100.0	100.0
10	0.3	0.4	1.1	1.8	99.7	99.6	98.9	98.2
20	0.6	1.1	2.7	3.7	99.4	98.9	97.2	96.1
30	0.7	1.7	3.9	5.2	99.3	98.3	95.9	94.5
40	0.9	2.3	4.7	6.6	99.1	97.6	95.1	93.0
50	1.1	2.7	5.8	7.9	98.9	97.2	93.9	91.6
60	1.2	3.0	6.6	8.8	98.7	96.9	93.0	90.7

Table 4. Change in the concentration of isopropyl-*para*-xylol and relevant hydroperoxide during oxidation in the presence of NHPI (2% wt.).

The total concentration of reaction by-products ([Pr]) was determined by the difference in the experimental values according to the equation (4). In order to simplify the calculations, the change in mass ratios of the reaction mixture components due to the absorbed oxygen was neglected. Tables 2 – 4 show that the increase in reaction temperature leads to an increase in the degree of hydrocarbon conversion to the corresponding hydroperoxides. High selectivity is preserved even at temperatures up to 140°C.
The resulting kinetic data was processed in two stages. Initially, the authors processed data related to the regularities of by-products formation, and the obtained values were used in the simulation of results related to hydroperoxide formation. Experimental data related to the consumption of hydrocarbons was used to test mathematical models of these processes.

Consistent patterns of the reaction by-products formation.

The first stage of experimental data processing implied the use of dependencies related to the formation of by-products during the reaction time, calculated with regard to the data presented in a-d (Figure 2).

Afterwards, using differential analysis of the kinetic curves (6), the authors determined the approximate numerical values of the constants of the Equation 5. The differential processing was conducted as follows: polynomial equations were initially prepared for each curve; these equations approximated the current [Pr] concentrations on the time *t*. The approximation reliability (R^2) for each kinetic curve made $R^2 \approx 0.99$.

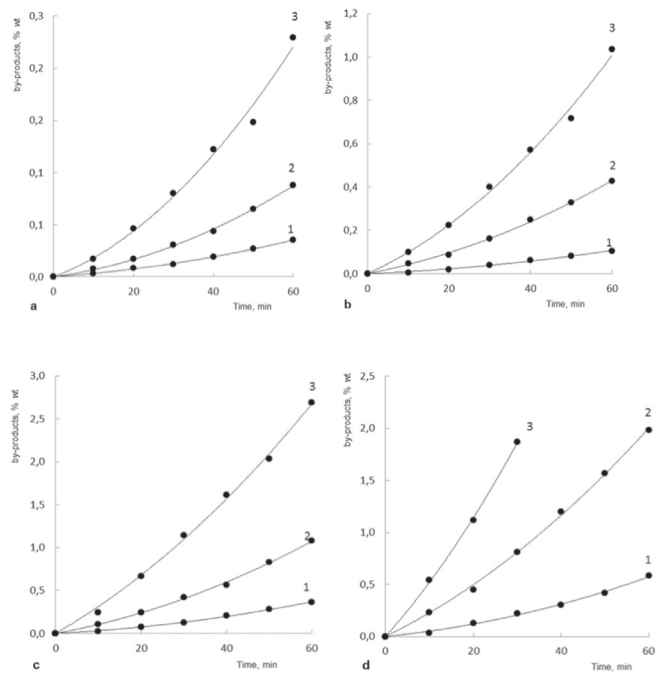

Figure 2. Experimental points and the estimated kinetic curves of by-products formation during the oxidation of hydrocarbons: a – 110°C, b – 120°C, c – 130°C, d – 140°C. 1 – 2,5-DMC, 2 – 3,5-DMC, 3 – 3,4-DMC.

Formation rate of by-products ($^{d[Pr]}/_{dt}$) were calculated after time differentiation of the obtained equation. The calculated numerical values of by-product formation rate were correlated with hydroperoxide concentrations, corresponding to the relevant reaction time (Figure 3).

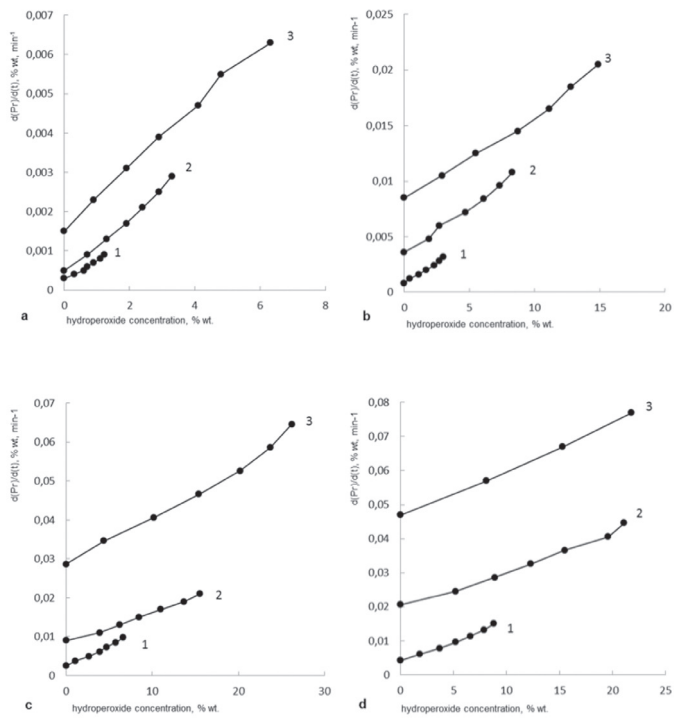

Figure 3. Dependencies of hydrocarbon oxidation rate expressed as $^{d[Pr]}/_{dt}$ (% wt·min^{-1}) on the current hydroperoxide concentrations under various temperatures: a – 110 °C, b – 120 °C, c – 130 °C, d – 140 °C. 1 – 2,5-DMC, 2 – 3,5-DMC, 3 – 3,4-DMC.

Statistical analysis of trend lines shows high accuracy of the linear approximation, the R^2 values are within $0.98 < R^2 < 0.99$. The analysis of the graphs indicates that each of the resulting correlations corresponds to the equation (5). The separated parts of Y-axis that do not depend on the current hydroperoxide concentration can be interpreted as the rate of initiation reaction (r_0). Slope of the curve corresponds to the numerical value of the dependency $\{(f+1)\cdot k_1\}$ of the equation (Eq. 5), i.e. it reflects the processes of radical and non-radical decomposition of hydroperoxide.
In this regard, the calculated numerical values (r_0) and multiplications $\{(f+1)\cdot k_1\}$ were used as the initial approximations during modeling of experimental values of [Pr], using the equation (5). The numerical values of relevant [ROOH] concentrations required for integration were determined by polynomial equations that approximate the current concentration of [ROOH] from time *t*. The approximation reliability (R^2) of each kinetic curve indicating [ROOH] formation by quadratic polynomials made $R^2 \approx 0.99$. After integration the authors compared the values calculated according to equation (5) and the experimental values of the current [Pr] concentrations for a given reaction time. By varying the values of the parameters maximum reliability of the R^2 linear regression approximation was achieved being defined by the standard program Microsoft Excel 2003. Within the high-level reliability ($R^2 = 0.98 - 0.99$) numerical values of the desired parameters were determined. During the calculations the r_0 and $\{(f+1)\cdot k_1\}$ values calculated during processing data displayed by Figure 3 were somewhat specified. The obtained values of the desired parameters are given in Table 5.

Description of the kinetic curves related to the formation of the reaction by-products during the oxidation of various DMC isomers by the equation (5) corresponds to the mechanism of the oxidation reaction, which can be described by the above system of equations (1 (÷) 5) and allows you to go to the next step of the study - the description of the reaction kinetics of education corresponding hydroperoxides.

Regularities of hydroperoxide formation

At the second stage of data processing, the obtained expressions $\{f+1)\cdot k_1\}$ and the initiation rate (r_0) were used in the co-processing of all experimental dependencies (concentration of by-products on temperature (Figure 4) and the concentration of hydroperoxide on the temperature, (Figure 4) using the least squares method for nonlinear functions.

To this end the equations (Eq. 1), (Eq. 2), (Eq. 3), and (Eq. 5) were solved by replacing the expression $(k_0[RH]+k_{01}[NHPI])\cdot\sqrt{2k_i}$ in the equations (Eq. 1) and (Eq. 2) with constant K, whereas this expression is insufficiently changed during the reaction (24). K, K_1 and multiplication $(f\cdot k_1)$ were chosen as the independent parameters of optimization. The choice of $(f\cdot k_1)$instead of (f) is determined with a view to avoid inflexible values of possible change in the value $(0<f<2)$ and to leave the possibility for the appearance of any other formation mechanism for the free radicals from hydroperoxide along with corresponding changes in the equation (Eq. 3).
By varying parameters, the minimum sum of squared deviations of the experimental and desired values of hydroperoxide and reaction products concentration was determined. The high approximation accuracy of

DMC isomer	Parameter	Temperature, °C			
		110	120	130	140
3,4-DMC	$r_0 \cdot 10^{-4}$, (% wt·min^{-1})	19	100	280	400
3,5-DMC	$r_0 \cdot 10^{-4}$, (% wt·min^{-1})	5	38	100	170
2,5-DMC	$r_0 \cdot 10^{-4}$, (% wt·min^{-1})	2	8	23	35
3,4-DMC	$(f+1)\cdot k_1 \cdot 10^{-4}$, (min^{-1})	7	9	11	14
3,5-DMC	$(f+1)\cdot k_1 \cdot 10^{-4}$, (min^{-1})	6	8	11	14
2,5-DMC	$(f+1)\cdot k_1 \cdot 10^{-4}$, (min^{-1})	7	9	11	14
Approximation reliability, R^2		0.98-0.99	0.99	0.99	0.99

Table 5. The dependence of r_0 and $(f+1)\cdot k_1$ during oxidation of different DMC isomers on the temperature, calculated with regard to processing experimental data related to [Pr].

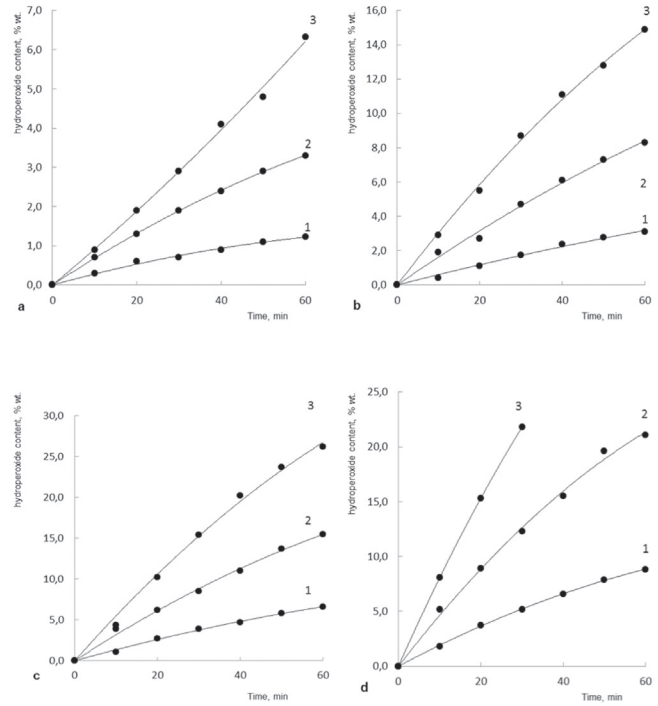

Figure 4. Experimental points and the estimated kinetic curves of by-products formation during the oxidation of DMC isomers (1 – 2,5-DMC, 2 – 3,5-DMC, 3 – 3,4-DMC) under various temperatures: a – 110 °C, b – 120 °C, c - 130 °C, d – 140 °C.

the desired and experimental concentration values of hydroperoxide and by-products within $0.95 < R^2 < 0.99$ was obtained given the parameters displayed in Table 6.

The obtained data give the possibility to set various DMC isomers in a row with regard to their reactivity in liquid phase oxidation: 3,4-DMC > 3,5-DMC > 2,5-DMC. This is seen both with regard to the change in the rate of the process initiation (r_0, Table 5), and with regard to the rate of chain prolongation constant (*K*, Table 6). Apparently, the resulting order of hydrocarbons activity is determined by the "classical" effects of substituted benzenes: methyl groups being close to the isopropyl group have a negative impact on the stabilization of p-electrons in the substituted cumene radical (Figure 5)

DMC isomer	Parameter	Temperature, °C			
		110	120	130	140
3,4-DMC	K (% wt$^{1/2}$·min^{-1})	1.86	2.34	2.93	3.61
3,5-DMC	K (% wt$^{1/2}$·min^{-1})	1.90	2.00	2.51	3.11
2,5-DMC	K (% wt$^{1/2}$·min^{-1})	1.24	1.58	2.00	2.48
3,4-DMC	$k_1 \cdot 10^{-4}$ (min^{-1})	3.4	4.7	6.8	8.3
3,5-DMC	$k_1 \cdot 10^{-4}$ (min^{-1})	3.9	4.1	6.4	9.0
2,5- DMC	$k_1 \cdot 10^{-4}$ (min^{-1})	4.8	5.7	7.5	10.0
3,4- DMC	$f \cdot k_1 \cdot 10^{-4}$ (min^{-1})	3.6	4.3	5.0	6.0
3,5- DMC	$f \cdot k_1 \cdot 10^{-4}$ (min^{-1})	3.0	4.0	4.5	4.9
2,5- DMC	$f \cdot k_1 \cdot 10^{-4}$ (min^{-1})	2.2	3.3	3.5	4.2

Table 6. The values of K, K_1, $(f \cdot k_1)$ in the system of equations (Eq. 1) ÷ (Eq. 5).

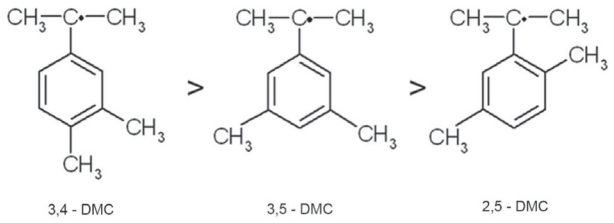

Figure 5. The reaction ability of DMC radicals.
Further experiments showed that the reactivity of DMC meta-isomers with methyl and isopropyl groups being close (e.g., 4-isopropyl-1,3-dimethylbenzene) is comparable to the para-isomer reactivity. This is confirmed by the fact that during the acid decomposition of the 3,5 DMC hydroperoxide, only 3,5-xylenol is formed, which corresponds to 3.5 DMC.

DISCUSSION

The proposed kinetic oxidation model for various isomers of isopropyl dimethylbenzene (the system of equations (Eq. 1) - (Eq. 5)) with high approximation reliability of the experimental and desired concentrations of hydroperoxides and by-products is described by the parameters presented in Tables 5 and 6. The above Figures 1 and 3 graphically represent a good description of the experimental data (in the form of points) by the calculated kinetic curves.
The main distinction of the proposed scheme describing oxidation of isopropyl xylene derivatives of isomers from the well-known ones (28-30) lies in the fact that constant (r_0) was introduced into the kinetic model. It corresponds to the initiation rate of N-hydroxyphthalimide(24). Keeping in mind that the values of these speeds vary depending on the nature of the oxidizing DMC, it is believed that hydrocarbon molecule should participate in the initiation process. Previously, the isopropyl benzene oxidation gave reason to believe that the initiation of the oxidation reaction is determined not by the formation of N-oxyl radicals, but by their interaction with hydrocarbon:

$$PINO^{\bullet} + RH \xrightarrow{r_0} NHPI + R^{\bullet} \qquad (6)$$

Thus, these data confirm the hypothesis regarding involvement of the latter into the formation of radicals according to reaction (Eq. 6) (24). It should be noted

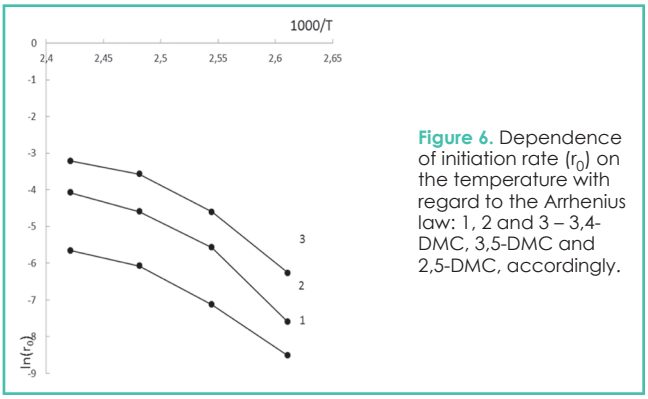

Figure 6. Dependence of initiation rate (r_0) on the temperature with regard to the Arrhenius law: 1, 2 and 3 – 3,4-DMC, 3,5-DMC and 2,5-DMC, accordingly.

that the temperature dependence (r_0) is not subject to the Arrhenius law (Figure 2). By increasing the reaction temperature from 110 ° C to 140 ° C, the effective activation energy of initiation is reduced from 130 kJ / mol to a relatively low value - 50 kJ / mol.
The Arrhenius equation is observed for calculation of the K constants, which describe the interaction of the ROO • radical with hydrocarbon and NHPI, and the corresponding constants have the following functional form:

$$K\,(3,4\text{-}DMC) = 1.74 \cdot 10^4 \cdot \exp(-3500/T) \quad (7)$$

$$K\,(3,5\text{-}DMC) = 1.82 \cdot 10^4 \cdot \exp(-3580/T) \quad (8)$$

$$K\,(2.5\text{-}DMC) = 1.17 \cdot 10^4 \cdot \exp(-3510/T) \quad (9)$$

However, the calculated values of (proceeding from these data) activation energy for the oxidation of various DMC were approximately equal (29.1; 29.8 and 29.2 kJ / mol, respectively), but low in their absolute values. This confirms the identity of interaction of peroxyl and *N*-oxyl radicals with isopropyl derivatives of aromatic hydrocarbons.
The tendency of decrease in the activation energy (33) and even lowering the reaction rate under the increased temperatures was repeatedly observed in NHPI - catalytic processes, in the studies devoted to the oxidation of alkylaromatic compounds (20). Violation of the Arrhenius law in the reactions related to transfer of the hydrogen atom from the hydrocarbon radical to PINO is of interest for various researchers (34, 35). Usually, the obtained anomalies related to the temperature dependence, along with sufficient kinetic isotope effect discovered during the study of this system are explained by the effect of macro particle tunneling (2, 16, 36).
The resonance dramatically reduces the energy barrier of the reaction, which lowers the activation energy of the reaction up to its negative values (2,37,38).
In contrast to the temperature dependence of (r_0), and *K*, dependence of the rate constant related to the hydroperoxide decomposition (k_1) has a quite usual form (Eqs. 7 - 9),

$$k_1(3,4-DMC) = 1.02 \cdot 10^2 \cdot \exp(-4827/T) \quad (10)$$

$$k_1(3,5-DMC) = 6.55 \cdot 10^1 \cdot \exp(-4647/T) \quad (11)$$

$$k_1(2,5-DMC) = 1.24 \cdot 10^1 \cdot \exp(-3906/T) \quad (12)$$

their activation energy values being 40.1; 38.6 and 32.5 kJ / mol for hydroperoxides of 3,4-DMC, 3,5-DMC and 2,5-DMC, respectfully.
The data presented in Tables 5 and 6, was used to identify the proportion of (*f*) radicals formed from one molecule of hydroperoxide, and initiating a chain reaction (Table 7). The results show that more than half of hydroperoxide radicals being formed can not participate in the propagation of the Table 7 shows that the proportion of kinetically independent free radicals decreases with the increase in the reaction temperature. The obtained values f well reflect the reference data related to toluene (f = 0.44), ethyl benzene (f = 0.78), tert-butyl (f = 0,88-0,91) and are determined by two competing processes: the interaction of radicals in the solvent "cage" (which leads to their death) and their exit from this "cage" through diffusion (6). In contrast to chemical interaction, the diffusion rate is weakly dependent on the temperature, which causes the observed decrease in the proportion of (*f*) radicals formed from one molecule of hydroperoxide, and initiating a chain reaction, along with the increase in temperature.

DMC	Temperature, °C			
	110	120	130	140
3,4-DMC	1.1	0.9	0.8	0.7
3,5-DMC	0.9	0.8	0.7	0.5
2,5-DMC	0.6	0.6	0.5	0.4

Table 7. Temperature dependence of the proportion (f) of radicals, formed from one hydroperoxide molecule, which initiate the chain process.

CONCLUSIONS

This research provided study of regularities related to liquid-phase DMC oxidation to hydroperoxide in the presence of N-hydroxyphthalimide at

constant temperature (110 - 140 ° C) and the concentration of catalyst (2 wt.%). The mathematical model of the process was obtained on the basis of experimental data. Adequacy of the obtained kinetic model proves validity of the proposed mechanism of the DMC oxidation to hydroperoxide in the presence of N-hydroxyphthalimide.

This paper provided calculations of the rate constants related to the interaction of peroxide radicals with hydrocarbon (k_0), the rate constant for the interaction of the peroxide radical to the N-hydroxyphthalimide (k_{01}), the rate constant of hydroperoxide decomposition (k_1) and the rate constant of chain propagation (K). Also, the study defined the proportion of radicals formed from one molecule of hydroperoxide, which initiate the chain reaction (*f*) and the initiation rate (r_0).

Analysis of the above data suggests that DMC oxidation by oxygen is initiated and catalyzed by N-hydroxyphthalimide. The role of N-hydroxyphthalimide as the initiator of the process is that its interaction with the stationary concentration of oxygen results in the steady state concentration of *N*-phthalimide radicals, which initiate oxidation in interaction with hydrocarbon.

ACKNOWLEDGEMENTS

The authors express their gratitude for the financial support provided by the Ministry of Education and Science of the Russian Federation. The task was set by the Federal State Budgetary Educational Establishment of Higher Professional Education "D.I. Mendeleev Russian Chemical-Technological University", No. 4.2512.2014 / K within the project of the public task in the field of scientific activity and the task set by the Federal State Budgetary Educational Establishment of Higher Professional Education "Yaroslavl state technical university" No. 2014/259 on the implementation of public works within the framework of the basic part of the state task in the field of scientific research.

REFERENCES AND NOTES

1. Nikolai N. Lebedev. Chemistry and Technology of Basic Organic and Petrochemical Synthesis, Khimiya, Moscow, USSR (1988)
2. Ishii, Y., Sakaguchi, S., Iwahama, T. Innovation of Hydrocarbon Oxidation with Molecular Oxygen and Related Reactions. *Adv. Synth. Catal.*, 393-427 (5) (2001)
3. Francesco Recupero and Carlo Punta. Free Radical Functionalization of Organic Compounds Catalyzed by N-Hydroxyphthalimide. *Chem. Rev*. 107, 3800-3842 (2007)
4. Kurganova E.A., Koshel G.N. Liquid-phase oxidation of alkyl aromatic hydrocarbons and their cyclohexyl derivatives in the presence of phthalimide catalysts. *Russian chemical journal*, 2014, 58(3-4) 91-110 (2014)

   5. Kurganova E.A., Frolov A.S. Joint synthesis of 3,4-xylenol and acetone by liquid phase oxidation of isopropyl-o-xylene. *Chemistry and Chemical Technology*, 57(10) 72-73 (2014)
6. E.T. Denisov, I.B. Afanas'ev, *Oxidation and Antioxidants in Organic Chemistry and Biology*, CRC Press (an imprint of Taylor & Francis Group): Boca Raton, Florida, USA (2005)
7. Y. Ishii, K. Nakayama, M. Takeno, S. et al. Nishiyama A Novel Catalysis of *N*-Hydroxyphthalimide in the Oxidation of Organic Substrates by Molecular Oxygen, *J. Org. Chem.* 60(14), 3934-3935 (1995)
8. O. Fukuda, S. Sakaguchi, Y. Ishii. Preparation of Hydroperoxides by N-Hydroxyphthalimide-Catalyzed Aerobic Oxidation of Alkylbenzenes and Hydroaromatic Compounds and Its Application. *Adv. Synth. Catal*. 343 (8) 809-813 (2001)
9. Y. Aoki, N. Hirai, S. Sakaguchi, Y. Ishii. Aerobic oxidation of 1,3,5-triisopropylbenzene using *N*-hydroxyphthalimide (NHPI) as key catalyst, *Tetrahedron*, 61(46) 10995–10999 (2005)
10. T. Iwahama, K. Syojyo, S. Sakaguchi, Y. Ishii. Direct Conversion of Cyclohexane into Adipic Acid with Molecular Oxygen Catalyzed by *N*-Hydroxyphthalimide Combined with $Mn(acac)_2$ and $Co(OAc)_2$, *Organic Process Research & Development*, 2(4), 255-260 (1998)
11. Y. Ishii and S. Sakaguchi. A new strategy for alkane oxidation with O2 using N-hydroxyphthalimide (NHPI) as a radical catalyst. *Catalysis Surveys from Japan*, 3(1), 27-35 (1999)
12. L. Melone, S. Prosperini, G. Ercole, et al. Puntals it possible to implement *N*-hydroxyphthalimide homogeneous catalysis for industrial applications? A case study of cumene aerobic oxidation. *J Chem Technol Biotechnol*, 89(9), 1370-1379 (2013)
13. L. Melone, C. Gambarotti, S. Prosperini, et al. Hydroperoxidation of Tertiary Alkylaromatics Catalyzed By *N*-Hydroxyphthalimide and Aldehydes under Mild Conditions. *Adv. Synth. Catal.* 353(1), 147-154 (2011)
14. F. Minisci, F. Recupero, G. F. Pedulli, et al. Transition metal salts catalysis in the aerobic oxidation of organic compounds Thermochemical and kinetic aspects and new synthetic developments in the presence of *N*-hydroxy-derivative catalysts. *Journal of Molecular Catalysis A: Chemical*, 204–205, 63-90 (2003)
15. R. Amorati, M. Lucarini, V. Mugnaini, et al. Hydroxylamines as Oxidation Catalysts: Thermochemical and Kinetic Studies. *J. Org. Chem.* 68(5), 1747-1754 (2003)
16. I. O. Opeida, YU. E. Litvinov, O. V. Kushch, et al. Kinetic Studies of Acenaphthene Oxidation Catalyzed by N-Hydroxyphthalimide. *International Journal of Chemical Kinetics.* 45(9) 514-524 (2013)
17. I.A. Opeyda, M.A. Kompanets, O.V. Kusch, et al. On the role of N-hydroxyphthalimide in the alkylarene oxidation by molecular oxygen. *Petrochemistry*, 49 (5), 409-412 (2009)
18. K. Kasperczyk, B. Orlińska, J. Zawadiak. Aerobic oxidation of cumene catalysed by 4-alkyloxycarbonyl-N-hydroxyphthalimide. *Cent Eur J Chem*, 12 (11), 1176-1182 (2014)
19. O. Fukuda, S. Sakaguchi, Y. Ishii. Preparation of Hydroperoxides by *N*-Hydroxyphthalimide-Catalyzed Aerobic Oxidation of Alkylbenzenes and Hydroaromatic Compounds and Its Application. *Adv Synth Catal*, 343 (8), 809-813 (2001)
20. B. Orlińska, J. Zawadiak. Aerobic oxidation of isopropylaromatic hydrocarbons to hydroperoxides catalyzed by N-hydroxyphthalimide. *Reac Kinet Mech Cat*, 110(1), 15-30 (2013)
21. R.A. Sheldon, I.W.C.E. Arends. Catalytic oxidations mediated by metal ions and nitroxyl radicals. *Journal of Molecular Catalysis A: Chemical*, 251(1-2), 200-214 (2006)
22. Frolov A.S., Kurganova E.A., Koshel' G.N., et al. Aerobic Oxidation of 2-isopropyl-1,4-dimethylbenzene to tertiary hydroperoxide. *European Journal of Analytical and Applied Chemistry*, 1, 16-22 (2015)
23. E.A. Kurganova, Y.B. Rumyantsev, G.N. Koshel', et al. Liquid phase oxidation of p-cymene to hydroperoxide in the presence of N-hydroxyphthalimide. *Chemical Industry Today*, 4, 20-23 (2012)
24. V. N. Sapunov, G. N. Koshel', Yu. B. Rumyantseva, et al. The Role of N-Hydroxyphthalimide in the Reaction Mechanism of Liquid-Phase Oxidation of p-Cymene. *Petroleum Chemistry*, 53(3), 171–176 (2013)
25. G.N. Koshel', E.V. Smirnova, E.A. Kurganova, et al. Liquid-phase oxidation of isopropylbenzene in the presence of N-hydroxyphthalimide. *Catalysis in the industry*, 1, 7-11 (2012)
26. G.N. Koshel', E.A. Kurganova, E.V. Smirnova, et al. Liquid-phase oxidation of alkyl derivatives of cyclohexylbenzene. *Journal of Organic Chemistry*, 44(4), 558-561(2008)
27. Ewing G.W. *Instrumental Methods of Chemical Analysis*. McGraw-Hill, Inc., New York, USA (1985)
28. A. Bhattacharya. Kinetic modeling of liquid phase autoxidation of cumene. *Chem. Eng. J.* 137(2) 308-319 (2008)
29. K. Hattori, Y. Tanaka, H. Suzuki, et al. Kinetics of liquid phase oxidation of cumene in bubble column. *J. Chem. Eng. Japan*, 3(1) 72-78 (1970)
30. Peter R. Makgwanea, Nigel I. Harmsea, Ernst E. Fergb, Ben Zeeli. Selective oxidation of p-cymene catalyzed by VPO catalyst: Process performance and kinetics studies. *Chemical Engineering Journal,* 162(1) 341-349 (2010)

Readers interested in a full list of references are invited to visit our website at **www.teknoscienze.com**


S. Devyatkov


N. V. Kuzichkin

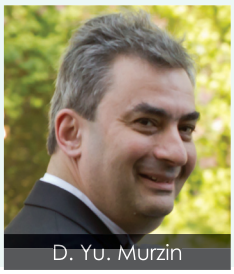
D. Yu. Murzin

S. DEVYATKOV[1], N.V. KUZICHKIN[1], D.YU. MURZIN[2]

1. St. Petersburg State Technical University, Russia
2. Åbo Akademi University, Turku/Åbo, Finland

On comprehensive understanding of catalyst shaping by extrusion

KEYWORDS: Sulfated zirconia, extrusion, zeta-potential, binder, alkylation.

Abstract A brief introduction into catalyst shaping and its importance is given. Some challenges and key aspects are discussed. A special attention is paid to visualization of the structure of catalyst extrudates. Hydrous sulfated zirconia, as a promising catalyst for acid catalyzed transformations of hydrocarbons such as alkylation, is considered from the viewpoint of its shaping via extrusion. Rheology and zeta potential measurements are presented for this material, addressing also the influence of PVA addition as a surface-modifying agent. The quality of the green bodies of the shaped catalysts is shown to be strongly dependent on particles surface properties in molding masses.

INTRODUCTION

Immense importance of catalysis in chemical industry is manifested by the fact, that roughly 85-90% of all chemical products have seen a catalyst during a course of the production. The number of catalytic processes in industry is very large with mainly heterogeneous catalysts applied. Such catalysts come in many different forms as porous solids. Contribution of catalysts to the overall cost of a product made with an aid of catalysts on average is not very high (ca. 3%). In theory catalysts are not consumed in a chemical reaction, while in industrial practice many industrial catalysts deactivate, requiring gradual replacement. Even taking such replacement into account a part of catalyst sales in relation to the gross domestic product (GDP) is marginal (ca. 0.1%). At the same time the share of products made by catalysts in GDP could be as high as 25%.
In the areas where heterogeneous catalysts are used in industry, almost one third is used in crude oil refining and petrochemistry (1). Among the current trends driving catalysts demands in the future, the following should be mentioned: improving process efficiency and expansion of the feedstock base to include coal, natural gas and biomass. In particular lignocellulosic biomass, not competing with the food chain, has attracted a lot of attention. It is fair to say that utilization of such feedstock might require fundamental changes in processing technology.
Microscopic understanding of catalysis (i.e. nm scale – active site) is the main goal of academics s working in the field of heterogeneous catalysis. At the same time shaped catalysts particles (mm range) are applied industrially on a macroscopic level. Thus, in addition to intrinsic kinetics, also transport phenomena constitute an essential part of catalytic engineering. Moreover, understanding of the events occurring at macroscopic or reactor level (i.e. 1 m scale) requires description at the mm (shaped catalyst pellet) and micron scale.
The shaping of catalysts and supports is a key step in the catalyst preparation procedure.
Most academic research institutions, however, work only with small quantities of powders, and do not consider the influence of the scale-up. At the same time information about the distribution of components (for example zeolite and a binder) inside an industrial catalyst is very important.
In general, in the process of catalyst design, more attention should be attributed to the stage of scale-up, including shaping. Very few academic groups in Europe and globally have a proper infrastructure and skills to address the engineering aspects of catalyst shaping on a quantitative level. The required work needs expertize in catalyst preparation, elucidation of catalytic activity, characterization and imaging, rheology, kinetics and mass transfer. The complexity of the work apparently explains why catalyst shaping is not in the focus of research done in academia.
One example of a sophisticated characterization work for an industrial catalyst is related with fluid catalytic cracking catalysts. This examples involves integrated laser and electron microscopy. In fluorescence microscopy, a focused laser light

scans a catalyst detecting fluorescence emission from the focal points. The technique contrary to electron microscopy has limited spatial resolution and solely reveals fluorescent structures. The integrated laser and electron microscope (iLEM) developed by Weckhuysen and co-workers (2) is an imaging tool, combining strengths of both methods.
In order to generate a fluorescence signal, fluorogenic thiophene oligomerization is used, catalysed by acidic sites of zeolites. The product, oligomerized thiophene, emits green fluorescence. In this way location of acid sites can be made. Moreover, fluorescence intensity can be related to the strength of acid sites. The method allows a spatial resolution of ca. 20 nm. The iLEM setup shown in Figure 1a consists of a custom-designed laser scanning fluorescence microscopy (FM), mounted on a side port of a TEM. The laser beam is perpendicular to the path of the electron beam. For FM imaging, the grid with the catalyst sample is rotated to face the laser beam, while FM is partially retracted and the grid is tilted to enable TEM imaging.
The technique was applied to study a fluid catalytic cracking catalyst. The active phase, zeolite Y, is embedded in a matrix consisting of clay, silica, and alumina. Using iLEM technique location of active acidic centres could be determined by relation to fluorescence and could be correlated to the catalyst particle structure. Two different areas were found in the catalyst, one associated with the zeolite component giving the fluorescent products, while the other areas are mainly composed of the matrix material (Figure 1 b, c).

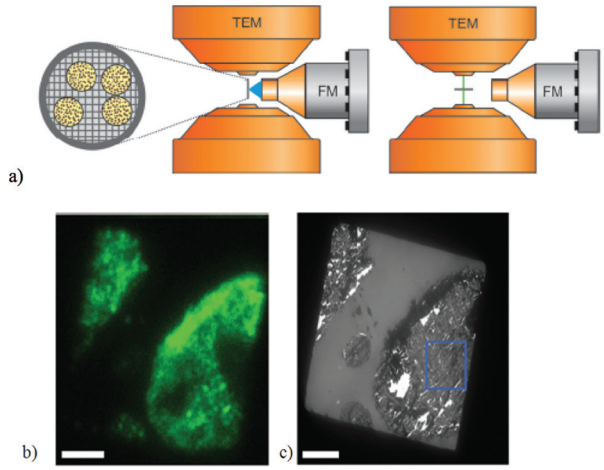

Figure 1. a) The iLEM setup, and iLEM analysis of a sectioned FCC catalyst particle: b) FM image, c) TEM image, taken from the same region (2) Copyright WILEY.
When the zeolitic structure is exposed to steam, Al atoms from the framework can be extracted creating extra-framework Al species. This results in lower amounts of Brønsted acid sites and, thus, eventual deactivation. The iLEM images of hydrothermally deactivated catalysts show much lower fluorescence intensity compared to the fresh FCC catalyst particles. In addition, a large fraction of the crystals is damaged and the large regions of clay are lost.

SHAPING OF CATALYSTS

Main principles of extrusion

The shape and size of the catalyst particles should promote catalytic activity, strengthen the particle resistance to crushing and abrasion, minimize the bed pressure drop, lessen fabrication costs and distribute dust build-up uniformly.

Small particle size increases activity by minimizing influence of internal and external mass transfer. At the same time the bed pressure drop increases. Thus, there is an apparent contradiction between the desire to have small catalyst particles (less diffusional length, higher activity) and to utilize large particles displaying lower pressure drop.
For reactors with fixed beds, often applied in industry, relatively large particles are in use (several mm) to avoid pressure drop.

Extrusion (Figure 2) is the most economic and commonly carried out shaping technique for catalysts and supports. During extrusion, a wet paste from a hopper at the top is forced through a die. The emerging ribbon, passing through holes in the die plate, is cut to the desired length using a suitable device. The pressure, which is developed in the screw extruder as the paste moves towards the die, is affected by the screw geometry and the paste rheology.
Too viscous pastes can block the extruder, while the opposite leads to unstable extrudates.
Usually the catalyst powders obtained after the thermal treatments behave like sand, i.e. do not have by themselves the required moldability and plasticity, even when water is added. Various additives are used in formulation of pastes, such as: a) compounds for improving the rheological behaviour (clays or starch); b) binders (aluminas or clays); c) peptizing agents to de-agglomerate the particles (dilute acetic or nitric acid); and d) combustible materials to increase the porosity (carbon black, starch, etc.). The operating variables include mixing time, additive content, water content, ageing and extrusion temperature. The quality of the extrudates also depends on the drying and calcination procedure. Special shapes (trilobates, rings, hollow cylinders, monoliths or honeycombs) can be obtained using proper dies.

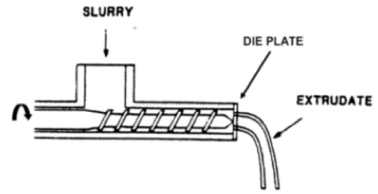

Figure 2. Principle of extrusion.

Catalyst forming is seldom considered in academic research. It is, however, extremely important for preparation of catalysts, influencing the final performance. Information about catalyst forming is typically proprietary and primarily empirical, leading to uncertain/sub-optimal processes, decreased quality and increased costs. It is, thus, apparently clear, that solid engineering approaches are needed also in this field.
Although extrusion is thoroughly studied in ceramic science the use of porous materials (3–5), such as for example zeolites relevant for catalysis is much more rare.
Compared to other preparation methods extrusion process affords high throughput at relatively low costs and gives a variety of possible extrudate shapes (Figure 3).

Figure 3. Shapes of extrudated catalysts.

The downside of the method is a nonuniform shape of extrudates and lower abrasion resistance compared to pellets. The key factor in wet shaping is preparation of pastes of catalytic powder (concentrated suspensions).
The desired product during extrusion (high shear rates) is achieved for pseudoplastic pastes with low viscosity, since after leaving the die at a low shear rate the viscosity is increased leading to stable extrudates. Most catalyst pastes are prone, however, to shear deformation. The flow behaviour of molding masses is well described by

$$\tau = k \cdot \gamma^n$$
$$\eta = k \cdot \gamma^{n-1} \quad (1)$$

where τ is the shear stress, γ is the shear rate, k is the consistency constant (Pa s^n), η is the viscosity and n is the flow behaviour index. The later characterizes deviation of the flow from the Newtonian fluids behaviour where n=1. At n <1 the fluid is thixotropic, while n>1 characterizes dilatants fluids.
More adjustable parameters resulting in more acc urate fitting of experimental data are included in the Herschel-Bulkley model (6)

$$\tau = \tau_0 + k \cdot \gamma^n$$
$$\eta = \frac{\tau_0}{|\gamma|} + k \cdot |\gamma|^{n-1} \quad (2)$$

where additional parameter τ_0 is the shear yield stress. This parameter has the meaning of the minimum stress, above which material starts to flow. Herschel-Bulkley model can be used to quantitatively describe the dependence of shear stress and viscosity on the shear rate for suspensions with different concentrations of additives, binder, etc.
There is a radial profile of flow velocity in the die channel, as the flow velocity decreases with an increasing distance from the flow axis. If the velocity gradient is significant, the defects will be generated after a granule leaves a die channel because of the velocity equalization. Subsequently efficient molding will not be possible. A small flow behaviour index corresponds to less significant velocity gradients. Ideally plug flow is achieved at $n \rightarrow 0$. The flow behaviour index of the paste for simple shapes is at most 0.7. The extrusion process is influenced by the paste preparation method, composition, namely water content (typically 20 and 40 wt. %), presence of peptizing agents (to adjust the colloid chemical properties of the paste), binders, plasticizers, lubricants and porogenes. It is also important that no large solid particles are present for extrusion of complex shapes. The operating variables also include mixing time, ageing and extrusion temperature. If the amount of water is much lower than the solid pore volume, smooth processing of such dry paste can be troublesome. On the contrary significant water content will not allow the paste to settle after the extruder. The influence of water could be even more complicated. For example, shaping of TiO_2 monolith (7) showed that distribution of the small pores is only influenced by the starting material particles sizes. The amount of large pores was, however, affected mainly by the water content of the molding pastes. Presence of large pores can drastically reduce the crushing strength of the monolith body.

Additives to molding masses

Peptizing agents (for example nitric acid, formic acid or acetic acid solutions) influence the colloid–chemical interactions between particles. This is done by assuring that pH deviates from the point zero charge. Otherwise the liquid phase might start to agglomerate. Binders are required during extrusion in order to make the extrudates strong enough (Figure 4). The negative side of the binder presence can be elevation of the flow index (n in eq. 1 and 2). Such elevation can lead to a pronounced velocity profile in the paste and deteriorated properties of extrudates due to inadequate adhesion during extrusion.

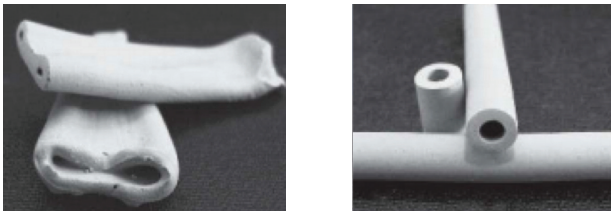

Figure 4. Extrudates with and without binders (7).

Typically inorganic binders such as alumina, silica sols, or clays are utilized. Alternative organic binders will be burned away at the calcination step. When alumina is added in the form of boehmite or pseudoboehmite, it is transformed into transition alumina during calcination. Gelation of silica sols and agglomeration of delaminated fragments of clays are responsible for the extrudates stability, when these binders are applied. There are several examples of the mutual influence of the main active component and the binder. This has a consequence in terms of the final catalyst physico-chemical properties. Extrusion of zeolites was considered in (5) with aluminum phosphate as a binder. Figure 5 displays temperature programmed desorption of ammonia from fresh forms of H-ZSM-5 zeolite and γ-alumina and with AlPO binder. Changes in acidity upon addition of a binder can be associated with the phosphor migration from the binder to the crystal structure of zeolite. This case serves as a clear example of the binder influence on the catalytic properties.
In general, well-known binders are added to the active phase in order to obtain the required physico-mechanical properties. Nonuniformity of the active component distribution can lead to zones with a high concentration of it and enhanced reaction

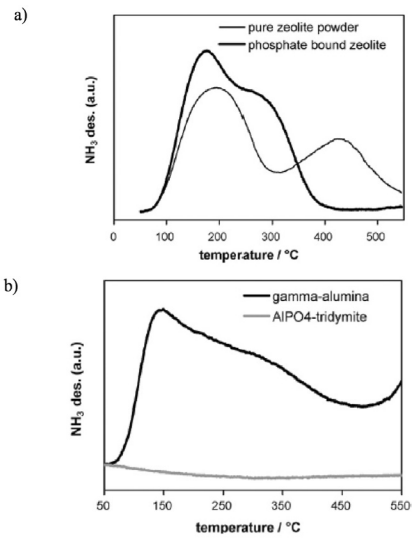

Figure 5. Ammonia TPD of a) H-ZSM-5 powder after calcination and AlPO4 bound extrudate containing the same zeolite b) AlPO4 and -alumina (5).

rates. In other zones the active phase concentration is much lower. As a result, local zones are formed inside a catalyst granule. In such zones the reaction rate is controlled not by kinetics, but mass transfer, decreasing the overall effectivity compared to uniform distribution of the active phase and the binder. Optimal activity profiles have been a subject of extensive mathematical analysis in the chemical engineering literature (8–10) without, however, explicitly taking into account the binder properties.

Selection of plasticizers or their mixtures to improve the rheological behaviour of the paste is often empirical. A wide variety of plasticizers is available with clays, starch, sugars, cellulose derivatives, polyethylene glycol and polyvinyl alcohol being among them.

Porogenes (carbon black, starch, and sawdust) are added to the paste to create porosity, which is generated during calcination also because besides porogenes, plasticizers and lubricants are burned away. Such porosity, being beneficial for mass transfer, deteriorates, however, mechanical stability.

SHAPING THE CATALYST FOR OLEFINS ALKYLATION BY ISOPARAFFINS OVER SOLIDS

Modern alkylation trends

Few guidelines exist regarding the optimal formulation of the shaped body in the light of rheology as well as possible mass transfer and chemical effects.

Below alkylation of isobutane with butenes with acid catalysts (1) will be considered, reflecting the experience of the authors in shaping of sulphated zirconia catalysts for this reaction. Alkylate (the target product of the process) has a low saturated vapor pressure and does not contain sulfur, oxygen, nitrogen, and aromatic components. In industrialized countries the amount of alkylate in high octane gasoline reaches 13% vol. Currently there are two main industrial methods of alkylate production – alkylation of isobutane with butenes using sulfuric and hydrofluoric acids as a catalyst, or their mixtures with addition of other acids. Both processes exhibit high product yields, selectivity and alkylate quality. However, the use of liquid acid (homogeneous) catalyst is associated with several drawbacks such as the acid high specific flow rate and acid corrosivity. In addition there is a necessity of the catalyst-product mixture separation with a subsequent disposal of the spent acids. Such procedures, along with the toxic properties of the acids, constitute risks to personnel health.

Modern trends in industrial alkylation processes are mainly associated with the substitution of liquid acids catalysts by solid ones. Use of a solid catalyst allows to avoid the above problems and to gain several technological and economic advantages. The main drawback in the use of solid catalysts for isobutene alkylation is a high rate of their deactivation (short catalyst lifetime) and low selectivity to trimethylpentanes (high octane number components). A solid acid catalyst is applied in the AlkyClean process developed by ABB and Neste, which employs several reactors. A demonstration unit of this technology comprises three reactors. The first one is used for alkylation, another one for mild regeneration (mild liquid-phase regeneration using isobutane and hydrogen) and high temperature regeneration is done in the third one . A simplified block diagram of the alkylation process is given in Figure 6.

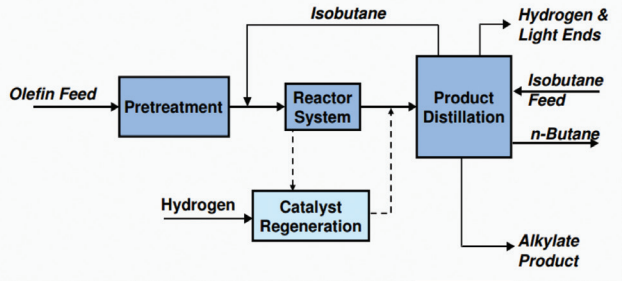

Figure 6. Alkylation of olefins with isobutene (1).

As alkylation catalysts, zeolites (11–13) or sulphated zirconia (14–17) can be used. Below we will focus more on the latter type of catalysts. The key parameters in designing adequate shaped sulphated zirconia catalysts for this process should be its texture, surface properties including zeta potential, nature of additives, liquid content, particle size distribution, extrusion temperature, paste ageing to name a few.

Rheology of sulphated zirconia based pastes

The challenge is to quantify the influence of various parameters and develop quantitative correlations for rheological curves. A complex rheological behaviour is expected from sulphated zirconia suspensions, when the material has a distribution of shapes and particle sizes. IT should be also kept in mind that the molding paste consists of several types of materials (namely the binder and the active component), each having their own surface properties. From the rheological viewpoint the paste properties should be optimized leading to a mechanically stable catalyst with the structure favouring kinetic control of the reaction. This is critical, for example, in reactive distillation processes (18) with extremely strong hydrodynamics stresses on the catalyst pellets.

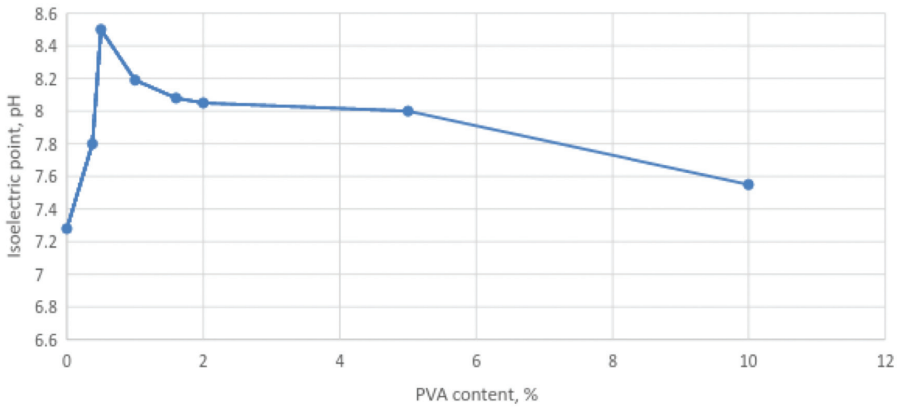

Figure 7. Point zero charge as a function of PVA content (28).

Special attention should be given to zeta potential measurements. Zeta potential, usually expressed as ζ-potential, is a physical property of any particle in colloidal systems. It refers to as an electrostatic voltage caused by the ions aggregated on colloidal particles. The magnitude of zeta potential partly shows the stability of the colloidal system. Larger zeta potential values indicate stronger resistance to aggregation, otherwise, the system is not stable and flocculation occurs. Thus, zeta potential measurements are a useful method to predict and control the long-term stability of suspensions and emulsions helping to understand aggregation or flocculation process. Few systematic measurements of zeta potential have been reported in the literature for zeolites (19–24). As an additive influencing the surface properties in suspensions, water soluble polymers are applied (24–27), such as poly(ethylene glycol) or polyvinylalcohol (PVA). Changes in the zeta-potential, namely point zero charge (also so-called isoelectric point), as a function on pH in the presence of PVA are presented in Figure 7.

The most interesting is the region with PVA content up to 2 wt%. Further increase of the polymer content does not change substantially the surface properties, while negatively influencing the strength of granules.
Dependence of shear yield stress on zeta-potential for water suspension of sulphated zirconia at different amounts of PVA is shown in Figure 8. Experimental results are well explained using the following expression (29),

$$\tau_y = \tau_{y\max} - k \cdot \tau_{y\max} \cdot \xi^2 \qquad (3)$$

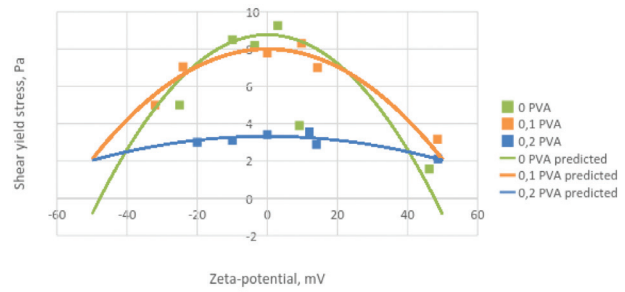

Figure 8. Dependence of sulphated zirconia suspensions shear yield stress on zeta-potential at various PVA content (28).

Addition of a binder influences the surface and rheological properties of suspensions, namely higher alumina content in sulphated zirconia suspensions leads to a shift of point zero charge towards higher pH. Introduction of alumina increases viscosity and the shear stress. This is a sign of a more stable coagulation structure of such suspensions (Figure 9).

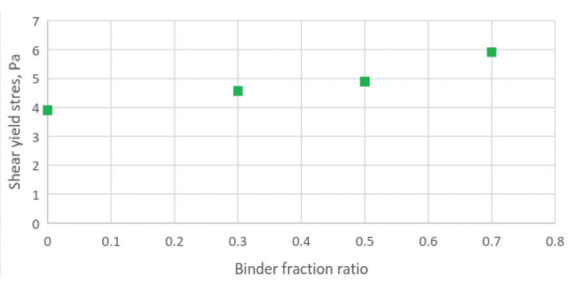

Figure 9. Dependence of shear yield stress on the binder content of sulfated zirconia suspensions (28).

SEM image of sulfated zirconia and alumina binder mixed together is presented in Figure 10. A near-spherical shape of the particles is beneficial for a smooth rheological behavior, a lower flow index *n* in the rheological model, thus, leading to a more mechanically stable extrudate.

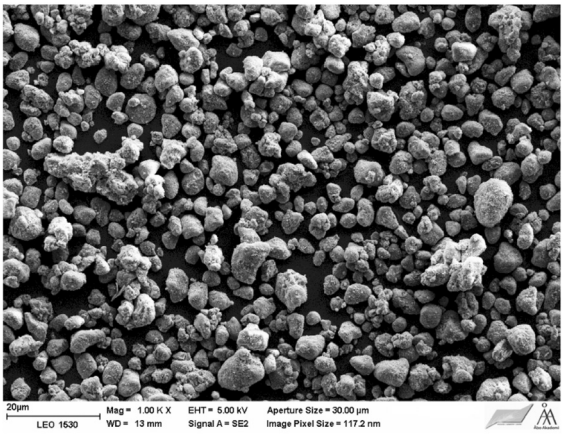

Figure 10. SEM image of sulphated zirconia and alumina binder mixed together (28).

Results for elucidations of the PVA impact on the shear yield stress and shear stress (value taken at 1000 1/s) for sulfated zirconia suspensions at different amount of PVA, binder content of 30 wt% and zeta-potential of 14 mV are illustrated in Figure 11.

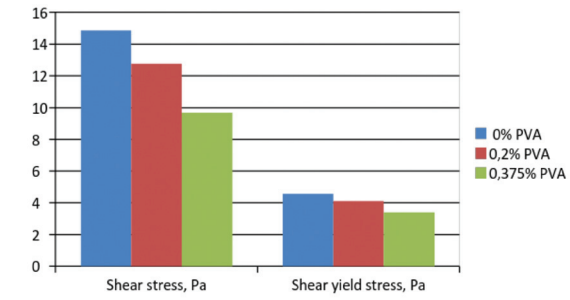

Figure 11. Shear rate impact on the shear stress and shear yield stress for sulfated zirconia suspensions at different amount of PVA and binder content of 30 wt% and zeta-potential of 14 mV (28).

Catalysts shown in Figure 12 were extruded at different pH, which was gradually adjusted by adding sodium hydroxide (0.1 M) from 4.1 (Figure 12, a) to 7.2 (Figure 12, f). An increased amount of defects accumulated in green bodies corresponds to changes in the rheological properties and surface characteristics of particles in the pastes.

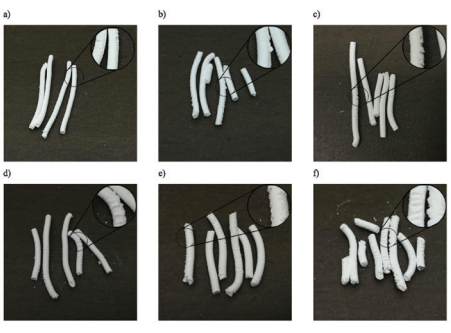

Figure 12. Extruded sulfated zirconia catalysts with alumina binder (30 wt%) and 0.3wt% PVA obtained at different pH (28).

Addition of the binder obviously increases the mechanical strength, thus, improving the life time, as the same time decreasing the concentration of the active component. As the consequence, the catalyst volume should be increased, obviously giving a rise to catalyst and reactor costs.

FURTHER TECHNIQUES FOR CATALYST'S STRUCTURE VISUALIZATION AND UNDERSTANDING

Understanding of the heterogeneous system (the binder and the active component), which has its optimum (porous) structure (30), requires advanced characterization methods allowing spatial visualization of catalyst granules (31. Such visualization include g several methods, e.g. Raman, UV–vis–NIR and infrared microspectroscopies, magnetic resonance imaging, and X-ray absorption and diffraction microtomography (micro-CT).
For example, positron emission tomography (PET), a well-known method in nuclear medicine for molecular imaging of biochemical functions (Figure 13), can be also applied to molecular imaging of the chemical processes on the surfaces of heterogeneous catalysts.
Recently, a study was published on application of PET imaging technique in combination with radio-gas chromatographic analysis for investigation of catalytic processes on A- type zeolites (31).

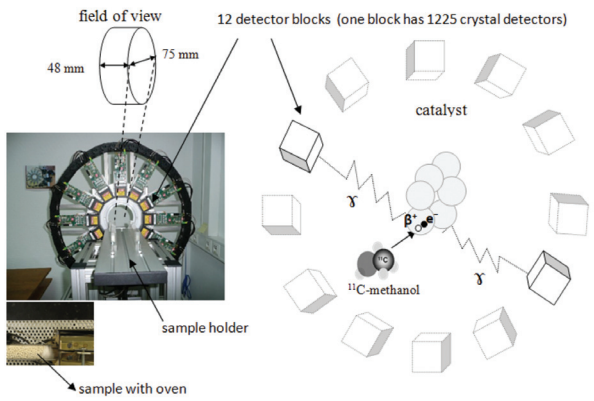

Figure 13. The scheme of PET system.

Another powerful technique of components mapping in the catalyst pellets is SEM EDX – scanning electron microscopy in combination with energy-dispersive X-ray spectrometry. This technique is based on the ability of atoms to emit characteristic X-rays under conducted high-energy electrons beam. As the result the map profile of components distribution in the domain of interest can be obtained and readily visualized (Figure 14).

SEM could be equipped with a BSE (backscattering electrons) detector, as heavy atoms of high atomic number tend to scatter electrons stronger than light ones. Corresponding images recorded with BSE (Figure 15) display, therefore, compositional information. A higher contrast of some parts of the image reflect nonhomogeneous distribution in the catalyst body.

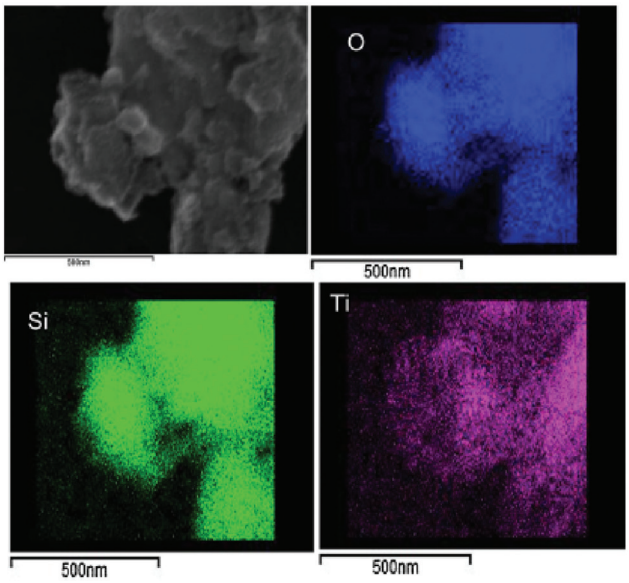

Figure 14. SEM-EDX element mapping of zeolite composition (33).

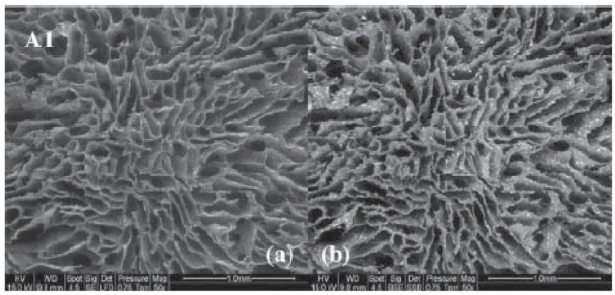

Figure 15. SEM and BSE image for determination of heavy elements in catalytic composition (34).

CONCLUSIONS

Shaping of catalysts and supports is a key step in the catalyst preparation procedure. Most academic research institutions, however, work only with small quantities of powders, and do not consider the influence of the scale-up. At the same time information about the distribution of components (the active component and a binder) inside an industrial catalyst is very important.
Considering as an example sulphated zirconium hydroxide, this material as such cannot be extruded, while addition of aluminium hydroxide or another binder makes extrusion possible. From the viewpoint of rheology it is important to find an extrusion mass with sufficient shear yield stress and viscosity, maintaining relatively low flow index. However, these characteristics sometimes should be chosen as a compromise with the resulting rupture strength, surface area, pore volume distribution, etc. The rheological characteristics could be reliably fine-tuned by adjusting the surface characteristics of particles in suspensions through the zeta-potential using numerous surface modifying agents.
Selection of the type and amount of the binder, thus, substantially influences the catalyst structure and its

effectiveness and should be considered carefully. The research work in the area of catalyst shaping, besides focusing on the active phase preparation and characterization, typically done in the academic labs, should include:

- rheological studies of suspensions
- determination of the relationship between rheological behavior of the active phase paste and the key parameters, such as concentration of suspension; concentration and types of additives, binders, peptizing agents, porogenes; mixing time; ageing and extrusion temperature
- preparation of extrudates including special shapes
- visualization of the shaped bodies by advanced techniques addressing potential structural inhomogeneity
- analysis of mechanical properties of shaped catalysts
- and, finally, elucidation of catalytic behavior.
- Thus, scaling up of catalyst synthesis from an active phase *per se* to a catalyst granule is a complex process.

ACKNOWLEDGEMENTS

The work was performed as part of the state contract awarded on the basis of a grant of the Government of the Russian Federation for support of scientific research conducted under the supervision of leading scientists at Russian institutions of higher education, research institutions of State Academies of Sciences and state research centres of the Russian Federation on March 19, 2014, no. 14.Z50.31.0013.

REFERENCES

1. Murzin DYu. Chemical Reaction Technology, deGruyter, 2015
2. Karreman MA, Buurmans ILC, Geus JW, et al. Integrated laser and electron microscopy correlates structure of fluid catalytic cracking particles to Brønsted acidity, *Angew Chemie - Int Ed*. 2012, 51, 1428–1431.
3. Gordina NE, Prokof'ev VY, Il'ina AP, Extrusion molding of sorbents based on synthesized zeolite, *Glas Ceram*. 2005, 62, 282–286.
4. Li Y, Perera S, Crittenden B, et al. The effect of the binder on the manufacture of a 5A zeolite monolith, *Powder Technol*. 2001, 116, 85–96.
5. Freiding J, Patcas F-C, Kraushaar-Czarnetzki B, Extrusion of zeolites: Properties of catalysts with a novel aluminium phosphate sintermatrix, *Appl Catal A Gen*. 2007, 328, 210–218.
6. Herschel WH, Bulkley R, Konsistenzmessungen von Gummi-Benzollösungen., *Kolloid-Zeitschrift*. 1926, 39, 291–300.
7. Forzatti P, Orsenigo C, Ballardini D, et al. On the relations between the rheology of TiO_2-based ceramic pastes and the morphological and mechanical properties of the extruded catalysts. *Prep. Catal. VII. Elsevier Masson SAS*, pp 787–796, 1998.
8. Johnson DL, Verykios XE, Effects of radially nonuniform distributions of catalytic activity on performance of spherical catalyst pellets, *AIChE J*. 1984, 30, 44–50.
9. Nyström M, Effectiveness factors for non-uniform catalytic activity of a spherical pellet, *Chem Eng Sci*. 1978, 33, 379–382.
10. Morbidelli M, Servida A, Varma A, Optimal catalyst activity profiles in pellets. 1. The case of negligible external mass transfer resistance, *Ind Eng Chem Fundam*. 1982, 21, 278–284.
11. Yoo K, Smirniotis PG, The influence of Si/Al ratios of synthesized beta zeolites for the alkylation of isobutane with 2-butene, *Appl Catal A Gen*. 2002, 227, 171–179.
12. Costa BOD, Querini C, Isobutane alkylation with solid catalysts based on beta zeolite, *Appl Catal A Gen*. 2010, 385, 144–152.

13. Guzman A, Zuazo I, Feller A, et al. On the formation of the acid sites in lanthanum exchanged X zeolites used for isobutane/cis-2-butene alkylation, *Microp Mesop Mater*. 2005, 83, 309–318.
14. Guo C, Yao S, Cao J, et al., Alkylation of isobutane with butenes over solid superacids, SO_4^{2-}/ZrO_2 and SO_4^{2-}/TiO_2, *Appl Catal A Gen*. 1994, 107, 229–238.
15. Guo C, Liao S, Qian Z, et al. Alkylation of isobutane with butenes over solid acid catalysts, *Appl Catal A Gen*. 1994, 107, 239–248.
16. Smirnova MY, Toktarev AV, Ayupov AB, et al. Sulfated alumina and zirconia in isobutane/butene alkylation and n-pentane isomerization: Catalysis, acidity, and surface sulfate species, *Catal Today*. 2010, 152, 17–23.
17. Corma A, Martnez A, Martnez C, The effect of sulfation conditions and activation temperature of sulfate-doped ZrO_2, TiO_2 and SnO_2 catalysts during isobutane/2-butene alkylation, *Appl Catal A Gen*. 1996, 144, 249-268.
18. Sladkovskiy DA, Kuzichkin NV, Semikin KV, et al. Optimal design of catalytic distillation for alkylation of isobutane with 2-butene on a solid catalyst, *Chem Today*. 2015, 33, 32–42.
19. Au P-I, Leong Y-K, Liu J, Sequential yield stress and zeta potential measurements on the same suspensions for platelet and spherical alumina, *Colloids Surf A Phys Eng Asp*. 2014, 441, 360–366.
20. Gustafsson J, Mikkola P, Jokinen M, et al. The influence of pH and NaCl on the zeta potential and rheology of anatase dispersions, *Colloids Surf A Phys Eng Asp*. 2000, 175, 349–359.
21. Ong BC, Leong YK, Chen SB, Yield stress-zeta potential relationship of oxide dispersions with adsorbed polyacrylate — Steric effect and zeta potential at the flocculated-dispersed transition state, *Powder Technol*. 2008, 186, 176–183.
22. Ece I, Gu N, The viscosity and zeta potential of bentonite dispersions in presence of anionic surfactants, *Materials Lett*. 2002, 57, 420–424.
23. Laxton PB, Berg JC, Relating clay yield stress to colloidal parameters, *J Colloid Interface Sci*. 2006, 296, 749–55.
24. Tsai C-J, Chen C-N, Tseng WJ, Rheology, structure, and sintering of zirconia suspensions with pyrogallol-poly(ethylene glycol) as polymeric surfactant, *J Eur Ceram Soc*. 2013, 33, 3177–3184.
25. Tunç S, Duman O., The effect of different molecular weight of poly(ethylene glycol) on the electrokinetic and rheological properties of Na-bentonite suspensions, *Colloids Surf A Phys Eng Asp*. 2008, 317, 93–99.
26. Avadiar L, Leong Y-K, Fourie A, Effects of polyethylenimine dosages and molecular weights on flocculation, rheology and consolidation behaviors of kaolin slurries, *Powder Technol*. 2014, 254, 364–372.
27. Wiśniewska M, Grządka E, Mendrek B, Influence of the solid type on the adsorption mechanism of nonionic polymers in the metal oxide/water solution system—temperature effect, *Powder Technol*. 2013, 246, 682–688.
28. Devyatkov SYu, Peltonen J, Kuzichkin NV, et al. (unpublished results)
29. Foundas M, Britcher LG, Fornasiero D, et al. Boehmite suspension behaviour upon adsorption of methacrylate–phosphonate copolymers, *Powder Technol*. 2015, 269, 385–391.
30. Kong X, Liu J, Influence of alumina binder content on catalytic performance of Ni/HZSM-5 for hydrodeoxygenation of cyclohexanone, *PLoS One*. 2014, 9, e101744.

Readers interested in a full list of references are invited to visit our website at **www.teknoscienze.com**

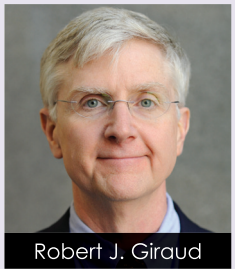
Robert J. Giraud

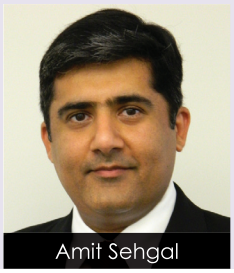
Amit Sehgal

ROBERT J. GIRAUD[1], AMIT SEHGAL[2], CHRISTIANA BRIDDELL[3], DAVID CONSTABLE[3], ANN LEE-JEFFS[3]

1. Engineering Technology Principal Consultant, The Chemours Company, Wilmington, USA
2. Senior Staff Scientist and Project Manager(R&I), Solvay USA Inc., Bristol, USA
3. ACS Green Chemistry Institute®, Washington, USA

Less energy-intensive alternative separations: creating a roadmap to accelerate industrial adoption

KEYWORDS: Energy efficiency, industrial roundtable, Green Engineering.

Abstract

Separation processes account for over 35% of energy used in chemical manufacturing. To advance the availability of less energy-intensive separations for industrial adoption, the Chemical Manufacturers Roundtable at the ACS Green Chemistry Institute® in partnership with AIChE sought a NIST AMTech planning grant to collaboratively create an innovation roadmap. Since receiving the award in May 2015, the collaboration has expanded to include researchers from universities and national labs, suppliers of commercial separations equipment, and a growing list of interested manufacturers and sustainability leaders. Successful roadmap development depends on the involvement of a wide range of chemical science and engineering innovators.

Separating mixtures into valuable components is central to chemical manufacturing. Distillation is the approach generally used to effect these separations because it is a dependable, well-understood method that works. The problem is that distillation is a very energy intensive operation. Over 35% of total energy use in U.S. chemical manufacturing is consumed by distillation (1).

At a time when chemical manufacturers are focused on cutting energy use to reduce costs and greenhouse gas emissions, a key challenge for the sector is transforming the energy efficiency of separation processes. Volatile energy prices and the high capital investment required for conventional separations equipment present an opportunity for change.

Manufacturers need effective and less energy-intensive alternative separation technologies that are appropriate for specific industrial separation tasks and that have demonstrated performance and available design tools for predictable scale-up. To achieve this, a diverse and inclusive group of stakeholders must come together and meet this 21st century challenge head-on.

Collaborators include:

ACS GCI Chemical Manufacturers Roundtable (Ajinomoto North America, Inc., Albemarle, Arizona Chemical, Chemours, Dixie Chemical, DuPont, Pen A Kem, Sigma-Aldrich, and Solvay USA Inc.)

American Institute of Chemical Engineers (AIChE) (including its Institute for Sustainability, Separations Division, and Computational Molecular Simulation & Engineering Forum)

NIST Materials Measurement Laboratory

Industrial Fluid Properties Simulation Collective

Pine Chemicals Association

AstraZeneca, GlaxoSmithKline, Merck, Sanofi

Ingevity, Compact Membrane Systems, University of Toledo, Rowan University

ALTSEP

With use of distillation in common and with reducing the energy consumption in chemical manufacturing as a shared aim, the Chemical Manufacturers Roundtable at the American Chemistry Society Green Chemistry Institute (ACS GCI) began a pre-competitive joint effort in 2013 to investigate less energy-intensive alternative separation (ALTSEP) technologies (2). The Roundtable sought processes that could competitively displace distillation when new or replacement equipment is being specified.

This collaboration provided the basis for a proposal to the U.S. National Institute of Standards and Technology (NIST) Advanced Manufacturing Technology (AMTech) program for a highly competitive planning grant.

Awarded in May 2015, the two-year NIST AMTech planning project is aimed at creating an innovation roadmap for advancing the rational design and predictable, widespread industrial

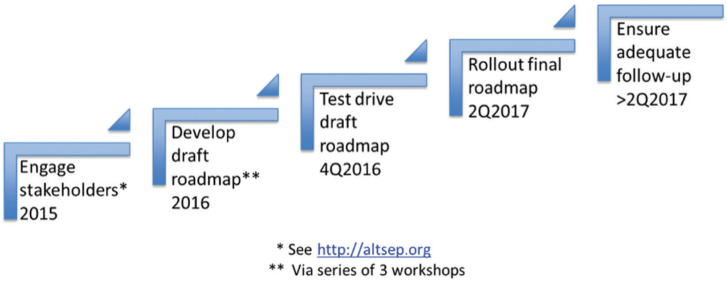

Figure 1. Roadmapping Timeline.

application of less energy-intensive separation processes as alternatives to distillation (Figure 1). The roadmap will identify and prioritize research, development, and demonstration needs for technology initiatives with the potential to transform the competiveness and sustainability of the chemical industry. Successful development of the roadmap depends on a collaborative effort among innovators from chemical and pharmaceutical manufacturers, universities, research institutions, and professional organizations such as ACS and AIChE.
The ultimate aim of this effort is to establish and maintain a robust ecosystem across the chemistry enterprise that enables industrial implementation of less energy-intensive alternative separations technologies.
In order to achieve these goals, the ACS GCI Chemical Manufacturers Roundtable would like you to get involved and contribute. We are soliciting input from companies in the chemical and allied manufacturing sector on the types of separations currently performed via distillation so that we can assure roadmapping stays in tune with industrial needs.

Please contact **gciroundtables@acs.org** with your input. To learn more and to get involved, please visit **http://altsep.org**.

REFERENCES

1. NRC. *Sustainability in the Chemical Industry: Grand Challenges and Research Needs - A Workshop Report*; The National Academies Press: Washington, D.C., 2005.
2. Giraud, R.J., Williams, P.A., Sehgal, A., et al. Implementing Green Chemistry in Chemical Manufacturing: A Survey Report. *ACS Sustainable Chemistry & Engineering* 2014, 2, 2237-2242.

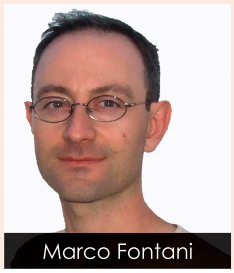
Marco Fontani

MARCO FONTANI[1]*, MARY VIRGINIA ORNA[2], SILVIA SELLERI[3], CECILIA BARTOLI[3]
*Corresponding author
1. Department of Chimica "Ugo Schiff", University of Florence, Via della Lastruccia 13, 50019 Sesto F.no, Firenze, Italy
2. College of New Rochelle, 29 Castle Pl, New Rochelle, NY 10805, New York, USA
3. Department of Neuroscienze, Psicologia, Area del Farmaco e Salute del Bambino, University of Florence, Via Ugo Schiff 6, 50019 Sesto F.no, Firenze, Italy

PEER REVIEWED

A feminine task:
Karlik's and Bernert's discovery of the last natural occurring element

KEYWORDS: Astatine, radioactive elements, missing and spurious elements, women in science.

Abstract The conviction that knowledge acquired via scientific research could be out of the ordinary, or on a higher level, with respect to other forms of knowledge, whether artistic or cultural, was very deep-rooted among 20th century male scientists. At the same time, many scientists emphasized the objective character of their discoveries that allowed them access to an atmosphere of "reality" removed from value judgments and social ideologies, although this interpretation could also be debated. Perhaps "male Science" never held such a romantic position, nor its very name was always associated with the greatest opportunity and the highest ideals.
This paper takes into consideration the academic impact of Karlik and Bernert in their search for the last natural occurring element (astatine, Z=85) and it discusses pertinent topics, such as the increased number of discoveries in the nineteenth century due not only to female scientists working with their husbands (Curie and Noddack).

THE ELUSIVE EIGHTY-FIFTH ELEMENT

From the 1920s into the 1950s, scientists tried a variety of techniques to locate element 85, the heaviest halogen, based on its presumed properties (1). The claimed discovery in 1931 at the Alabama Polytechnic Institute (now Auburn University) by Fred Allison (1882-1974) and associates, led to the spurious name for the element of *alabamine* (Ab) for a few years(2). This discovery was later shown to be one of the biggest scientific blunders of all time.
In 1937, at Dhaka university, the unknown radio-chemist, Rajendralal De, published the discovery of a pair of elements found in the mineral monazite, one of which was presumably *eka-iodine*, long sought after by chemists all over the world (3).
In the second half of the 1930s, other names attributed to this elusive element appeared. The presumed discoveries of Horia Hulubei (1896-1972) and Yvette Chaucois (1908-1999) of elements 87, 93, and 85 - observed by X-rays apparatus in the late 1930s - had as unique results the christens of these elements with the euphonious names of *moldavium*, *sequanium* and *dor* (4).
Soon after these facts Walter Minder (1905-1992), a Swiss radio-chemist, who received his degree in chemistry at Bern in 1930, quickly became interested in understanding the radioactive decay series of the thorium and uranium families. During 1936 he travelled to Berlin where he got in touch with the most renowned German atomic physicists of the time: Walther Bethe (1906-2005), Siegfried Flügge (1912-1997) and Carl Freidrich von Weizsäcker (1912-2007). In 1938 he was named assistant to professor Adolf Liechti (1898-1946) at the local Radium Institute of Bern hospital. That year he published his first article in which he hypothesized on the existence in nature of *eka-iodine* and *eka-cesium*. He also conducted tests to characterize halogens, after which, convinced of having discovered *eka-iodine* (5) wrote: "The beta-decay of Ra-A leads us certainly to hypothesize the formation of element 85. For this reason we suggest the name *helvetium*".
In 1942 Minder became acquainted with a young and beautiful English physicist, Alice Leigh-Smith, née Prebil (1907-1987). Alice Leigh-Smith approached Walter Minder and, exploiting all of her feminine charms, sought to convince him to re-locate to work with her German friends and colleagues in Berlin with the purpose of picking up important information on the status of atomic research in Germany (6). An analogous plan for the construction of an atomic bomb was advancing in great secrecy in the United States. The English, not having the same means of allying themselves with Americans, preferred to send a hugely remunerated spy to Berlin to discover the enemy's plans. Minder was not exactly enchanted with this proposition and refused to accompany Leigh-Smith. However, a strong bond grew between them anyway, culminating in their joint publication of their work in radiochemistry on December 26th, 1942 (7). At the conclusion of their work, they both expressed a desire to name the 85th element: "As a tribute to the scientific work

of our two countries, we propose to name element 85 *anglo-helvetium*".
A bitter criticism to this work arrived from England in the form of a letter from the radiochemist F. A. Paneth (1887-1958). On May 23rd, 1942, he wrote(8): "There is so far no trustworthy indication of a branching of any of the main radioactive series leading to an element 85. Nor has a stable form of this element been found." Paneth's second criticism relative to the existence of stable isotopes of element 85 was addressed to Hulubei's spectroscopic work.
Shortly after Paneth's intervention a young Viennese radiochemist Berta Karlik and her assistant Gertrud Cless-Bernert came to the limelight, succeeding in discovery of the only natural isotope of element 85, but it soon turned out to be not the same one "identified" by Minder...

KARLIK'S AND TAUSCHINSKI'S SEARCH FOR THE NATURAL ASTATINE ISOTOPES

For several reasons, maybe in part because of the encouragement offered by Stefan Meyer (1872-1949), the head of the institute, and in part because the boundary between chemistry and physics had been more open to women physicists, the *Institut für Radiumforschung* became a *mecca* for women exploring the complex of the fields surrounding nuclear physics, radio-chemistry, and radio-physics. Meyer brought in, among others, Berta Karlik and Marietta Blau (1894-1970); the former was able to co-author paper with Gertrud Cless-Bernert, the latter was able to supervise the dissertations of at least five other women, in the years 1930-1937: Elizabeth Rona (1891-1981), Elisabeth Kara-Michailowa (1897-1968), Hertha Wambacher (1903-1950), Stefanie Zila, and Elvira Steppan.
Berta Karlik was born in Vienna on January 24th 1904, eldest of three children of Carl Karlik, director of the *Landeshypothekenanstalt* of Lower Austria, and Karoline née Baier. In her infancy Berta enjoyed private lessons, but later she attended public school in Mauerbach. In the summer 1923, she graduated with distinction. She entered the University of Vienna and on October 10th 1927 she discussed her thesis, under the tutorage of Stefan Meyer: "Über die Abhängigkeit der Szintillationen von der Beschaffenheit des Zinksulfides und das Wesen des Szintillationsvorganges" (9).

Figure 1. Berta Karlik at the Radium Institute in Vienna, 1920s.

On March 8th 1928 she obtained her Ph.D. "*Philosophiae Doctor*" at the University of Vienna.
From November 1930 to December 1931 she worked at the Royal Institution of Great Britain in London, headed by Nobel laureate Sir William Bragg (1890-1971), during which period her researches were focuses on X-ray studies of crystal structures.
Berta Karlik took advantage of the time she spent in England and visited a large number of physical, chemical and biological Institutes. She had several opportunities to stay for a long time at the Cavendish Laboratory in Cambridge, which was led by Lord Rutherford (1871-1937), the famous pioneer in the field of nuclear physics. She could become familiar with this institution and in particular with the radioactive research and devoted herself, while in London, studying the medical application of radium, also attending the physical divisions of six leading hospitals.
In summer 1931 she travelled from London to Paris and she visited the laboratory of Louis de Broglie (1892-1987), the Pasteur Institute and the Curie Institute, where she personally met the legendary figure of Madame Curie (1867-1934).
When eventually she came back to Vienna she dedicated her scientific research at the *Radiumforschung*. On April 1st 1933 Berta Karlik was appointed graduate assistant. In 1937 she received the *Venia Legendi* of physics at the University of Vienna and two years later she was appointed lecturer. In October 1940 she was appointed research assistant at the Institute for Radium Research.
During the World War II, she and her colleague Traude Cless-Bernert succeeded in collecting a very significant discovery: they managed to close the last gap in the periodic table of the elements. In autumn 1944 heavy bombardments of Vienna began. Alongside the valuable equipment of the Institute and radium stocks were brought to safety outside Vienna, and the hunt for element 85 had a sudden stop.
However this work was, for Karlik alone, crowned with the 1947 "Haitinger Prize" for chemistry with the following motivation: *Frau Karlik ist durch die Entdeckung des Elements 85 in die Namen der Gelehrten von internationalem Ruf eingetreten.*
Her boss and mentor professor Gustav Ortner died in late April 1945. Under the difficult conditions due to war, Berta Karlik, was requested by the Academy of Science to take the provisional directorship of the Institute for Radium Research. She reported in her diary: "Als im April 1945 Wien zum Kriegsschauplatz wurde, tobte der Kampf einige Tage hindurch auch in der unmittelbaren Umgebung des Instituts. (...), das Radiuminstitut kam glücklicherweise ohne größeren Schaden davon. (...) Es bot einen traurigen Anblick: Die leeren Räume waren bedeckt mit Glasscherben und Schutt und Staub, der von Bombentreffern der Umgebung hereingeschleudert worden war"(10).

In 1950 Berta Karlik was appointed associate professor and later full professor (*ordentliche Professor*), position never reached before by a woman in Austria. In 1954 Berta Karlik became a corresponding member of the Austrian Academy of Sciences. When on September 1st 1974 the Faculty of Science asked Berta Karlik to retire she replied "yes", with the condition that professor Dr. Herbert Vonach could be her successor the next day.
On February 4th 1990 having just turned her 86th birthday, Berta Karlik died peacefully in her home. Vonach Herbert wrote her obituary in which he stated: "Eine ganze

Figure 2. Berta Karlik (right) and Gertrud Cless-Bernert (left) in their laboratory, 1942.

Generation von Physikern wurde von ihr in die Welt der Atome und Kerne eingeführt(11)".

The life of Gertrud Tauschinski (born in Vienna on June 27th 1915), Karlik's assistant, gave so much less satisfaction and professional recognition than that of her boss. She graduated on June 22nd 1933; later she expressed the desire to study architecture at the Technische Hochschule but before the end of winter semester she left her architecture studies for physics at Vienna University. In 1938, one year previous her promotion, she spent a semester in Leipzig. Eventually she discussed her thesis on July 12th 1939 under the supervision of professors Gustav Ortner (1900-1945), Eduard Haschek (1875-1947) and Egon von Schweidler (1873-1948) at the *Radiuminstitut*.
In 1940 Gertrud Tauschinski married Mr Bernert from which she had a son. She occupied the position of "volunteer assistant" at the *Institut für Radiumforschung*, and there she had the opportunity to work closely with Dr. Berta Karlik eleven years her senior. Together they found the natural isotope of element 85. In 1945 she was appointed as laboratory technician at the same Institute and later she spent one year (1948-49) in Sweden, but her "finest hour" in scientific research of high level was fatally fading away.
Since 1959 she was appointed "scientific secretary" for the *Konferenz Atoms for Peace* at Geneva. Later she became a salaried consultant for industrial applications of isotopes. In 1961 she married for the second time with the engineer F. Cless. Her hopes and plans of future work were soon frustrated by an accident that forced her to retire early. Gertrud Cless-Bernert née Tauschinski died on 20th February 1998. Although she was four months short of her 83rd birthday, her death was regarded by friends and relatives as sudden as unexpected.
Coming back to the history of the discovery of element 85, Berta Karlik and Traude Bernert observed the alpha particle emissions of ^{218}At as early as 1942. The experiments of Minder and Leigh-Smith were repeated by Karlik and her colleague Traude Bernert, but they did not observe the weak beta radiation that Minder and Leigh-Smith claimed was characteristic of *anglo-helvetium*. Karlik considered the work of the two Bern physicists as the height of error. Using a methodology totally different from that used to "discover" *anglo-helvetium*, Berta Karlik discovered the short-lived natural isotope of *eka-iodine* (^{218}At) with a half-life of about two minutes.
In 1943, Karlik and Bernert were working with an intense sources of RaA (^{218}Po). RaA preparations were made by electronic activation and short exposure (10-15 seconds) of ^{222}Rn (~100 milliCurie) and immediately tested by a 4-stage tube electrometer and oscillograph for α-rays of range beyond these of RaA. Successively, a second group of RaC› rays was found, originating a very α-unstable isotope of mass number 218 (^{218}85). The range of the new α-ray was 5.53 cm, with the energy of 6.63 meV, and a half life of about 2 seconds(12). The amounts of β-decompositions *per* α-decomposition for RaA (in other words, the *ratio* of "element 85" and RaC' formed from RaA) was found to be 3.3×10^{-4}.
The following year, while the face of German and Austrian cities was drastically altered by the Anglo-American bombing, Berta Karlik and Traude Bernert found that the new α-rays (13) in the thorium and actinium series corresponded to the isotopes ^{216}85 and ^{215}85. Besides in contrast to the results of Minder, the β-activity of RaA was in agreement with theoretical predictions. With RaA a group of α-particles of range 5.53 cm was found and attributed to isotope 218 of element 85. Similar observations with thorium emanation and actinium emanation were related to isotopes 216 and 215 of element 85. These isotopes fit-in well in curves of disintegration energy vs. mass number. Good agreement was also found for the energy balance of the Ra series, while for the Th and Ac series a hypothesis of isomeric nuclei was proposed although with some difficulties (14).

This element occurs in the natural decay chains as a result of product after with very low branching ratio taking place β-decay of Ra (218Po), ThA (216Po) and AcA (215Po); Karlik and Bernert observed the radiation of the formation and decay of that isotope (mass 218) of element 85 and were able to demonstrate that it appeared at the uranium-radium series. However, other researchers in the USA had induced nuclear reactions and produced artificially this item in 1942 previously – exactly two years earlier than Karlik and Bernert.

Actinium chain											
					At-219 0.9 m ←	Fr-223 22 m ←		Ac-227 22 y α/β	Th-231 25.6h α/β⁻	Pa-231 3.3×10^4y	U-235 7×10^8y
		Pb-211 36.1m α/β⁻		Po-215 1.8ms α	Rn-219 3.9s α	Ra-223 11.4d α		Th-227 18.7d			
	Tl-207 4.8m α/β⁻		Bi-211 2.15m								
		Pb-207 stable									

Table 1. The actinium (4n + 3) series runs from uranium 235, via actinium 227, to lead 207.

They synthesized element 85 and in the mean time they were recognised as the true discoverer of it; Karlik and Bernert, who had identified a natural isotope of element 85 - despite the immense credit for this success - did not come right of naming it. They would have chosen the name *Viennium*(15). Later researchers in the United States called the element Astatine. In the fall of 1944, heavy allied bombardment of Vienna began. The valuable equipment of the Institute and the radium stocks were brought to safety outside city and the two women abruptly had to interrupt their radiochemical researches.

Astatine (At) has 37 known isotopes, all of which are radioactive; the range of their mass numbers is from 191 to 229. There also exist 23 metastable excited states. The longest-lived isotope is ^{210}At, which has a half-life of 8.1 hours; the longest-lived isotope existing in naturally occurring decay chains is ^{219}At with a half-life of 56 seconds (16). Actinium-219 was chemically separated from a natural source only in 1953 by Earl K. Hyde (1920-1997) and Albert Ghiorso (1915-2010)(17). However the accepted proof of element 85's existence came in 1940 from the Berkeley group of Dale R. Corson (1914-2012), Kenneth R. MacKenzie (1912-2002), and Emilio Gino Segré (1905-1989), who synthesized the element by alpha particle bombardment of bismuth (18). The turmoil of World War II and the fundamental question of artificial *vs.* natural elements, leads to the delay of the discovery credit and the honor of naming the element until 1947 (19).

CONCLUSION

It is well consolidated that the difficulties facing women scientists are deep-rooted. It is not a personal speculation that in the late nineteenth century and in the first decades of twentieth century there were almost no initiatives to support them in their academic careers. And, in some Country, in addition to these considerable barriers, their admission to the University was banned.

Berta Karlik worked for the University of Vienna and eventually become the first female professor at that institution. She discovered that the element 85, astatine, is a product of the natural decay processes, after several scientists in vain searched for it in radioactive minerals. Berta Karlik was not the only chemist influenced by her mentor but, she was one of those who, without marrying him, took his direction seriously enough to influence other women in research, high in quality.

ACKNOWLEDGEMENTS

The author would like to thank Professor Stefano Cicchi and Dr. Costanza Montis – of the Department of Chemistry of the University of Florence – for their advices and guidance; we would also like to express sincere appreciation to Dr. Andreas Pavlik – of the Nuclear Physics Group of the University of Vienna – for his earnest efforts and for providing many biographical data concerning Dr. Tauschinski.

REFERENCES AND NOTES

1. Fontani, M., Costa, M. DE REDITU EORUM, Sulle tracce degli elementi scomparsi, (2009), Società chimica italiana Ed., Roma, 359-69. Fontani, M., Costa, M., Orna M.V. THE LOST ELEMENTS: THE PERIODIC TABLE'S SHADOW SIDE, (2014), Oxford University Press, Hardcover, 576 Pages, 55 pictures.
2. Allison, F., Murphy, E. J., Bishop, E. R. et al. "Evidence of the Detection of Element 85 in Certain Substances," *Physical Reviews*, 37(9), 1178-80, (1931). Allison, F., Bishop, E. R., Sommer, A. L. , "Concentration, Acids and Lithium Salts" of Element 85," *J. Am. Chem. Soc.*, 54, 616-620, (1932).
3. Das, A., De, R., *J. Indian Chem. Soc.*, 13, 197, (1936). De, R., "Twin Elements in Travancore Monazite", *Separate* (Bani Press, Dacca), 18, (1937). De, R., *Indian Journal of Physics*, 13, 407, (1939). R. De, "New Elements in Monazite Sand", *Sri Gouranga Press*, Calcutta, 21, (1947).
4. Hulubei, H., "Recherches relatives à l'élement 87", *Compt. Rend.*, 202, 1927-29, (1936). Hulubei, H., *Compt. Rend.*, 205, 854, (1937). Hulubei, H., Cauchois, Y., "Spectres de l'émission propre ondulatorie du radon et de ses dérivés. Raies attribuables à l'élément 85," *Compt. Rend.*, 209, 39-42 (1939). Hulubei H., "Sur L'Element 85", *Bull. Section Scientifique de l'Academie Roumaine, 27*, 124-134 (1944). Hulubei H.,, "État Actuel des Informations Sur Les Isotopes de Numéro Atomique 85," *J. Chim. Phys. Phys.-Chim. Biol., 44*, 225-229, (1947).
5. Minder, W., "Über die β-Strahlung des Ra A und die Bildung des Elementes mit der Kernladungzahl 85", *Helvetica Physica Acta*, 13, 144-152, (1940).
6. Minder, W., *Gheschichte der Radioaktivität*, Springer Ed., (1981).
7. Leigh-Smith, A., Minder, W., "Experimental Evidence of the Existence of Element 85 in the Thorium Family", *Nature*, 150, 767-8, (1942).
8. Paneth, F. A., *Nature*, 149, 565, (1942).
9. "On the dependence of scintillations on the nature of the zinc sulphide and the essence of scintillation process"
10. When in April 1945, Vienna was the set of war, the battle raged for several days passed in the immediate vicinity of the institute. (...), the Radium Institute fortunately was not seriously damaged. (...) I provided a sad sight: The empty spaces were covered with broken glasses and rubbles and dust provoked by the bombs.
11. A whole generation of physicists was introduced by her into the world of atoms and nuclei.
12. Karlik, B., Bernert, T., "Eine Neue Natürliche α-Strahlung", *Naturwissenschaften*, 31, 298-99, (1943). Karlik, B., Bernert, T., "Ein Weiterer Dualer Zerfall in der Thoriumreihe," *Naturwissenschaften*, 31, 492, (1943). Karlik, B. Bernert, T. "Über eine dem Element 85 Zugeordnete α-Strahlung", *Sitzber. Akad. Wiss. Wien, Math.-naturw. Klasse*, 152, 103-110, (1943).
13. Karlik, B., Bernert, T., *Anz. Akad. Wiss. Wien, Math.-naturw. Klasse*, 81(No. 1), 2, (1944). Karlik, B., Bernert, T., "Das Element 85 in der Actiniumreihe," *Naturwissenschaften, 32*, 44, (1944).
14. Karlik, B., Bernert, T., "Das Element 85 in den Natürlichen Zerfallsreihen", *Zeitschrift für Physik*, 123, 51-72, (1944).
15. Strohmaier B., Österreichischer Verband für *Strahlenschutz*, "Berta Karlik (1904–1990) Kernphysikerin, Wissenschaftsmanagerin, erste Ordinaria an einer philosophischen Fakultät in Österreich", 42(1), 20-29, (2008).
16. Audi, G., Wapstra, A. H., Thibault, C. et al. "The Nubase evaluation of nuclear and decay properties", *Nuclear Physics A*, 729, 3–128, (2003).
17. Hyde, E. K., Ghiorso, A., "The α-branching of Ac K and the presence of astatine in nature", *Phys. Rev.*, 90, 267, (1953).
18. Corson, D. R., MacKenzie, K. R., "Artificially Produced Alpha-Particle Emitters," *Phys. Rev.*, 57, 250, (1940). Corson, D. R., Mackenzie, K. R., Segré, E. G., "Possible Production of Radioactive Isotopes of Element 85" , *Phys. Rev.*, 57, 459, (1940). Corson, D. R., Mackenzie, K. R., Segré, E. G., "Some Chemical Properties of Element 85" , *Phys. Rev.*, 57, 1087, (1940). Corson, D. R., Mackenzie, K. R., Segré, E. G., "Artificially Radioactive Element 85" , *Phys. Rev.*, 58, 672-78 (1940). Corson, D. R., "Astatine," *Chem. Eng, News*, 81, 158, (2003).
19. Corson, D. R., Mackenzie, K. R., Segré, E. G., "Astatine: Element of Atomic Number 85" , *Nature*, 159, 24, (1947).

PostEVENTS

Summary of the 5th Conference on Frontier in Organic Synthesis Technology (FROST5) (21-23 October 2015, Budapest)

The 5th FROST conference on flow chemistry, organized by the Flow Chemistry Society in collaboration with the Akadémiai Kiadó was held in Budapest in October this year. The conference focused on innovative areas of organic chemistry, such as end-to-end production technology, innovative applications in oil industry, nanotechnology and green chemistry. The event, which was opened by Ferenc Darvas, President & Chairman of the Society, attracted 63 participants from 15 countries. During the 5-section conference 18 very high-quality, inspiring lectures and nearly 20 posters were presented. From the 3 keynote speakers, Rigoberto Advincula highlighted that flow chemistry is an ideal process for the oil and gas industry, Holger Löwe presented how chemical reactions can be accomplished in microemulsion droplets, and Walter Leitner expounded new flow catalysis possibilities by the usage of carbon dioxide. In the further lectures latest research results of acknowledged flow chemistry experts were demonstrated. Hungary was represented by 3 lecturers, illustrating that the country has been playing a pioneering role in flow chemistry from the beginnings, mainly owing to the reactors of ThalesNano Inc. (e.g. H-Cube®). The regular panel discussion on the current state and future of flow chemistry was moderated by Richard V. Jones (ThalesNano). Among other topics the debate forum discussed the integration of flow chemistry into the organic chemist BSc education, as it is an ever-growing need of the industry. In the topic of development trends in the next 10 years, the comprehensive integration of real-time analytics was examined, which may facilitate remote control over chemical reactions, thus revolutionize laboratory or plant work culture. Four companies (Advion, Syrris, ThalesNano and Vapourtec) also took part in the conference as exhibitors and sponsors. At the gala dinner the award for the best poster was handed over to Nicholas Holmes, PhD student of the University of Leeds. The IUPAC – ThalesNano Flow Chemistry Award 2016 was also announced at the dinner by its initiators, Ferenc Darvas (ThalesNano) and János Fischer (IUPAC Hungary). Overall, the event was a great success due to the enthusiasm and hard work of its organizers: Ferenc Darvas (Chairman), Mimi Hii (Vice-Chair) and the members of the Local Organizing Committee (Oliver C. Kappe, Paul Watts, Szilvia Gilmore and Balázs Réffy).

PostEVENTS

Pharma Booming at CPhI Worldwide 2015

CPhI Worldwide is the largest global exhibition for the pharmaceutical industry. Together, with its co-located events, the 26th edition welcomed impressive attendee numbers of over 36,500 and around 2500 exhibitors. Held in Madrid for 2015, the pharma industry's largest event saw representatives from 140+ countries, an expanded conference platform and a plethora of networking, learning and sharing opportunities.

Mirroring the growth of the industry over the last decade, CPhI Worldwide remains integral to the pharmaceutical community agenda, offering engaging, world-class content. The event provides the best opportunities for networking and is the global hub for suppliers and buyers in the industry.

This year there was a significant increase in content-sharing platforms, specifically through the introduction of the CPhI Pharma Forum. This new initiative took centre stage during the event, acting as a dedicated content village where all CPhI attendees had the opportunity to examine thought leadership from media partners, exhibitors and the CPhI Pharma Insights Reports.

The Pharma Insight Innovation Briefings were another notable highlight with impartial, in-depth sessions on regional updates and specialist topics covering regulation, QC, traceability, sustainability and health to name but a few. In addition, an expanded CPhI Pharma Awards also returned, with four new categories to further honour the industry's achievements and innovations across all areas of the pharmaceutical supply chain.

Prior the main exhibition, the Pre-Connect Congress took place – a full day of conferences showcasing senior executives and influential speakers discussing the latest innovations, trends and market developments from across the industry in a series of market-led educational modules. This year, the conference was organised along two main

tracks, with sessions in *track one* including 'Formulation & Drug Delivery'; 'Biologics, Biosimilars & Biobetters'; and 'API Sourcing & Manufacture'. *Track two* features modules across 'generics'; 'Pharmaceutical Packaging'; and 'Mergers and Acquisitions'.

The success of CPhI Worldwide 2015 has further cemented its reputation as the global hub for insight and analysis, networking, and it is now the definitive barometer of the industry's future direction and health. In 2016, CPhI Worldwide will return to Spain and, for the first time, it will take place in amongst the thriving biotech and pharma manufacturing cluster, as it visits the great city of Barcelona, 4-6 October.

CPhI worldwide

PostEVENTS

Seven prestigious winners from over 70 entries in the CPhI Pharma Awards 2015

The worthy winners of the 2015 CPhI Pharma Awards were announced live during a dedicated ceremony at CPhI Worldwide in Madrid, Spain, 13-15 October. The entries included innovations and new service offerings from across the entire spectrum of the pharmaceutical supply chain, with the awards honouring companies and individuals driving the industry forward.
With the launch of four new categories this year, the awards received a record number of entries, covering: 'Best Innovation in Packaging'; 'Best Innovation in Process and Formulation Development'; 'Excellence in Partnering & Outsourcing'; Best Innovation in APIs and Excipients'; 'Innovation in Supply Chain & Logistic Management'; 'Best Innovation in Manufacturing Technology'; and 'CEO of the Year'.
The 16 finalists shortlisted were invited to present their case during the first day of CPhI Worldwide, and after extensive deliberations, the judges announced the winners during a live ceremony on the first day of the event.

The 2015 CPhI Pharma Award Winners:

- Best Innovation in Supply Chain & Logistic Management: **TraceLink**
- Best Innovation in Manufacturing Technology – *in cooperation with Pharmaceutical Technology:* **Harro Hoefliger**
- Best Innovation in Packaging: **Sulzer**
- Best Innovation in APIs and Excipients: **OMYA International AG**
- Excellence in Partnering & Outsourcing – *in cooperation with Pharmaceutical Outsourcing Magazine*: **Centroflora CMS**
- Best Innovation in Process and Formulation Development: **Catalent**
- CEO of the Year *in cooperation with PharmaBoardroom*: **Vivek Sharma, CEO - Pharma Solutions, Piramal Enterprises Ltd**
- CPhI Sustainable Stand Award 2015: **Novo Nordisk Pharmatech and Novozymes**

Rutger Oudejans, CPhI Brand Director, added: "*What impresses me most are the innovative contributions that all the nominated companies are making in improving pharmaceutical processes, enhancing quality and pushing new boundaries. On behalf of CPhI Worldwide and UBM EMEA, I would like to commend all of the finalists and offer my warmest congratulations to this year's worthy winners.*"

informEx

FEBRUARY 2-4, 2016

Morial Convention Center • New Orleans, LA, USA

www.informex.com

InformEx is a dynamic event held to build partnerships among buyers and sellers of fine and specialty chemicals—the only show of its kind in the US. The three-day event is returning to New Orleans, LA, USA from February 2-4, 2016, and will once again foster profitable partnerships and innovation in the high-value chemical industry.

InformEx is uniquely positioned to help chemical companies transform into science and technology companies. For over thirty years, the innovation focused show has aimed at building a global network of customers, suppliers and colleagues in some of the most rapidly growing chemical markets, including medical devices, agrochemistry, biopharma and green chemistry.

Don't miss your chance to get involved in the 2016 event!

Interested in attending InformEx? Use **PROMO Code CHEMTODAY10** when you register before January 01, 2016 and get a 10% discount!*

For more information on exhibiting at InformEx, email sales@informex.com.

UBM

*Discount applicable to non-exhibiting badge types only.

Pharma&Biotech

Lonza

Anywhere, Anytime

Explore Lonza's Custom Manufacturing Facilities From Your Mobile Device

Save yourself a costly and time consuming flight by touring our modern custom manufacturing sites from any electronic device. Take your first in-depth look at our state-of-the-art biological and chemical development and production facilities.

To view Lonza's online tours, visit www.lonzavirtualtours.com

Custom Services Include:

- Protein Design and Optimization
- Cell and Viral Therapies
- Mammalian Biopharmaceuticals
- Microbial Biopharmaceuticals
- Antibody Drug Conjugates
- Cytotoxics
- Highly Potent APIs
- Peptides
- Small Molecules
- Vaccines

Lonza Inc.
US: +1 201 316 9200
Europe: +1 41 61 316 81 11
custom@lonza.com

www.lonza.com/oursites